The functional role of theta-gamma oscillations in human motor neurophysiology

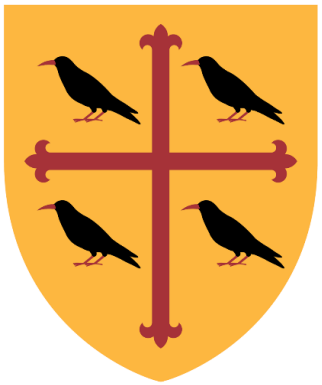

Camille Lasbareilles

St Edmund Hall

University of Oxford

Physiological Neuroimaging Group

Wellcome Centre for Integrative Neuroimaging

Nuffield Department of Clinical Neurosciences

A thesis submitted for the degree of

Doctor of Philosophy

2025

40,520 words

Abstract

BACKGROUND: Motor cortical theta-gamma (θγ) oscillations have recently gained the attention of neuroscientific literature following recent results from Akkad *et al*. (2021) in which artificially entraining 75Hz γ oscillations, phase amplitude coupled to the positive half of a 6Hz θ envelope (θγ peak; TGP) using transcranial alternating current stimulation (tACS) significantly modulated motor behaviour. Such an effect was not seen when entraining 75Hz γ oscillations, phase amplitude coupled to the negative half of a 6Hz θ envelope (θγ trough; TGT). There is a limited understanding of the neurophysiological mechanisms underpinning such behavioural effects. To this end, this thesis explored the effects of θγ oscillations on healthy human motor learning behaviour, TMS-metrics of receptor-mediated inhibition and excitation, and MRI-measured functional connectivity within the sensorimotor network. Taken together, these results provide novel insights into the neurophysiological mechanisms underlying human motor cortical θγ oscillations and showcase the potential of driving such oscillations on noninvasively modulating healthy human motor neurophysiology.

METHODS: I artificially entrained motor cortical θγ oscillations using tACS. Depending on the research question of each experiment, I delivered different types of θγ oscillations (e.g. 45Hz versus 75Hz TGP waveforms or TGP versus TGT). I also investigated two different potential mechanisms of action for tACS: entrainment (delivering three second bursts of tACS) versus neuroplasticity (delivering 20 minutes continuous tACS).

EXPERIMENT 1: I first investigated whether the positive behavioural effects reported by Akkad *et al*. (2021) were frequency-specific. I compared the effects of driving 45Hz versus 75Hz γ TGP on motor behaviour. The tACS was delivered in a movement-locked manner, such that participants only received three seconds bursts of tACS per three seconds trial. I found that participants receiving 45Hz TGP tACS hit significantly fewer targets than participants receiving sham tACS. I found no significant difference in the *number of targets hit* between participants receiving 75Hz TGP tACS and sham tACS. This was unexpected, given the previously reported behavioural effect of 75Hz TGP tACS on motor behaviour (Akkad *et al.*, 2021). This suggests that short bursts of 75Hz TGP tACS potentially engages different neurophysiological mechanisms than longer stimulation periods. Furthermore, I found that that these same participants receiving 45Hz TGP tACS had significantly reduced force outputs compared to participants receiving sham tACS, as quantified by extracting the slope of the first instance of force production. Overall, these results suggest that 45Hz TGP tACS impedes behavioural gains, potentially via reductions in force output.

EXPERIMENT 2: Next, I investigated the phase-specific effects reported by Akkad *et al*. (2021) such that TGP, and not TGT, significantly modulated motor behaviour. Given the relationship between motor learning and GABA, it is possible that TGP uniquely modulates GABA. Here, using Transcranial Magnetic Stimulation (TMS), I sampled single and paired-pulse TMS to assess cortical excitability and receptor-mediated inhibition and excitation before, during, and after 20 minutes of continuous 75Hz TGP tACS. I found that TGP significantly reduced extrasynaptic GABAergic tone, serving to explain the positive behavioural findings of Akkad *et al*. (2021).

EXPERIMENT 3: Finally, I investigated whether the positive behavioural effects of TGP tACS reported by Akkad *et al*. (2021) were mediated by local changes in neuronal activity or by wider, network level changes in sensorimotor network functional connectivity. Using a combined tACS-functional MRI approach, I compared the effect of TGP tACS on sensorimotor functional connectivity at rest versus during motor learning. I found that TGP tACS significantly reduced the functional connectivity between the sensorimotor network and the right somatosensory cortex from pre- to late-tACS during motor learning. I also found that TGP tACS significantly increased the functional connectivity between the sensorimotor network and the right supramarginal gyrus from late- to post-tACS during motor learning.

DISCUSSION: Together, the findings of the present studies address the different facets of the complex neurophysiological mechanisms of motor cortical θγ oscillations in healthy human motor behaviour.

Acknowledgements

First and foremost, I would like to thank my primary supervisor Professor Charlotte (Charlie) Stagg. It has been a genuine honour to work with you. Your leadership, expertise, and unwavering kindness has made my DPhil journey so positive. Thank you for trusting and believing in me since day one and for always encouraging me. I have learnt so much from being at PiNG, as a scientist and as a person, things I will keep with me for the rest of my life. Thank you for this incredible opportunity.

I would like to thank M. Jean Chagnon for his incredibly generous financial support throughout my DPhil. I had the pleasure of meeting Jean on multiple occasions both in the UK and in Canada and always loved telling him about all the weird and wonderful things I have been doing in Oxford. Thank you for making this once-in-a-lifetime journey possible for me.

Thank you to my second supervisor, Professor Huiling Tan and her team (especially Alek Pogosyan) for their support in providing invaluable expertise, lab space, and equipment.

Thank you to my St Edmund Hall College advisor, Professor David Dupret. You are one of the brightest minds as well as one of the most genuine and caring people I have encountered in Oxford. Thank you for your continued support throughout my DPhil and for believing in me at times when I did not.

I would like to thank St Edmund Hall (Teddy Hall) for being my second home and providing a safe space throughout my DPhil. I would also like to thank St Edmund Hall Boat Club (SEHBC) for the wonderful memories, friendships, fun races (Summer VIIIs, Torpids, WeHoRR, Quintin Head, Molesey), training camps (Sabaudia and Cambridge), and courage to join the OUBC Development Squad.

***

To those in my personal life without whom any of this would have been possible. My mother, Christine-Louise Lasbareilles. Thank you for always believing in me. I am eternally grateful for all of the love, support, and strength you have given me throughout my life to get me to this point. My love for science is thanks to you and none of this would have been possible without you.

My partner, Oliver Stark. Thank you for your unconditional support and unwavering love throughout this journey. Again, this would not have been possible without you.

My father, Antoine Breton, thank you for calling me every Sunday night and visiting me in Oxford as much as you did. I have loved sharing my love of Oxford with you.

***

Thank you to the wonderful Radiographer and core staff team at WIN (Jon, Nicky, David, Mike, Juliet, and Seb). Thank you for your support and patience on my 7T MRI project. Thank you for training me as a scanner operator (thank you, Nicky!). Being an MRI scanner operator at WIN has been one of the highlights of my DPhil and certainly got me through the last few months of writing. Thank you to the Public Engagement Team (Hanna and Carinne) for introducing me to the world of public engagement and giving me so many fun opportunities to showcase my work to the general public.

Thank you to all of the students I had the pleasure of supervising. Syed (Hur) Shah, Sarah Zhang, Charlotte Austin, Helen Zhang, Charlotte Burney, thank you all for your hard work and friendship. I am proud to have worked with you all and see you grow into the scientists you have become.

***

Thank you to the incredible postdoctoral team at PiNG:

Poly - You are a wonderful scientist and even more wonderful friend. The hours we spent fighting with the force gripper really brought us closer together! I am so proud to have worked with you and learnt from you. Thank you for your kindness, support, and for always being on my side.

Ioana - Thank you for always being there for me and providing the best hugs! You got me through some of the toughest times in my DPhil. You are an incredible scientist and one of the most genuine people I have met in Oxford.

Justin - Thank you for teaching me the insane world of (f)MRI analysis. Thank you for your patience and encouragement as I battled through learning bash and FSL. It has been a pleasure working with you.

Valentina - Thank you for being a wonderful friend and source of support throughout my DPhil. From fighting with the Digitimer during our tACS-TMS project, to having lunch outside in summertime Oxford, it has been a pleasure getting to know you and working with you.

Catha - Without your support during my MSc, I may not have even made it here! Thank you for being a constant source of strength, inspiration, and kindness. It has been a genuine pleasure working with and learning from you. I am so proud to have worked with you and seen you bloom into a wonderful mother as well as an incredible scientist.

And last, but certainly not least, I would like to thank my fellow PiNGWINs and WIN friends over the years. Lara, Lucy, Juju, Aislin, Hanna, Barbara, Eva, Izabelle, Mat, James, Ben, Nilgoun, Tim, Faye, Jake, Alekhya, Jess, Patricia, Birtan, Oana, Mareike, Felix, Loic, Alexanne, Fabio, Judith, Vera. You have all provided different sources of strength and happiness to me throughout my DPhil. A special thank you to Lara and Max for truly keeping me sane and getting me through the last few months of my DPhil. Thank you for listening to my rants, buying me tea from Pret, and generally encouraging me. I am grateful to you both for being there for me so consistently in the final push. Finally, thank you to all of my wider Oxford friends: James, Maria, Alex, Sarah, Frances, Verity, Ed, Theana, Nikola, Angelica, Emma, Rohit, Natalie, and many others. Thank you for making this DPhil filled with friendship and laughter.

***

Related publications

A subset of the data presented in Chapter 3 was submitted by Charlotte Burney for her FHS project report.

A subset of the data presented in Chapter 4 was submitted by Helen Zhang and Charlotte Austin for their MSc project reports.

A subset of the data presented in Chapter 5 was submitted by Sarah Zhang for her MSc project report and by Syed Shah for his FHS project report.

Contents

CHAPTER I - Introduction

In this Chapter, I first contextualise the significant clinical and socioeconomic problem that stroke poses to society. I then discuss how the acquisition of a novel motor skill in the healthy brain is likened to the reacquisition of a lost motor skill in the post-stroke brain and how, as such, I use healthy human motor learning as a model of post-stroke motor skill recovery. I then define "motor learning" for the purposes of the experimental chapters and outline the role of the primary motor cortex and other motor areas in supporting motor learning. Next, I explore the neurophysiology of excitatory pyramidal cells, inhibitory interneurons, and their interactions leading to theta and gamma oscillations, with a focus on cross-frequency coupling (particularly theta-gamma phase amplitude coupling) in hippocampal- and (possibly) non-hippocampal-dependent learning. Finally, I outline transcranial alternating current as a non-invasive neuromodulatory technique as well as provide an overview of its hypothesised mechanisms of action.

1.1 Current landscape of post-stroke motor recovery

Stroke represents a significant global health challenge with up to 15 million new cases per year, resulting in around five million deaths (Donkor, 2018; Ursin *et al.*, 2019). Up to 50% of stroke survivors are left with long-term disabilities of varying severity including cognitive, motor, visual, and sensory impairments that can significantly impact quality of life, independence, and ability to work (Donkor, 2018). Therefore, there is an urgent clinical need to develop adjuvants to physical therapy that can boost and potentially accelerate the rehabilitative process.

The current gold-standard for post-stroke motor recovery is intense and tailored physical therapy such as task-specific training and Constraint-Induced Movement Therapy (CIMT) soon after the onset of stroke where the potential for functional recovery through local and network-level neuroplasticity-related effects are at their peak (Maier, Ballester and Verschure, 2019). Within environments with high pressures on these resources, such as the National Health Service in the United Kingdom, this represents an ongoing challenge as the impact of stroke continues to increase on a macro socio-economic scale. As such, research is invested in the development and optimisation of novel rehabilitative tools that can be implemented as an adjuvant to physical therapy.

1.2 Relationship between post-stroke motor recovery and motor learning

In practice, we liken the reacquisition of a lost motor skill in the chronic stages of post-stroke recovery to the acquisition of a new motor skill in the healthy brain. Recovery from hemiparesis has been suggested to be a form of motor learning as training on specific tasks leads to specific skill improvement. In fact, several rehabilitation approaches, such as CIMT, are based on theories of motor learning (Krakauer, 2006). Furthermore, the neurophysiological underpinnings of improved motor performance in stroke and healthy controls appear to be mediate by similar neurophysiological mechanisms such as changes in excitation/inhibition (E/I) balance (Bachtiar and Stagg, 2014; Grigoras and Stagg, 2021). Therefore, in order to improve post-stroke motor recovery, it is vital to develop an intervention that could be delivered alongside physical therapy, and which modulates neuronal activity in a meaningful way to support motor learning.

1.3 Human motor learning

The acquisition and retention of complex motor skills such as learning how to write, ride a bicycle, type on a keyboard, or learn a musical instrument plays a central role in our daily lives. Motor learning is a multifaceted phenomenon, encompassing elements of low level motor control such as force and speed, as well as high level cognitive planning, memory, sensory integration, visuomotor, and sensorimotor mechanisms. At a behavioural level, motor learning can focus on facets such as improvements in outcome, consistency, stability, adaptability, reorganization of existing skills, changes in coordination dynamics, speed-accuracy trade-offs, and many others (Ranganathan, Lee and Krishnan, 2022). Once a new motor skill has been acquired, the motor system is able to adapt this learnt behaviour in the face of new challenges. This is known as motor adaptation.

Human motor learning involves a complex network of distributed systems across cortical, subcortical, and spinal regions. These regions and associated circuits adapt and reorganise in response to practice and feedback and are involved in different stages of motor behaviour and learning. Cortical regions consistently involved in motor learning include the primary motor cortex (M1), (pre)supplementary motor area (SMA), primary somatosensory cortex (S1), dorsal/ventral premotor cortex, prefrontal cortex (PFC), posterior parietal cortex and their associated networks (Krakauer *et al.*, 2019). These cortical regions are often part of a wider network that involve subcortical regions such as the basal ganglia, thalamus, hippocampus, and cerebellum.

Here, I have defined motor learning as an experience-dependent improvement in performance of a novel motor skill (Krakauer *et al.*, 2019). I have further separated motor learning into two key processes: (1) early skill acquisition: the processes by which an individual acquires the ability to identify appropriate movements given a particular task context, select the correct action given a

sensory stimulus and/or the current state of the body and the world, and execute that action with accuracy and precision; and (2) later skill maintenance and refinement: the ability of the individual to maintain performance levels of the acquired skill and gradually reduce error.

1.4 Neuronal subtypes

Broadly speaking, there are excitatory and inhibitory neurons that govern neuronal activity in the healthy brain. The intricate balance of activity between excitatory and inhibitory populations of neurons is known as excitation-inhibition (E/I) balance and is essential for healthy brain function. When E/I balance is disrupted, this can result in a variety of neurodevelopmental (e.g. autism spectrum disorder) and psychiatric (e.g. schizophrenia) disorders (Gandal *et al.*, 2012).

Most neocortical neurons (70-80%) are excitatory pyramidal neurons, characterised by their pyramidal shape and extensive dendritisation that allows for the reception and integration of inputs from multiple sources. Pyramidal cells primarily release the neurotransmitter glutamate, which facilitates the propagation of signals across synapses and contributes to the overall excitability of a neuronal network (Markram *et al.*, 2004; Mo *et al.*, 2015). Modulation of glutamatergic synapses facilitates synaptic plasticity, including long term potentiation-like (LTP) plasticity, a key mechanism that underpins learning.

The remaining 20-30% of neocortical neurons are interneurons, the vast majority of which are inhibitory cells that release the neurotransmitter gamma-aminobutyric acid (GABA) (Markram *et al.*, 2004; Vithlani, Terunuma and Moss, 2011). Circuits containing interneurons allow for more complex computation than excitatory cells alone by modulating the rate and temporal structure of the network output provided by excitatory neurons (Buzsáki, 2006; Mo *et al.*, 2015). There are many subtypes of inhibitory neurons, but sensorimotor areas are dominated by output-modulating parvalbumin-positive (PV+) interneurons (Kim *et al.*, 2017). PV+ interneurons are known for their fast-spiking capabilities and are integral in synchronizing the spike timing activity of excitatory neurons, thereby contributing to the generation of high frequency oscillations (Kim *et al.*, 2017; Antonoudiou *et al.*, 2020).

1.5 Inhibition and motor learning

Reductions in inhibitory GABAergic signalling appear to be necessary to permit the neuroplastic changes underpinning motor learning to occur (Stagg, Bachtiar and Johansen-Berg, 2011; Bachtiar and Stagg, 2014; Nowak *et al.*, 2017; Bachtiar *et al.*, 2018; Grigoras and Stagg, 2021). For example, cortical LTP-like plasticity has been shown to be blocked in the presence of a GABA agonist (Trepel and Racine, 2000) and rats trained on a novel motor skill showed a significant reduction in the frequency of inhibitory post synaptic potentials, suggestive of decrease in presynaptic GABA release probability (Kida and Mitsushima, 2018). The quantification of GABA in humans is more challenging; however, by using Magnetic Resonance Spectroscopy (MRS), research has shown that the concentration of GABA in M1 decreases during motor learning (Floyer-Lea *et al.*, 2006; Kolasinski *et al.*, 2019). Overall, reductions in GABAergic signalling appear to be a central mechanism for healthy human motor learning.

1.6 Oscillations

A key neurophysiological phenomenon that is ubiquitous across the human brain is its engagement in neuronal oscillatory activity. Oscillations are not an epiphenomenon of neuronal activity, but rather are thought to play a key role in dynamically modulating network connectivity to subserve behaviour. Neuronal oscillations are transient, cooperative, rhythmic patterns of electrical activity generated by the summed synaptic activity of a local neuronal population (Canolty and Knight, 2010). Oscillations are thought to bind neurons into cell assemblies that engage in specific computational functions (Canolty and Knight, 2010; Igarashi *et al.*, 2013).

As populations of neurons rhythmically fire together, they generate group-level electrical activity which can be detected non-invasively through the scalp with magneto/electroencephalography

(M/EEG) and/or invasively using local field potentials. Mammalian cortical neurons have been shown to fire within several oscillatory "bands" that have been clustered into canonical frequency bands (delta ~0.5-4Hz, theta [θ] ~4-8Hz, alpha ~8-12Hz, beta [β] ~12-35Hz, gamma [γ] >35Hz). These different frequency bands are thought to involve different neuronal populations contributing to different type of neuronal computation (Canolty and Knight, 2010).

Oscillations are fundamental to neuronal communication, acting as mechanistic regulators of input (Buzsáki, 2006). They provide temporal coordination of neuronal processes by rhythmically modulating membrane potentials, thus defining time windows during which neuronal spiking must occur to enable communication both within and across brain regions (Buzsáki, 2006; Canolty and Knight, 2010; Onitsuka and Kanba, 2013; Cabral-Calderin and Wilke, 2020). Oscillations mediate neuronal communication such that only coherently oscillating neuronal groups interact efficiently since their communication windows for input/output are open at the same times (Fries, 2005). This is known as the "communication through coherence" hypothesis (CTC). This temporal gating is especially important for distant, but functionally-connected, regions whose communication would otherwise be metabolically expensive (fluctuating the membrane potential is energetically cheaper than keeping it in a constant depolarised state).

1.6.1 Individual frequency bands and their role

This next section will explore two frequency bands used throughout this thesis: γ and θ, their neurophysiological underpinnings, and their role in motor behaviour and learning.

1.6.1.1 Gamma oscillations

The γ frequency is commonly defined as oscillations occurring within 30 to 100Hz, encompassing different γ-frequency sub-bands (slow-, mid-, and fast-γ at 30-60Hz, 60-90Hz, and 90Hz+, respectively) that, in terms of slow- and mid-γ at least, appear to have distinct physiological and behavioural characteristics for motor learning (Zich *et al.*, 2021).

It is well-established that networks containing GABAergic inhibitory interneurons have a prominent role in the generation of γ band activity (White *et al.*, 2000; Whittington and Traub, 2003; Vida, Bartos and Jonas, 2006; Fries, Nikolić and Singer, 2007; Buzsáki and Wang, 2012). The γ cycle starts with an excitatory input to the pyramidal cell. When this cell fires, it activates inhibitory interneurons. The interneurons fire with a slight delay compared to the pyramidal cells because their firing is driven by the pyramidal cells' excitatory input. Activation of these interneurons inhibits the pyramidal cell. This inhibition prevents pyramidal cells from firing during this period. However, as the inhibitory signal from the interneuron fades, a brief window opens where the pyramidal cell can respond to excitatory input again. This window is crucial for the timing of the next round of firing. γ oscillations thus depend on the spiking of inhibitory interneurons which synchronise the firing of excitatory pyramidal cells via fast synaptic inhibition (Traub *et al.*, 1996; Fries, Nikolić and Singer, 2007). In other words, γ oscillations arise as a result of synchronised, inhibitory interactions between populations of excitatory pyramidal cells and local inhibitory GABAergic interneurons (pyramidal-interneuron network γ or PING) (Fries, Nikolić and Singer, 2007; Börgers, 2017).

One of the strongest cases made to date for the importance of cell-specificity in rhythm induction is the role of parvalbumin-positive fast-spiking GABAergic interneurons (PV-FSis) in generating γ oscillations (Cardin *et al.*, 2009). PV-FSis are GABAergic cells that influence the downstream effects on signalling and ultimately change behaviours (Nahar, Delacroix and Nam, 2021). They are present in all layers of cortex, with the exception of layer I, indicating specific cognitive and behavioural functional relevance in the cortex (Nahar, Delacroix and Nam, 2021). PV-FSis

modulate local excitatory pyramidal cell activity by controlling spike timings of neighbouring excitatory glutamatergic pyramidal cells via inhibitory postsynaptic effects (Nahar, Delacroix and Nam, 2021). The membrane properties of PV-FSis favour γ-frequency activity (Pike *et al.*, 2000; Whittington and Traub, 2003) and are seen to generate γ frequency outputs in the neocortex (Whittington and Traub, 2003). Additionally, PV-FSis strongly synapse onto other interneurons, disinhibiting their functioning such that there is decreased synaptic inhibition of excitatory neurons. Together, they are thus able to precisely modulate local pyramidal excitation levels (Nahar, Delacroix and Nam, 2021). These networks of fast-spiking interneurons provide large, synchronous inhibitory post-synaptic potentials to local excitatory neurons generating a narrow window for effective excitation (Cardin *et al.*, 2009). Overall, γ band oscillations are thought to relate to the activity of PV-FSis which, together, form a network that control the spike timing of local excitatory neurons.

The relationship between γ oscillations and GABAergic inhibitory interneuronal networks is also evidence by computational studies. Such studies have found that rhythmic activity within the γ-frequency range is spontaneously detected in a computer simulated random network of interconnected GABAergic fast-spiking interneurons (Wang and Buzsáki, 1996). This suggests that GABAergic synaptic transmission is a neurophysiological mechanism for synchronised γ-frequency oscillatory neuronal activity (Wang and Buzsáki, 1996). Furthermore, only three requirements are needed for γ oscillations to emerge in a network model consisting of only inhibitory interneurons: 1) mutually connected inhibitory interneurons, 2) a time constant provided by GABAa receptors, and 3) sufficient drive to induce spiking in the interneurons (Buzsáki and Wang, 2012). This supports the hypothesis that γ oscillations are driven by inhibitory interneurons, specifically those that act around the time constant provided by GABAa receptors.

The role of γ oscillations in further setting up the necessary neurophysiological environment to promote synaptic plasticity (and thus potentially [motor] learning) is also increasingly recognised (Hazime *et al.*, 2021; Li, Liang and Zhou, 2021). The induction of neuroplasticity across a network as a consequence of learning (or, putatively, re-learning post-stroke) is an activity-dependent process driven by the Hebbian principle of temporal coincidence of pre- and post-synaptic firing (Hebb, 1949). Oscillation of neuronal membrane potential at the γ frequency is beneficial to synaptic potentiation via the synchronisation of neuronal firing within a temporal window that is optimal for spike-timing dependent plasticity processes (Hasenstaub *et al.*, 2005; Hazime *et al.*, 2021; Li, Liang and Zhou, 2021). For example, the γ-cycle-related lifetime of a cell assembly is closely related to the time constant of GABAa and AMPA receptors as well as the membrane time constant of cortical pyramidal cells (Buzsáki and Wang, 2012). In other words, under a γ rhythm of oscillation, the probability of associating relevant information together to assemble a neuronal circuit, increases, thus increasing the probability of a pro-plastic environment (Hazime *et al.*, 2021). Therefore, γ oscillations likely play a key role in neuroplasticity via the modulations of local pyramidal cell excitation within a time constant that is in line with the necessary neurophysiological properties required for neuroplasticity. In support of the role of γ oscillation in plasticity, several studies have demonstrated that the power of γ oscillation is associated with plasticity potential in visual (Galuske, Munk and Singer, 2019), auditory (Van Wassenhove and Nagarajan, 2007), and motor (Aliakbaryhosseinabadi *et al.*, 2021) tasks.

It has classically been difficult to study γ oscillations via neuroimaging in humans with sufficient signal-to-noise ratio to accurately separate out the different frequency

sub-bands. However, new acquisition approaches, such as Optically Pumped Magnetometers (Boto *et al.*, 2018) and analysis techniques (Zich *et al.*, 2020) are beginning to allow us to fully interrogate this activity *in vivo* and associate these to changes in GABAergic signalling and behavioural performance. The importance of separating these distinct processes has been highlighted in a recent MEG study, which demonstrated not only that slow- and mid- γ activity have distinct spatial and temporal patterns, but differentiable physiological bases and behavioural relevance (Zich *et al.*, 2021). A further investigation into the role of slow- versus mid- γ on motor behaviour can be found in Chapter 3. The higher γ frequencies are thought to be involved in higher-levels of motor behaviour including motor learning. Past research has shown that driving 75Hz γ oscillations *in vivo* using brain stimulation led to a reduction in local GABAergic activity, the magnitude of which predicted motor learning on a subject-by-subject basis (Nowak *et al.*, 2017). The promotion of γ-band oscillatory activity thus appears to be a key element in healthy human motor learning as well as related to the role of GABA in motor learning.

Overall, γ-rhythm-related oscillatory dynamics are likely mediated by the effects of fast-spiking, GABAergic interneurons (PV-FSIs). These, in turn, provide the neurophysiological environment in which sensory processing and neuroplasticity can occur. Recent research has also looked at the relationship between γ and GABA *in vivo* and has demonstrated a relationship between distinct γ sub-bands and GABAergic signalling on motor learning. Whilst further studies are required to prove a causal role of γ oscillations in the induction of neuroplastic changes that translate to significant alterations in behavioural performance, this research provides the groundwork upon which future studies can start to interrogate the role of γ oscillations in motor learning.

1.6.1.2 Theta

θ oscillations are a prominent feature of hippocampal activity and play an important role in cognitive function including memory encoding and spatial navigation. Within the hippocampus, θ oscillations are produced by the coordinated activity of pyramidal cells and various types of interneurons, including basket cells and oriens-lacunosum moleculare (OLM) cells. These cells form interconnected networks that contribute to the rhythmic spiking necessary for θ oscillations (Hummos and Nair, 2017). θ oscillations play a key role in modulating synaptic activity thus making them fundamental players in mediating LTP. θ oscillations create optimal conditions for LTP by synchronising the timing of synaptic inputs and postsynaptic depolarisation, thus enhancing synaptic strength (Leung and Law, 2020). It is thus perhaps unsurprising that θ plays a fundamental role in hippocampal-dependent learning such as memory encoding and retrieval (Leung and Law, 2020). Furthermore, θ oscillations are well-suited for connecting widespread networks of neurons due to their ∼100-200ms period that can support longer conduction delays (Colgin and Moser, 2010).

In rodents, motor θ occurs in active periods when engaged in voluntary movements such as walking, running, jumping, bar-pressing, and exploratory sniffing (Karakaş, 2020). However, in humans, θ oscillations appear to play a role in higher level motor behaviour such as sensorimotor integration and motor planning by facilitating the coordination of sensory inputs with motor outputs (Caplan *et al.*, 2003; Karakaş, 2020). This coordination is crucial for tasks that require precise timing and synchronisation (Caplan *et al.*, 2003).

Overall, θ oscillations are thought to be involved in long-distance coordination of neuronal populations across different brain regions to promote multimodal sensory

integration to support cognitive processes such as attention, navigation, and exploratory learning (Caplan *et al.*, 2003; Fries, 2005; Karakaş, 2020).

1.6.1.3 Cross-frequency coupling

Oscillations can occur independently or can naturally couple with another oscillation in a process known as cross-frequency-coupling (CFC). Whether CFC is simply a mechanistic result of the way the brain is connected, or whether it plays a role in neuronal computation is unclear, though recent evidence favours the latter (Sotero, 2015). Recent interest has focused on how frequencies can be coupled and what the functional consequence of such coupling is. Since individual frequency bands are associated with the processing and integration of distinct dimensions of information processing, the integration of multiple frequencies may serve to provide enhanced computational power and opportunities for processing more complex information.

CFC has been hypothesised to play a role in neuronal communication, learning, and computation (Canolty and Knight, 2010). More specifically, a computational advantage of cross frequency coupling between one slow and one fast oscillation is that due to conduction delays, slower frequency oscillations are able to preferentially synchronise networks over long distances (inter-cortical processing) whereas faster frequency oscillations are thought to synchronise activity in local networks (intra-cortical processing) (Fries, 2005; Canolty and Knight, 2010; Sotero, 2015; Johnson *et al.*, 2017). Since fast and slow oscillations play distinct roles in coordinating and integrating information from local and distant brain regions, respectively, CFC is thought to serve as an information transfer mechanism between large-scale networks and fast, local cortical processes required for effective computation and synaptic modification (Canolty and Knight, 2010).

The most common type of CFC is phase-amplitude coupling (PAC) where the phase of one oscillation (typically slower) modulates the amplitude of another (typically faster) oscillation. PAC has been readily observed in rodent hippocampus (Bragin *et al.*, 1995; Buzsáki *et al.*, 2003). In humans, PAC has been observed across multiple cortical and subcortical sites (Mormann *et al.*, 2005; Canolty *et al.*, 2006; Demiralp *et al.*, 2007; Axmacher *et al.*, 2010) and appears to be related to behaviour. For example, the strength of PAC differs across brain areas in a task-relevant manner, changes quickly in response to sensory, motor, and cognitive elements, and correlates with performance in learning tasks (Canolty and Knight, 2010). In early training tasks, both PAC strength and task performance are low and PAC strength appears to be the most predictive neurophysiological marker of learning (Canolty and Knight, 2010). Therefore, PAC plays a central role in neuronal computation subserving behaviour and warrants further investigation. Across a wide range of phase and amplitude frequency pairs, the PAC between θ and γ is strongest (Canolty and Knight, 2010). In this thesis, I exclusively investigate PAC between θ (6Hz) and γ (45Hz and/or 75Hz).

1.6.1.4 θγ phase amplitude coupling

A prominent feature of hippocampal θ rhythm is its cooccurrence with faster γ oscillations (Lopes-dos-Santos *et al.*, 2018). In hippocampal CA1, γ oscillations occurring at different frequencies (slow [~30-50Hz], mid [~50-100Hz)] and fast [~100-140Hz]) appear at distinct phases of the θ cycle, supporting distinct network operations with different contributions to memory processes such as encoding and retrieval (Lisman and Jensen, 2013; Lopes-dos-Santos *et al.*, 2018). As such, hippocampal θγ PAC is typically thought of as a *neuronal signature of learning*.

Hippocampal γ rhythms are thought to temporally link the activity of pyramidal neurons to promote coordinated firing during memory processes (Colgin and Moser,

2010; Bott *et al.*, 2016). Due to their high frequency, γ oscillations are well-suited for the rapid coordination of neuronal activity, which is essential in hippocampal processes. These processes include quickly selecting inputs, organizing neurons into functional groups, retrieving memories needed for performing learned tasks, and determining which aspects of an experience will be retained for future recall (Colgin and Moser, 2010). Together with the temporal coordination provided by the θ envelope, θγ PAC plays a key role in mediating learning and memory (Canolty and Knight, 2010; Lisman and Jensen, 2013).

A recent rat study demonstrated, using local field potentials (LFPs), that the coupling strength between θ and high γ (60-90Hz) in rat hippocampus increased during rule-guided behaviour compared to a no rule condition (Nakazono, Takahashi and Sakurai, 2019). Intriguingly, this change in CFC strength was not seen for θ and low γ (30-60Hz) alone. These findings highlight the importance of such CFC between θ and γ bands during rule learning and further highlights the fact that high- and low-γ bands likely play different roles in learning. Similarly, (Bott *et al.*, 2016) found that θγ coupling in the hippocampal dentate gyrus is modulated during spatial reference memory tasks, suggesting that this coupling mechanism is critical for encoding and retrieval of spatial information.

In humans, θγ coupling has also been shown to support episodic memory processes. A cohort of recent studies recorded LFPs directly from the hippocampus of patients with epilepsy and found similar results. The first found that γ amplitude is coupled to opposed hippocampal θ-phase states during the encoding and retrieval of episodic memories, with the degree of phase opposition correlating with memory performance (Saint Amour Di Chanaz *et al.*, 2023). The second found that increased θγ coupling was associated with improved task performance (Vivekananda *et al.*, 2021).

Beyond a role in hippocampal-dependent learning, research is interested in whether the oscillatory code of hippocampal θγ coupling (which mediates hippocampal-dependent learning) can be extrapolated to cortical θγ coupling and serve non-hippocampal dependent learning, such as motor learning. In other words, is the θγ oscillation code a signature of learning across the brain? Until recently, it was unclear whether θγ coupling existed outside of the hippocampal-cortical memory axis, whether θ oscillations had any role in motor ensemble coding, and whether θγ oscillations coordinate unit spiking during motor behaviour.

The pattern of θγ PAC in human neocortex is consistent with the θγ PAC observed in rodent hippocampus and has been suggested to potentially have similar cellular and network origins, despite the relative complexity of the neocortical layers (Grillner *et al.*, 2005; Canolty and Knight, 2010). Furthermore, both hippocampal-based spatial exploration and neocortical-based motor behaviour both require the ability to store, recall, and process sequence information (Igarashi *et al.*, 2013). Therefore, it is plausible that the hippocampal θγ oscillations that serve hippocampal-dependent learning may be extrapolated to non-hippocampal dependent learning in the cortex.

Regarding the role of θγ oscillations in motor cortical activity, a seminal study by Igarashi *et al.* (2013) recorded neuronal spiking and LFP activity from rat motor cortex during reward-motivated movement. They found behavioural, state-dependent coordination of θγ oscillations during distinct movement states. The authors conclude that θγ oscillations aid in the selection of appropriate microcircuits for information transmission driving motor planning and output during animal movement (Igarashi *et al.*, 2013). This adds to the growing evidence that θγ coupling is a conserved oscillation code across the brain to support various behaviours (Canolty and Knight,

2010; Igarashi *et al.*, 2013). In humans, a key study that forms the basis of many questions in this thesis, found that driving θγ PAC (75Hz/6Hz) in human M1 resulted in a 26% acceleration gain in a low-level motor ballistic thumb abduction task, theorised to occur via the temporal structure the θγ oscillations created for neuronal excitability (Akkad *et al.*, 2021). Therefore, θγ oscillations may play a role in motor behaviour.

Overall, θγ PAC is crucial for hippocampal-dependent learning (Buzsáki, 2002; Bott *et al.*, 2016; Nakazono, Takahashi and Sakurai, 2019; Saint Amour Di Chanaz *et al.*, 2023) as θ oscillations form a temporal structure that organises γ-encoded units into preferred phases of the θ cycle, allowing specific processing and transmission of neuronal computations. θγ oscillations in rodent motor cortex (particularly in layer V) play a crucial role in facilitating the temporal coordination of neuronal firing to execute precise motor behaviours (Igarashi *et al.*, 2013; Johnson *et al.*, 2017). There is now increasing evidence that θγ oscillations exist in human (motor) cortex and modulate behaviour (Igarashi *et al.*, 2013; Akkad *et al.*, 2021). However, whether driving these oscillations in motor cortex reliably influences behaviour (Chapter 3), local neurophysiology (Chapter 4), and sensorimotor network connectivity (Chapter 5) remains to be investigated systematically.

To test the hypothesis that θγ oscillations play a functional role in modulating motor behaviour through changes in local and network-level functional connectivity, I needed a technique that was going to entrain neuronal oscillations to a specific frequency.

1.7 Transcranial Alternating Current Stimulation

Non-invasive brain stimulation (NIBS) has recently attracted the attention of neuroscientific and rehabilitation research and is increasingly gaining traction as a significant, non-invasive, adjuvant to physical therapy for post-stroke motor recovery. However, prior to implementing such interventions in clinical populations, there is a fundamental requirement to understand the effects these NIBS protocols have on local motor cortical neurophysiology and whether these neurophysiological/neurochemical changes are functionally-relevant to (motor) networks. The non-invasive modulation of various motor-related areas (and the downstream effects on the motor network within which they reside) have been investigated as potential targets for the improvement of novel skill acquisition using NIBS. Such motor-related areas include M1.

One key NIBS neuromodulation technique is transcranial electrical stimulation (tES). Under the umbrella term of tES lie three main techniques including transcranial direct current stimulation (tDCS), transcranial alternating current stimulation (tACS), and transcranial random noise stimulation (tRNS). In this thesis, tACS is used as the principal non-invasive neuromodulatory technique across the three experimental Chapters.

1.7.1 Introduction to tACS

It has been argued that if any given oscillation is essential for a cognitive, motor, sensory function, then modulating this oscillation should selectively interfere with its associated function. This is the basis of tACS research: modulating the spatiotemporal dynamics of endogenous neuronal oscillations and establishing their causal functional relationships to behaviour (Schmidt *et al.*, 2014; Vogeti, Boetzel and Herrmann, 2022). tACS involves the delivery of a small, external sinusoidal current to the scalp through rubber electrodes, at a specific frequency with alternating windows of excitation and inhibition, to selectively modulate local endogenous oscillations (Weinrich *et al.*, 2017). tACS is a sub-threshold neuromodulatory technique such that is does not induce any action potentials. Instead, tACS is thought to modulate local membrane potentials and change the likelihood of action potential generation (Huang *et al.*, 2021; Pozdniakov *et al.*, 2021; Vogeti, Boetzel and Herrmann, 2022).

The maximum current intensity induced in a region of interest with tACS depends on the electrode size and montage. A large proportion of current is shunted by the scalp such that only a small amount of the externally applied current ever reaches the cortex (Holdefer, Sadleir and Russell, 2006; Miranda, Lomarev and Hallett, 2006). Therefore, the intensity of current has to be sufficient to reach the cortical area of interest whilst remaining pain-free for the participant. Studies have shown that simulated tES montages using head models that account for conductance of skin, skull, bone, and CSF find that a threshold of 0.2V/m in the target area is sufficient to modulate neuronal activity using tACS (Reato *et al.*, 2010; Antal and Herrmann, 2016). A recent study measuring electric potentials intracranially in epilepsy patients showed that when stimulating with 2mA, cortical electric field reached up to 0.8V/m (Huang *et al.*, 2017). Therefore, 2mA tACS induces electric fields in cortical regions of sufficient intensity to modulate neuronal activity.

1.7.2 Mechanisms of tACS: Entrainment versus plasticity

The precise neurophysiological mechanisms by which tACS modulates endogenous oscillations remains under contention. There are currently two major hypotheses regarding the mechanisms of tACS: entrainment and spike timing dependent plasticity (STDP).

1.7.2.1 Entrainment

During one half of a tACS oscillation, one tES electrode acts as an anode and the other as a cathode. During the second half of the tACS, the pattern reverses and the former anode now acts as a cathode and vice versa (Antal and Herrmann, 2016). It has therefore been suggested that, on average, the membrane potential is likely not affected and tACS thus does not enhance of decrease the excitability of cortex, as is the case with tDCS overall. However, the brief depolarising and hyperpolarising phases of each half cycle may, instead, be strong enough to induce online effects via entrainment (Antal and Herrmann, 2016). Entrainment is defined as the temporal alignment (i.e. synchronisation) of endogenous oscillations to an exogenously applied alternating current (Pozdniakov *et al.*, 2021). In other words, tACS has been proposed to cause shifts in frequency and phase of neuronal spike timing (Thiele *et al.*, 2021). If tACS entrains endogenous oscillations to a known (exogenously applied) frequency, we can begin to investigate the causal role of specific frequencies in mediating particular behaviours, such a motor behaviour (Thiele *et al.*, 2021).

The ability of an exogenously applied oscillation to successfully entrain an endogenous oscillation is dependent on the exogenous oscillation frequency being at or close to the relevant endogenous frequency of the targeted neuronal network (Weinrich *et al.*, 2017; Lazzaro *et al.*, 2022; Vogeti, Boetzel and Herrmann, 2022). In the context of this thesis, the endogenous oscillators are motor cortical oscillations, and the external oscillator is tACS. Indeed, tACS with matched frequency has been shown to be most effective at entraining a network at the lowest amplitude (Ali, Sellers and Frohlich, 2013). This relationship between frequency and intensity is given by the Arnold Tongue model which posits that regions of high-synchrony between tACS and endogenous brain rhythms follow an upside-down triangular shape such that if the stimulation intensity is very low, the frequency of the endogenous oscillator and the applied frequency of the external driving force must be close to each other to achieve entrainment (Vogeti, Boetzel and Herrmann, 2022) (see Figure 1).

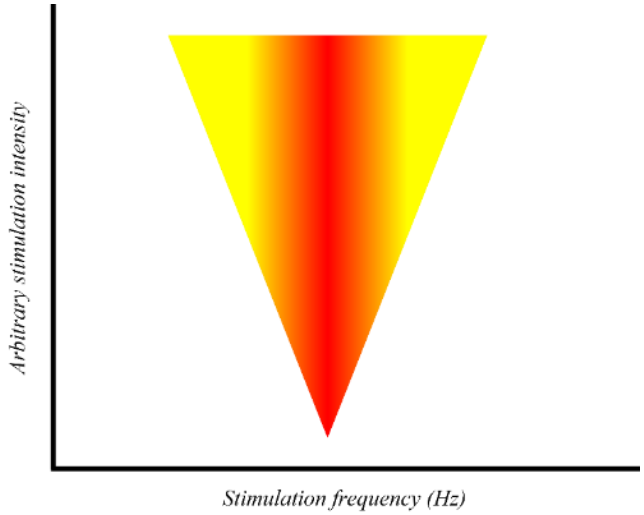

Figure 1 - Schematic representation of the Arnold Tongue Theory of Entrainment.

The only way to objectively assess the degree of entrainment is via invasive techniques such as LFP/spiking activities in animal models or with computational models. Animal studies often use ferrets due to their gyrencephalic brains, like humans, such that the distribution of electric field is nonuniform across neurons and thus more closely mimics the pattern of distribution in the human brain. Ali, Sellers and Frohlich (2013) performed electrophysiological measurements of multiunit activity (MUA) action potential firing in ferrets and found that tACS increased the rhythmic structure of the MUA firing. They found a pronounced increase in rhythmic power at the stimulation frequency with no pronounced outlasting effect after stimulation ended (Ali, Sellers and Frohlich, 2013). Likewise, a recent study also applied tACS and measured activity from the posterior parietal cortex of awake ferrets at several frequencies and intensities, including the individualised alpha frequency (Huang *et al.*, 2021). They found that matching the endogenous frequency with the stimulation frequency produced phase-locking of neuronal spikes, even at low stimulation intensities, in line with the Arnold Tongue theory (Huang *et al.*, 2021). These animal studies tell us that tACS can entrain a system to a specific frequency, in accordance with the Arnold Tongue, and that these entrainment effects do not outlast the stimulation period.

Providing evidence of entrainment during tACS in humans is more challenging because concurrent tACS-M/EEG data are significantly contaminated by the tACS oscillation artifact. Filtering out the tACS oscillation whilst keeping the endogenous oscillation is an ongoing engineering challenge. However, new analysis approaches are making this increasingly possible (Helfrich *et al.*, 2014). Much human tACS work bypasses this issue by looking at online behavioural effects and/or offline neurophysiological aftereffects. For example, there is a myriad of studies looking at the behavioural aftereffects of tACS on memory (Aktürk *et al.*, 2022), visual perception (Kar and Krekelberg, 2014), auditory activity (Wang *et al.*, 2023) and other sensory domains. In the motor domain, the aftereffects of tACS on motor behaviour are poorly replicated but do appear to be frequency-dependent. For example, a recent study found that 20Hz β-tACS increased MEP size during online application but did not produce significant offline effects (Pozdniakov *et al.*, 2021). In the γ band, a study by Nowak *et al*. (2017) found that driving γ oscillations using tACS resulted in significant, duration-dependent decreases in local resting-state GABAa inhibition, the magnitude of which correlated with subsequent behavioural performance, such that subjects who had greater increases in GABAa inhibition also

showed faster short-term learning (Nowak *et al.*, 2017). In a later study, Bologna *et al.* (2019) found that whilst β-tACS delivered during training inhibited the acquisition of the motor skill, γ-tACS improved the acceleration of the practiced movement during training but reduced motor retention. These results highlight the entrainment potential of tACS on neuronal oscillations serving behaviour.

Overall, there is increasing evidence from computational, animal, and human studies that the effects of tACS are mediated via entrainment. However, there is literature highlighting offline effects of tACS for up to 60 minutes post-stimulation (Wischnewski *et al.*, 2019; Akkad *et al.*, 2021). By definition, entrainment itself cannot outlast the stimulation period (Vosskuhl, Strüber and Herrmann, 2018; Vogeti, Boetzel and Herrmann, 2022). Therefore, research detecting post-stimulation effects suggests that tACS may act within a model of neuronal plasticity as opposed to entrainment (Thiele *et al.*, 2021).

1.7.2.2 Spike Timing Dependent Plasticity

STDP refers to neuroplastic changes that occur based on the order and timing of pre- and post-synaptic spikes (Song, Miller and Abbott, 2000; Feldman, 2012). STDP, as a theory, is often used in models of circuit-level plasticity and learning (Feldman, 2012). STDP is based on the Hebbian principle of plasticity which proposes that when one cell (e.g. cell A) reliably contributes to the spiking of another cell (e.g. cell B), the functional strength of the synapse from cell A to B is increased (Hebb, 1949). STDP was initially examined in cell cultures and brain slices demonstrating that the order of pre- versus post-cellular events and associated cellular spikes determines the induction of LTP or LTD (Vogeti, Boetzel and Herrmann, 2022). When pre-synaptic spikes occur prior to post-synaptic spikes this gives rise to LTP-like plasticity and when the opposite is seen, it induces LTD-like plasticity, at least in slice preparations (Vogeti, Boetzel and Herrmann, 2022).

Unlike the entrainment hypothesis, the STDP theory suggests that the exogenous oscillation does not interfere with ongoing oscillatory activity, but rather targets the membrane excitability of a neuron, making it more or less likely to fire (Antal and Paulus, 2013). The temporary modification of a synapse after being exposed to a rapidly alternating current may alter local biochemical mechanisms and induce neuroplastic changes (Antal and Paulus, 2013). tACS is thought to induce STDP by modulating the timing of neuronal firing. This mechanism can result in lasting changes in neuronal connectivity and function, persisting beyond the stimulation period (Vossen, Gross and Thut, 2015; Wischnewski *et al.*, 2019; Vogeti, Boetzel and Herrmann, 2022).

There is some evidence for the role of STDP without entrainment in underpinning the effects of tACS. Vossen, Gross and Thut (2015) applied different combinations of short (3 seconds) and long (8 seconds) bursts of individual alpha frequency tACS that was either in- or out- of phase (synchronous versus asynchronous). Changing the phase between stimulation trains is thought to disrupt entrainment but not STDP because changing the phase angle does not change the stimulation frequency (Vossen, Gross and Thut, 2015). They found significant increases in alpha power after the long bursts compared to short bursts, regardless of the phase. This effect has been replicated in computational studies demonstrating stimulation-outlasting connectivity changes between in- and anti-phase tACS (Schwab, König and Engel, 2021). Together, these results suggest that tACS may mediate more global neuroplastic changes as opposed to changes in local oscillatory dynamics.

Overall, online effects of tACS are typically attributed to entrainment. However, offline aftereffects observed in tACS studies point toward evidence for both entrainment and STDP. It remains unclear whether either mechanism alone can explain tACS' effects or whether a combined account is necessary (Vogeti, Boetzel and Herrmann, 2022). It is likely that a combination of entrainment and plasticity is necessary such that successful entrainment during stimulation might be a necessary requirement for the generation of synaptic plasticity (Vosskuhl, Strüber and Herrmann, 2018).

1.7.3 Driving θγ oscillations using tACS

Given the role of θγ oscillations in motor learning (Akkad *et al.*, 2021) and the wealth of evidence outlined regarding the role of γ and θγ is modulating local GABAergic signalling, I wanted to systematically explore the functional relevance of these oscillations. In this thesis, I used tACS as the primary neuromodulatory method, operating under the entrainment assumption. The work in the experimental Chapters investigates the effects of driving motor cortical θγ oscillations in healthy humans on behaviour, local neurophysiology (specifically GABAergic signalling), and global sensorimotor network functional network connectivity.

1.8 Aims of this thesis

Stroke is a leading cause of adult disability worldwide with significant socioeconomic impact. Research is interested in the development of NIBS interventions that can be used alongside physical therapy to boost, or even potentially accelerate, the rehabilitative process. The reacquisition of a motor skill post-stroke has been likened to the acquisition of a novel skill in the healthy brain and are likely served by similar neurophysiological mechanisms. As such, I used motor learning as a framework for post-stroke motor recovery. θγ oscillations have been shown to play a key role in hippocampal-dependent learning and a recent study demonstrated that artificially driving these oscillations using tACS can improve motor behaviour (Akkad *et al.*, 2021). However, there is a lack of understanding around why θγ oscillations (specifically 75Hz γ oscillations phase amplitude coupled to the positive half of a 6Hz θ wave) can modulate motor behaviour. This thesis took a systematic approach to unveiling the potential functional relevance of θγ oscillations and their associated neurophysiological mechanisms that mediate their effects on healthy human motor behaviour. Using a variety of methods (see Chapter 2: Methods), I explored the effects of θγ oscillations on behaviour (Chapter 3: Behavioural study), local receptor-mediated inhibition and excitation in M1 (Chapter 4: TMS), and sensorimotor network functional connectivity (Chapter 5: Neuroimaging). Together, the findings from this thesis provide an insight into the potential mechanisms that mediate the effects of θγ oscillations in healthy human motor behaviour.

CHAPTER II - Methods and Materials

In this chapter, I outline the methods used throughout this thesis to investigate the role of motor cortical θγ oscillations on healthy human motor skill acquisition. I first outline the neuromodulation technique adopted throughout the thesis: transcranial alternating current stimulation (tACS). I then outline the novel behavioural tasks I developed. I then explain how I investigated changes in corticospinal excitability and receptor-mediated inhibition and excitation before, during, and after tACS using transcranial magnetic stimulation (TMS). Finally, I describe how I used functional Magnetic Resonance Imaging (fMRI) to investigate functional connectivity across the sensorimotor network, before, during, and after tACS.

2.1 Neuromodulation: Transcranial Alternating Current Stimulation

The ability to non-invasively modulate neuronal activity in humans holds the potential to revolutionise clinical care for a variety of neurological conditions including stroke. In this thesis, tACS is used as the principal non-invasive neuromodulatory technique across the three experimental Chapters.

2.1.1 tACS in M1

This thesis focussed on the functional role of θγ oscillations and used tACS as the neuromodulatory technique to assess the effect of these oscillations on behaviour, GABAergic signalling, and sensorimotor functional network connectivity.

M1 is a key node in the wider sensorimotor network and thus by modulating activity in M1 it is thought that we are also able to yield network-wide level changes. This hypothesis is explored in more detail in Chapter 5 (Neuroimaging). M1 lies anterior to, and on the anterior bank of, the central sulcus. Due to its non-invasive nature, tACS is only able to successfully modulate neuronal activity in the superficial areas of the cortex. Fortunately, M1 is a good target for neuromodulation due to its role in behaviour and anatomy relative to the skull.

In current literature, a number of tACS montages exist that have been used to target M1, including "conventional" tES with two square/rectangular electrodes, one typically centred over M1 (C3; 10/20 International EEG electrode location) and one over a supraorbital frontal region (e.g. FP2) (Van Hoornweder *et al.*, 2022) or on the shoulder (Miyaguchi *et al.*, 2019), or various higher density tES involving multiple smaller electrodes centred around M1 (Ghafoor, Yang and Hong, 2022; Van Hoornweder *et al.*, 2022), or a small central electrode over M1 with an outer ring electrode (Van Hoornweder *et al.*, 2022). Current flow modelling, which has been validated against intracranial recordings (Liu *et al.*, 2018), has allowed us to model a variety of different montages to assess which one generates the largest electric field peak in a region of interest. One such current flow model-validated montage is the standard C3-Pz montage (Akkad *et al.*, 2021). I thus decided to adopt this montage for all experiments in this thesis to induce peak e-fields in M1 (see Figure 2).

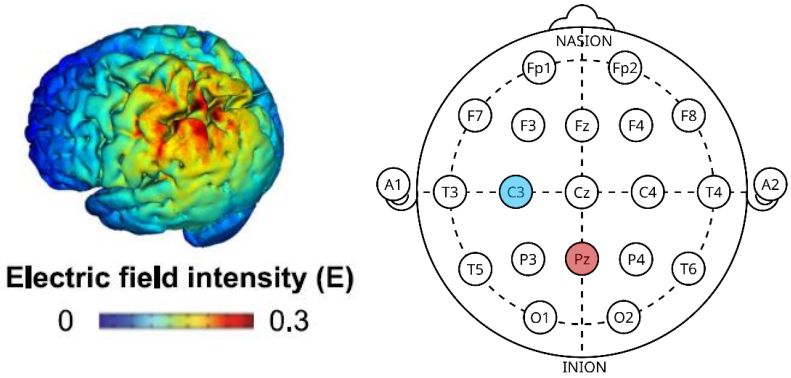

Figure 2: Electrode montage. Left: Current flow model of C3-Pz tES electrode montage placed to maximize electric field intensity in M1 (Akkad et al., 2021). Right: One electrode was centred over M1 (red, C3) and the other over the parietal vertex (blue, C4).

2.1.2 tACS waveforms used in this thesis

I used a cross-frequency phase-amplitude coupled (PAC) waveform of θ and γ, where the amplitude of a γ rhythm (45Hz or 75Hz) was modulated by the phase and amplitude of a θ rhythm (6Hz). These custom-coded waveforms mimicked the γ power distribution over the θ cycles that happens endogenously. Depending on whether the γ activity was coupled to the positive or negative half of the θ envelope, resulted in θγ-peak (TGP) or θγ-trough (TGT), respectively. Throughout this thesis, I delivered a combination of different θγ PAC tACS waveforms to understand which neurophysiological mechanisms (e.g. phase versus frequency) mediate its effects.

2.1.2.1 Phase: TGP versus TGT

Recent evidence points to TGP affecting behavioural performance differently compared to TGT (Akkad *et al.*, 2021). Whether this is because TGP and TGT engage different neurophysiological mechanisms or engage the same circuit in different ways remains to be demonstrated. In Chapter 4, I explored the changes in cortical excitability, GABAergic, and glutamatergic signalling that occur during and after 75Hz TGP versus 75Hz TGT (see Figure 3) using Transcranial Magnetic Stimulation (TMS; see section 2.3) to further elucidate the findings of Akkad *et al*. (2021).

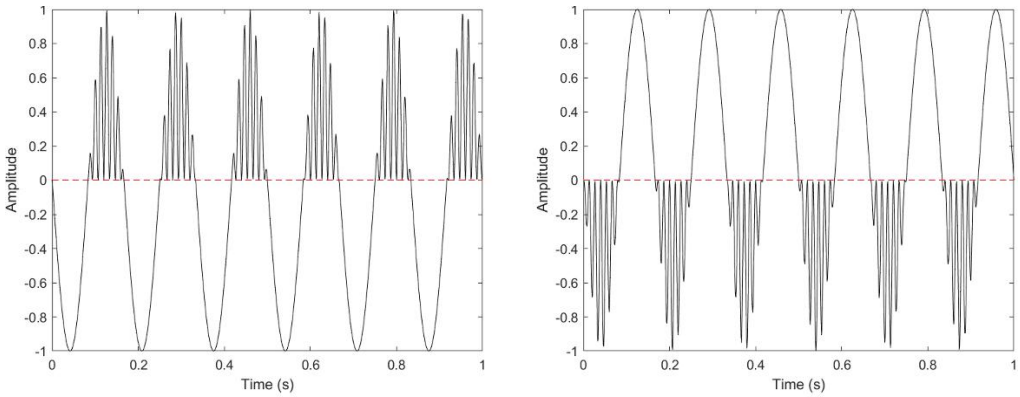

Figure 3: Schematic of 75Hz/6Hz θγ peak phase amplitude coupling (left) and 75Hz/6Hz θγ trough phase amplitude (right) as used in Chapter 4 (Neurophysiology study).

2.1.2.2 Frequency: 45Hz γ versus 75Hz γ

Following the finding that TGP improves motor learning compared to TGT (Akkad *et al.*, 2021), I then investigated whether this effect was specific to 75Hz. In Chapter 3, I investigated the causal effect of two γ frequencies (fast: 75Hz and mid: 45Hz) in a TGP waveform on changes in behaviour using a novel behavioural motor learning task.

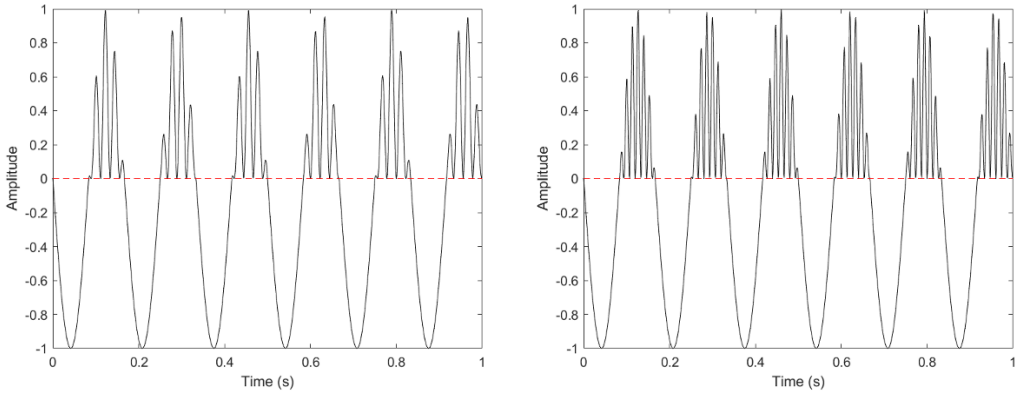

Figure 4: Schematic 45Hz/6Hz θγ peak phase amplitude coupling (left) and 75Hz/6Hz θγ peak phase amplitude coupling (right) as used in the behavioural study (Chapter 1).

2.2 Novel behavioural motor learning tasks

For the purposes of this thesis, I defined motor learning as a change in a pre-existing motor behaviour (e.g. force modulation) that persisted for a period of time, that led to an improvement in a behaviour that had not been trained before. An abundance of validated motor learning task exist such as serial reaction time tasks (Robertson, 2007), action selection tasks (Stewart, Tran and Cramer, 2014), and visuomotor adaptation tasks (Taylor, Krakauer and Ivry, 2014). Whilst the use of lab-based motor tasks can threaten generalisability to real-world motor learning, these tasks provide foundational insights into the components of learning that are likely necessary to account for how more complex skills are acquired (Krakauer *et al.*, 2019; Ranganathan, Lee and Krishnan, 2022). However, these validated tasks also often include higher level frontal and cognitive circuitries. Since the aim of this thesis was to understand how θγ oscillations interact uniquely with sensorimotor circuitry, I needed a task that engaged as little as possible other, extraneous, circuits. Force modulation tasks were a good candidate to this end since force is uniquely reliant on M1 local circuitry (i.e. force; Ashe, 1997). The two novel behavioural tasks in this thesis are thus inspired by force modulations tasks such as in (Steel *et al.*, 2016). In both tasks, the participant was required to learn how to map existing force schemas onto the task movement requirements to perform optimally (hitting targets or continuous tracking). The motor "learning" aspect thus came from adapting existing motor schemas for a specific function and for a specific amount of time.

2.2.1 Novel behavioural motor learning task 1 (Chapter 3)

In Chapter 3, I developed, piloted, and tested a novel motor learning task. This task was developed following the findings of a recent θγ stimulation optogenetic mouse study Sala-Bayo *et al.* (unpublished data). In this study, mice were trained to press a lever three consecutive times to obtain a reward. Mice had a set time window with both an upper- and lower- time limit to complete the lever presses (between 0.5-2.0 seconds). In this experiment, mice receiving active TGP stimulation were significantly more able to modulate and refine their newly learnt behaviour, compared to the control mice. Indeed, the control mice demonstrated continued increased speed at which the lever presses were performed, with a disregard for the time window (Figure 5). These results were argued to suggest that θγ stimulation allows "refinement" of a newly acquired skill. As such, in Chapter 3, I developed a behavioural task that captured a similar pattern of motor learning (three presses in quick succession that must follow a specific temporal pattern) with an initial steep "acquisition" phase followed by "refinement" in an attempt to replicate this finding in humans.

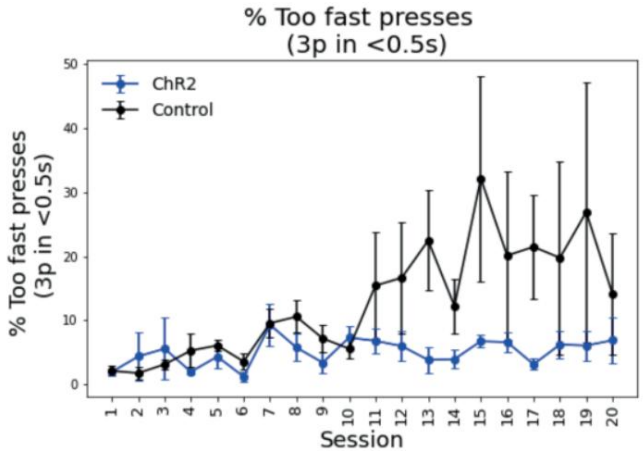

Figure 5: Mouse optogenetic results from unpublished data in our group showing the percentage of "too fast" presses (i.e. three lever presses in <0.5s) in mice receiving active "θγ tACS"(ChR2 genetically modified) and control mice.

A novel pinch force modulation motor learning task was developed for Chapter 3 (Behavioural). Briefly, participants used a pinchmeter held between their right index finger and thumb to trace a three-peak sinusoidal wave using smooth and small modulations in force (see Figure 6 and 7). A more detailed explanation of the pinch force modulation task can be found in Chapter 3 (section 3.2.2.3 *Behavioural task*). Behavioural metrics extracted from the behavioural task included **number of targets hit** and **tracing error**.

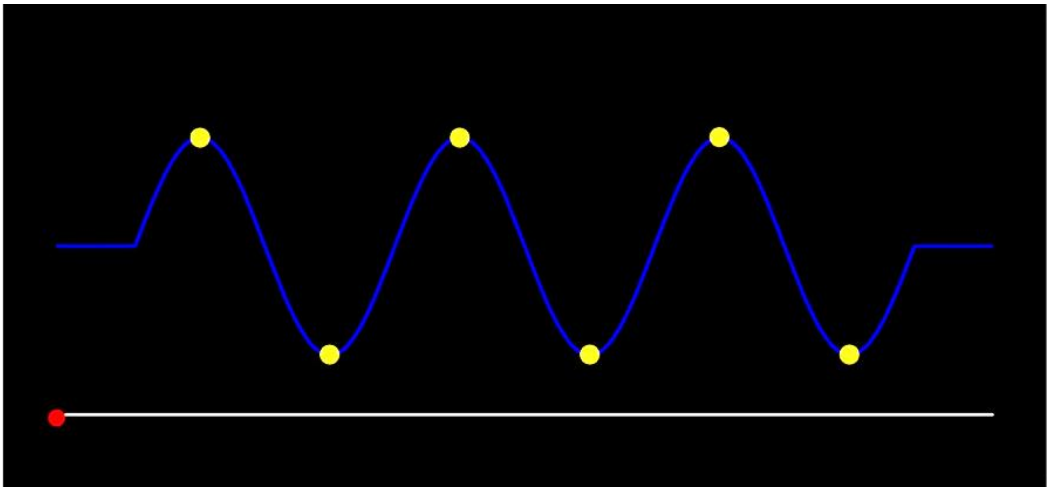

Figure 6: The behavioural task used in Chapter 3.

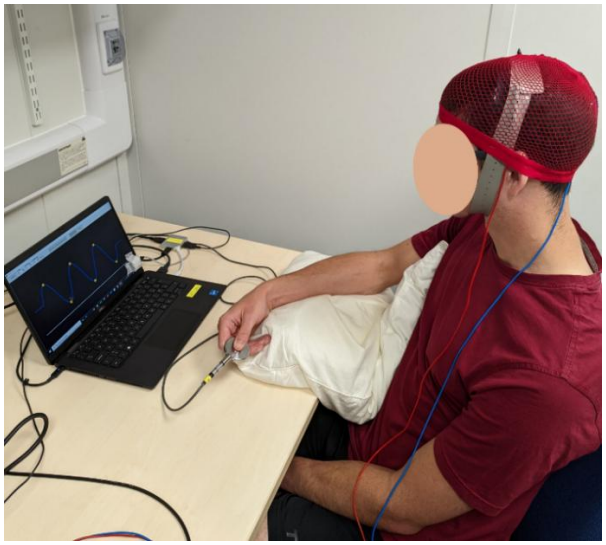

Figure 7: Example set up for the behavioural task in Chapter 3.

2.2.2 Novel behavioural motor learning task 2 (Chapter 5)

In Chapter 5, I developed, piloted, and tested a second novel motor learning task. The force modulation task that was developed for Chapter 3 was not suitable for use in an MRI study for two reasons. Firstly, each trial lasted three seconds which, for a functional MR study, is an insufficient amount of time to detect any BOLD/spectral changes. I considered increasing the duration of each trial but esteemed that the task was not challenging enough to elicit the anticipated motor learning effects. Additionally, the task in Chapter 3 was a pinching task. For an MRI study, this task would likely not produce sufficient signal to noise data for reliable quantification of functional connectivity changes and changes in GABA concentration, as the proportion of involved motor cortex is likely low. I therefore decided to adapt an existing, validated (Steel *et al.*, 2016), whole hand, grip force modulation task that would activate a wider spread of motor cortical neurons, thus increasing signal-to-noise ratio.

A custom-coded grip force modulation task was created using MATLAB (MathWorks, version 2022b). The task was translated and adapted from a previously validated task written in Python (Steel *et al.*, 2016). Participants were presented with a "target" (yellow vertical line) that moved smoothly along the X-axis of a 14" screen inside the MRI scanner (see Figure 8). Participants controlled a horizontally moving blue bar of the same width as the yellow target. A hand-held Fibre Optic Grip Force transducer (Current Designs, Inc., Philadelphia, PA) was held in their right hand to convert mechanical load into an electrical output signal that controlled the blue bar (see Figure 8). The task was coded such that the greater the amount of grip force applied, the greater the linear horizontal rightward movement of the blue bar. The aim of the task was to continuously track the yellow target by modulating grip force. The task was calibrated to each participant's 20% maximum voluntary contraction (MVC), such that maximum distance on the screen (right edge) was reached when applying 20% MVC. This was to ensure participants were not too fatigued and could perform the task continuously for 20 minutes.

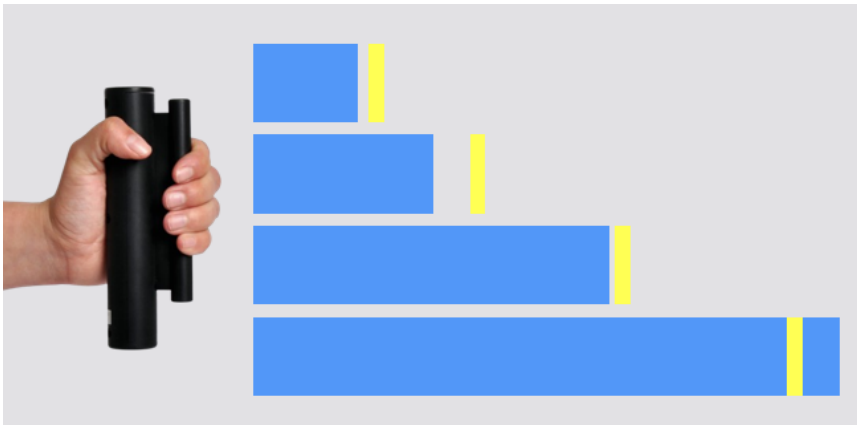

Figure 8: Experimental set up. Left: Grip force transducer. Right: Example of the grip-force modulation task. The yellow bar was a moving target which participants tracked with the blue bar using force.

The task consisted of six 17-trial runs. Each trial lasted for 14 seconds, during which the target moved horizontally in a sinusoidal manner. For runs **1** and **6**, the target motion was random and varied from trial to trial. For runs **2-5**, the target moved according to a predetermined sequence that was identical across trials (motor learning sequence). A schematic representation of the target output force required for one trial in each run can be found in Figure 9.

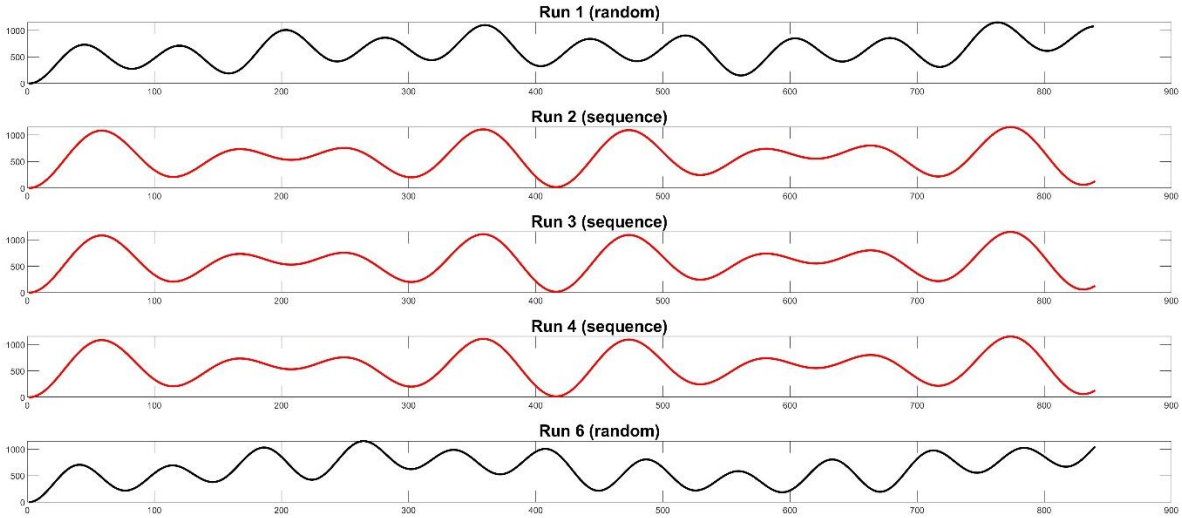

Figure 9: Schematic representation of the target output force required for one trial in each run. Runs 1 and 6 (black) were random sequences. Runs 2-5 (red) were a set force sequence to induce motor grip-force sequence learning.

2.3 Transcranial Magnetic Stimulation (Chapter 4)

Beyond assessing the effect of θγ oscillations on motor learning behaviour (Chapter 3 and 5), I also investigated their underlying neurophysiological mechanisms. One way of interrogating neurophysiology non-invasively in humans is with Transcranial Magnetic Stimulation (TMS).

2.3.1 Introduction to TMS

TMS is an in-vivo neurostimulation and neuromodulation technique based on the principles of electromagnetic induction of an electric field in the brain that is of sufficient magnitude and density to depolarise local neurons. If the current is large enough, and if the neurons are appropriately oriented in relation to the direction of the induced current (TMS preferentially activates neurons oriented horizontally and parallel to the coil at the brain surface), this results in neuronal depolarisation and neuronal firing of pyramidal cells in M1 (Zewdie and Kirton, 2016). In humans, TMS activates the cortex at a depth of 0.9-3.4 cm (Deng, Lisanby and Peterchev, 2013).

These neurons ultimately connect to the motor output pathways including the corticospinal tract (CST). The CST is the main descending motor pathway from the cerebral cortex to the spinal cord, and can be activated by TMS applied to M1 (Zewdie and Kirton, 2016). The CST originates from larger pyramidal cells located mainly in layer V of the cerebral cortex (Zewdie and Kirton, 2016). Axons of pyramidal cortical M1 neurons synapse onto motoneurons in the spinal cord, extending motor communication through to the peripheral muscles in the contralateral limb. When TMS is applied over M1, it induces a series of descending volleys in the CST and induces muscle contraction. This summed muscle contraction can be measured non-invasively using surface electromyography (EMG). When a muscle activated due to a TMS pulse, the EMG trace has a characteristic appearance and is known as a motor-evoked potential (MEP; see Figure 10). MEP latency and amplitude (as measured from peak-to-peak) primarily reflect the functional integrity of the CST and the number and excitability of activated corticospinal motor neurons (Cuypers and Marsman, 2021).

In Chapter 4 (TMS), I collected EMG data from the first dorsal interosseous (FDI) muscle of the right (dominant) hand. Although the target muscle varies between TMS studies, I chose the FDI for multiple reasons. Firstly, the FDI is easily accessible by EMG, and is the only muscle that abducts the index finger giving me spatial selectivity. Secondly, the FDI has a relatively large M1 representation and a relatively small motor unit-to-muscle fibre innervation ratio, making it an ideal candidate for TMS (Palmer and Ashby, 1992; Yao *et al.*, 2018). Finally, distal muscles are more sensitive to TMS than proximal muscles, meaning a lower TMS stimulator intensity is required, making it more comfortable for the participant (Yuasa *et al.*, 2022). In Chapter 4, I used a CE marked Magstim Bistim TMS unit with a standard figure-of-eight 70mm coil delivering monophasic pulses (Magstim Company Ltd).

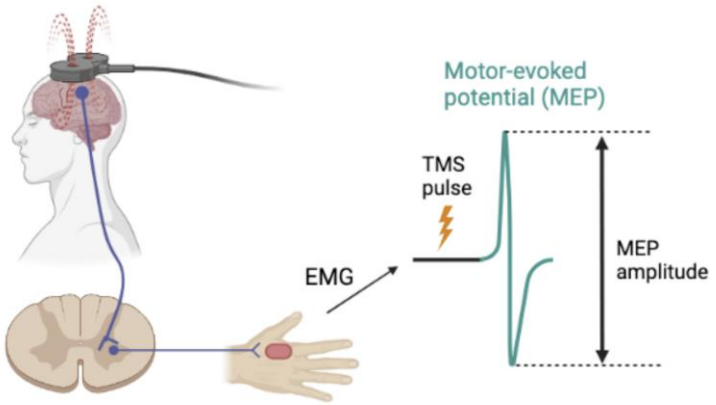

Figure 10: Schematic of TMS mechanism-of-action and detection of Motor Evoked Potentials (MEPs) using electromyography (EMG). Figure created in bioRender.

2.3.2 TMS pulses used in this thesis

I used a combination of single and paired pulse TMS to systematically investigate the effect of θγ oscillations on cortical excitability and receptor-mediated inhibition and excitation.

2.3.2.1 Single pulse TMS

TMS can be used to interrogate the overall excitability of the corticospinal tract using single-pulse TMS. As the intensity of the TMS stimulator is increased (i.e. the magnitude of the pulse), the size of the MEP amplitude increases, following a sigmoid function (Devanne, Lavoie and Capaday, 1997). If a higher stimulation intensity is required to achieve a certain amplitude of MEP (e.g. 1mV), this is thought to reflect lower excitability of M1 and spinal cord structures (Lazzaro, Ziemann and Lemon, 2008; Rosso and Lamy, 2018). However, factors such as inter-individual differences (e.g. skull thickness, cortical gyrification patterns) and intra-individual differences (changes in circadian rhythm, medication, sleep, physiological noise) also affect the stimulation intensity required to elicit MEPs.

I used single pulse TMS to determine the 1mV motor threshold (**MT_{1mV}**; see Figure 11A). This is the minimum stimulator intensity required to elicit a mean 1mV peak-to-peak MEP in the contralateral FDI over 10 consecutive trials, at rest. I also used single pulse TMS to determine the active motor threshold (**aMT**), the minimum stimulation intensity required to elicit a mean 0.2mV peak-to-peak MEP in the contralateral FDI over 10 consecutive trials at 30% maximum voluntary contraction of the FDI.

2.3.2.2 Paired pulse TMS

Whilst single pulse TMS can be used to quantify overall corticospinal excitability, paired pulse TMS can be used to measure receptor-mediated inhibition and facilitation by neurochemicals such as GABA and glutamate.

Following the ascertainment of the **MT_{1mV}** and **aMT**, I delivered paired pulse TMS at intensities personalised by these individual values. Paired pulse TMS involves the delivery of two single TMS pulses, one at 80% of **aMT** (*conditioning pulse*) and one at **MT_{1mV}** (*test pulse*). The first, *subthreshold*, conditioning pulse activates a population of smaller cortical interneurons which modulate the activity of larger pyramidal neurons (Kujirai *et al.*, 1993; Ilić *et al.*, 2002). The second, *suprathreshold*, test pulse depolarises pyramidal neurons leading to muscle activity, as described in single pulse TMS. These two pulses are delivered over one region of cortex (e.g. M1) through the same coil with differing interstimulus intervals (ISIs). The ratio of the size of the test pulse MEP to the conditioning pulse MEP is then calculated. Different receptors have different activation/deactivation times, thus varying the ISIs allows us to investigate the different types of receptors and neurotransmission happening on pyramidal neurons.

To probe **inhibitory neuronal populations** in M1, I used a paired pulse TMS protocol known as Short Intra-Cortical Inhibition (SICI; Kujirai *et al.*, 1993). SICI involves the delivery of a subthreshold conditioning pulse followed by a suprathreshold test pulse with an ISI of 1-5ms. Depending on the ISI, two distinct phases of inhibition can be distinguished with SICI (see Figure 11B and 11C). On one hand, SICI with an ISI of 2-4ms reflects short-lasting synaptic inhibition mediated through GABAa receptors as identified by TMS-combined pharmacological studies (Di Lazzaro *et al.*, 2000; Ilić *et al.*, 2002; Ziemann, 2004). On the other hand, SICI with an ISI of 1ms is less clearly understood but is hypothesised to reflect extrasynaptic GABAergic tone (Fisher *et al.*, 2002, p. 20; Roshan, Paradiso and Chen, 2003; Stagg *et al.*, 2011).

To probe **excitatory neuronal populations** in M1, I used a paired pulse TMS protocol known as Intra-Cortical Facilitation (ICF). ICF involves the delivery of a subthreshold conditioning pulse and suprathreshold test pulse with an ISI of 10-15ms. ICF results in an increase in MEP amplitude (see Figure 11D), which is thought to reflect a combination of both synaptic GABAa and glutamate activity through NMDA receptors (Stagg *et al.*, 2011). This is because NMDA antagonists, such as dextromethorphan have been shown to abolish ICF measured at 10 or 15ms (Ziemann *et al.*, 1998; Reis *et al.*, 2008).

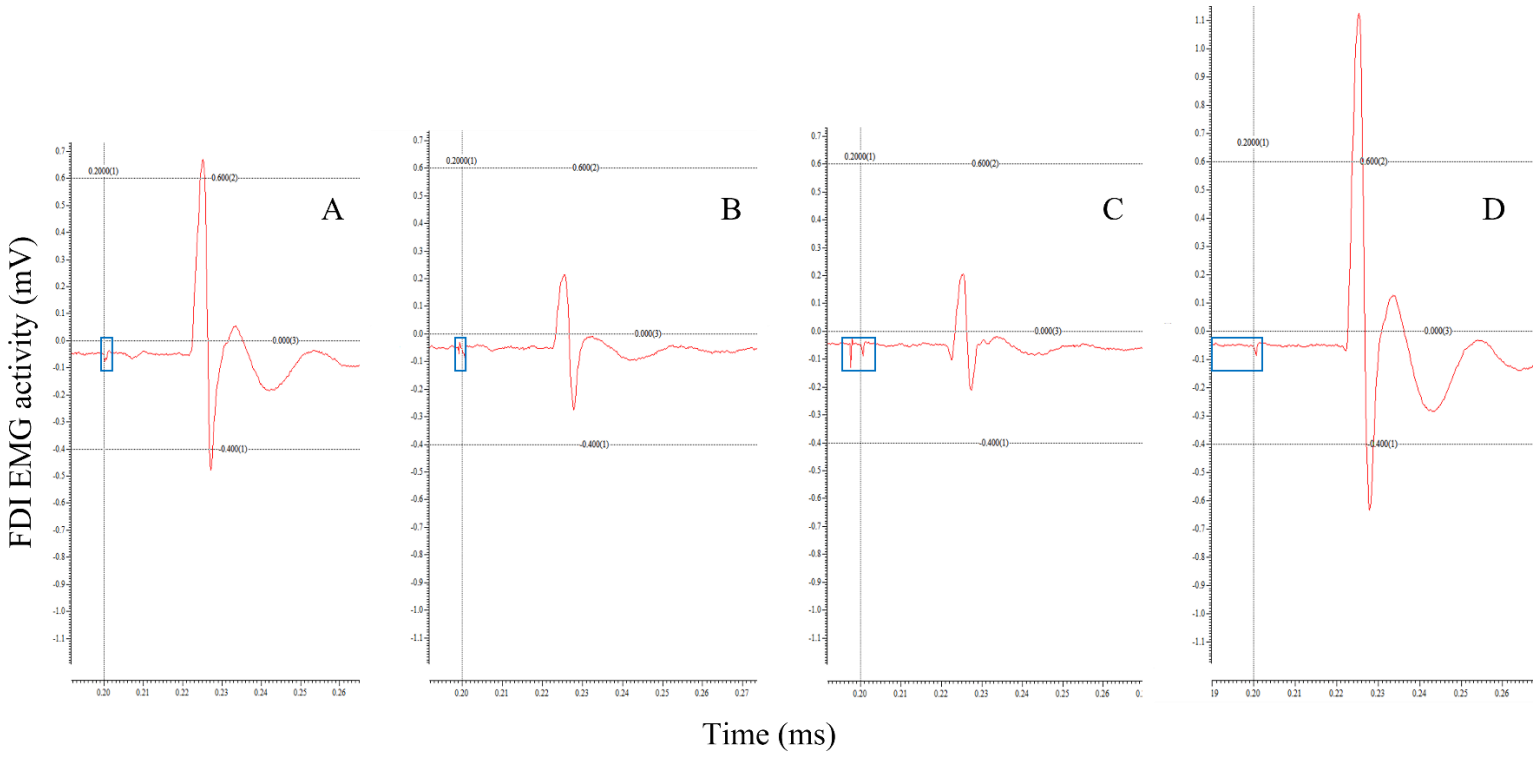

Figure 11: Example MEPs for MT1mV (A), SICI1ms (B), SICI2.5ms (C), and ICF12ms (D). Figures shown in Signal7 (CED, UK). Blue box highlights the TMS artefact (N.B. the conditioning pulse for ICF is not visible in this figure but are 12ms apart).

2.4 Neuroimaging (Chapter 5)

In the final experimental Chapter, I explored the effect of θγ oscillations on sensorimotor functional connectivity using functional Magnetic Resonance Imaging (fMRI). All MR data were acquired on using an ultra-high field 7T Siemens Magnetom (Siemens, Erlangen) with a 32-channel parallel-transmit head coil at the Centre for Functional MRI of the Brain, University of Oxford.

2.4.1 Introduction to Magnetic Resonance Imaging

Magnetic Resonance Imaging (MRI) is a non-invasive tool to look at structural and functional activity *in vivo*. MRI relies on the nuclear magnetic resonance phenomenon. MRI measures signal from water, specifically, signal from the protons present in the hydrogen nuclei (^{1}H) in water (H_2O). Protons are the most commonly used MR-sensitive isotope because most metabolites in the brain contain hydrogen, and its gyromagnetic ratio is higher than many other stable isotopes.

2.4.1.1 Spin

Atomic nuclei (such as the protons of hydrogen nuclei) exhibit a quantum mechanical property known as "spin". Spin causes the ^{1}H protons to behave like little magnets, with an apparent north and south pole. A hydrogen nucleus contains a single proton, so had a charge of +1. Thus, since 1H protons have a charge (+1) and motion (spin),

they create small electrical currents which in turn create small magnetic fields that interact with the local magnetic field, giving spins a magnetic moment. spins have a magnitude, and orientation, and a frequency.

2.4.1.2 B0, spins, and magnetisation (M)

Without an external magnetic field, spins are oriented randomly and spin around their own axis. However, when spins are placed in a large external magnetic field (*B0*), the majority of the spins algin parallel to B0. The signal from individual spins is too weak; therefore in MRI we measure the signal from spin packets (the average of several millions of protons experiencing the same magnetic field). The vector sum of all of the spins in the spin packet leads to a Net Magnetisation Vector (*M*).

2.4.1.3 Precession

The net magnetisation (*M*) does not remain stationary but instead precesses around B0 at a specific frequency. The resonance frequency (*f0*) at which the spins precess is proportional to the strength of B0 and a particle-specific proportionality factor known as the gyromagnetic ratio, given in the Larmor Equation:

$$\omega = \gamma * B0$$

For ^{1}H protons, this characteristic resonance frequency is in the radio-frequency range, meaning we are able to record its signal.

2.4.1.4 Excitation and relaxation

To understand the principles of excitation and relaxation in MRI, it is helpful to describe a three-dimensional coordinate system in which the vector *M* exists in relation to B0 (see Figure 12). Parallel to B0 is the z-axis and perpendicular to B0 are the x and y axes.

We can then separate *M* into two components: the first component is along the z-axis, also known as the *longitudinal axis* (M_z) and the second component is along the x-y axis, also known as the *transverse plane* (M_{xy}).

During scanning, *M* is tipped out of alignment with B0 (i.e. from M_z into M_{xy} or from the *longitudinal axis* towards the *transverse plane*) in a process known as ***excitation***. Excitation is achieved by applying a second, rotating magnetic field (B1). B1 is created by passing alternating current through a nearby RF coil, the transmit coil. This pulse causes the spin to be knocked from M_z into the M_{xy} plane. This results in greater signal in M_{xy} and less signal in M_z being detected by a received coil.

Following excitation, we remove B1, and the spins (*M*) will slowly realign with B0 and emit a signal. This process is called ***relaxation***. As *M* undergoes relaxation, the spins precess and return to alignment with B0 causing a changing magnetic field in M_{xy} over time. A changing magnetic field is the same as a radio wave and this signal is detected by a radio receiver in the MRI scanner. The signal in M_z increases exponentially and the signal along M_{xy} decays exponentially. The signal in the transverse plane (M_{xy}) is also called a free induction decay (FID).

2.4.1.5 T1 and T2 contrast

The relaxation process is governed by two time constants: T1 and T2. T1 (*longitudinal relaxation*) is the time constant for the growth of M_z after excitation due to spins returning to alignment with B0. T2 (*transverse relaxation*) is the time constant for decay of M_{xy} after excitation. Different tissues (e.g. grey matter, white matter, CSF) have different T1 and T2 values. Thus, the relative strength of the recorded signal will be different for each tissue type depending on their T1 and T2 values. This allows us

to create contrast between tissue types. Contrast is made by changing the repetition time (TR; time between excitations) and echo time (TE; time between excitation and measurement).

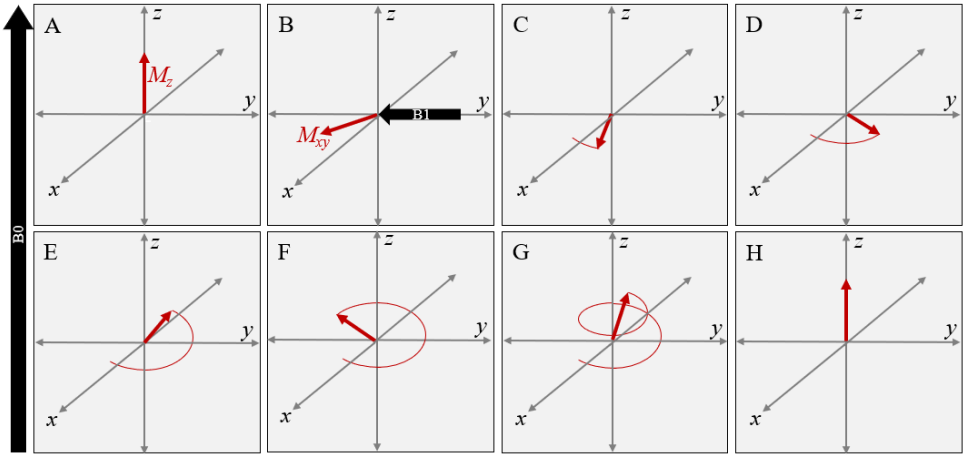

Figure 12: Schematic representation of a pulse MR experiment depicting alignment with B0 (A), excitation (B), and relaxation (C-G), ending with realignment with B0 (H).

2.4.2 Structural MRI

Structural MRI generates high resolution structural images of the human brain. This allows for the definition of cortical and subcortical structures as well as the differentiation between tissue types such as white matter and grey matter. Structural MRI has high spatial resolution with a standard spatial resolution of 1mm isotropically. A limitation to the use of structural MRIs is the susceptibility to motion. T1 weighted images have a short TE and TR times to create the T1 weighting and typically take around six minutes to acquire. I acquired one T1-weighted structural MRI image per participant, per session to overlay the resting state functional data onto and to plan the spectroscopy.

2.4.3 Functional MRI (fMRI)

Unlike structural MRI, fMRI looks at brain activity either in response to a task stimulus (task fMRI) or at rest (resting-state fMRI). fMRI detects changes in regional blood flow as an indirect measure of neuronal activity, known as the Blood Oxygenation Level Dependent (BOLD) signal. In fMRI, T2*-weighted images are acquired that are sensitive to the BOLD signal. T2* contrast includes the previously described T2 decay, but also incorporates additional dephasing due to field inhomogeneities and magnetic susceptibility effects. In Chapter 5, I used fMRI to investigate the effect of θγ oscillations on resting state functional connectivity in the sensorimotor network. I also look at whether combining θγ oscillations with a motor learning task further modulates the sensorimotor network functional connectivity compared to when delivered alone.

2.4.3.1 BOLD contrast

Haemoglobin can be either oxygenated (oxyhaemoglobin) or deoxygenated (deoxyhaemoglobin). fMRI is sensitive to blood oxygenation as the magnetic properties of oxy- and deoxy-haemoglobin are what give rise to the Blood Oxygenation Level Dependent (BOLD) signal. Deoxygenated haemoglobin is more paramagnetic, meaning it has a has a higher magnetic susceptibility and creates magnetic moments that interact and interfere with the local magnetic field, distorting it, and decreasing the MR signal. In physics terms, the spins in a voxel containing a blood vessel with deoxygenated blood will dephase and cancel each other out, resulting in signal loss and a faster T2* decay. On the other hand, oxyhaemoglobin does not create magnetic moments and thus does not interact with the magnetic field.

The BOLD signal is thought to be an indirect measure of neuronal firing. Neurons consume a lot of energy. Increase neuronal firing creates an initial increase in deoxyhaemoglobin compared to oxyhaemoglobin as the area requires more oxygen. Then, in response to this, the vasculature over-supplies oxygenated blood, increasing blood flow and blood volume to the region. This oversupply results in an increase in T2* signal. In other words, following an increase in neuronal firing, there is an initial dip in the BOLD signal (due to increased deoxyhaemoglobin which is paramagnetic) after which the MR signal quickly recovers and "overshoots" the baseline signal level (due to an increase in oxyhaemoglobin which does not interact with the magnetic field). The dynamic relationship between neuronal activity and BOLD is given by the Haemodynamic Response Function (HRF; see Figure 13). The HRF is delayed by approximately 0.5 seconds following neuronal activation as blood flow follows neuronal activity with a slower temporal resolution, meaning that the temporal resolution of fMRI is good, but not as good as neurophysiological methods such as M/EEG.

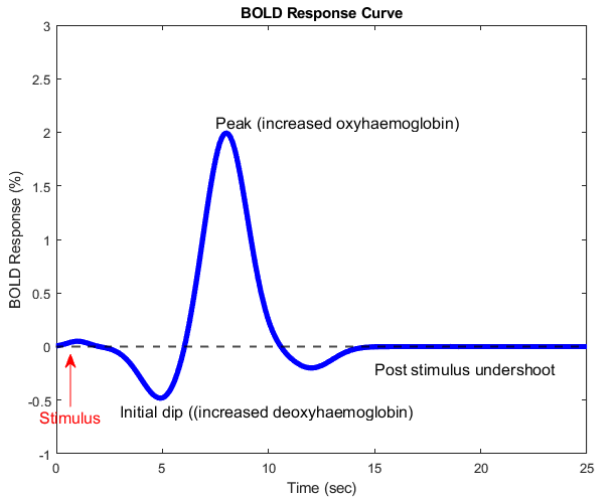

Figure 13: Schematic representation of the BOLD response curve in line with the haemodynamic response function.

2.4.3.2 Resting state and task fMRI

In this thesis, I used a combination of resting state and task fMRI to assess whether θγ oscillations impact functional connectivity across the sensorimotor network and whether the inclusion of a task further amplifies this effect.

fMRI can be used to quantify the BOLD response to an external stimulus, such as a task (known as task fMRI). However, fMRI can also be used in the absence of a task to study low-frequency spontaneous fluctuations of the BOLD signal. I can then compare the synchronicity of the BOLD signal changes across regions. The assumption is that areas that are connected in a functionally-relevant manner will show fluctuations in the BOLD signal that follow a similar temporal pattern (i.e. have correlated time courses of activation). This degree of correlation is thought to reflect functional connectivity between brain regions.

All fMRI scans in this thesis were whole-brain multi-band fMRI data (TR/TE/FA = 1000/20ms/90°; FOV(AP,FH,RL)=220×120×220mm^3; voxel size=2.0×2.0×2.0mm^3; multi-band factor of 2) in blocks of five minutes.

2.4.3.3 Pre-processing

As part of the analysis for this thesis, I developed a series of end-to-end, open-access, fMRI pre-processing pipelines, optimised for 7T MRI. fMRI data are inherently noisy

due to physiological processes (e.g. cardiac and breathing rhythms) as well as participant movement and hardware artefacts. As such, all fMRI data require extensive pre-processing.

The first stage of pre-processing was to the structural T1w scan. In this step, I prepared the structural T1-weighted MRI. First, I reoriented the image to standard orientation using fslorient2std. Then, I performed z-direction image cropping using the robustfov tool. I then performed brain extraction with Freesurfer using mri_synthstrip as I found that this significantly improved brain extraction (and subsequent registration). I then applied bias field correction to all brain extracted T1-weighted images. Bias field correction corrects inhomogeneities in the MRI signal intensity, which are caused by non-uniformities in the magnetic field or in the sensitivity of the receiving coils. I then expanded the bias field outside of the brain mask using fslsmoothfill. I applied the expanded bias field to the non-brain extracted T1-weighted images that had been reoriented and cropped. I performed tissue-type segmentation using FAST with three tissue type classes (corticospinal fluid, grey matter, white matter). I also performed subcortical structure segmentation using FIRST on the brain extracted image.

The next stage of pre-processing was to prepare the fieldmaps. In MRI (especially in high field MRI), there is greater magnetic susceptibility meaning that variations in B0 caused by differences in tissue composition, such as between air, bone, and brain, become more pronounced. These variations lead to geometric distortions. Field maps map the field and are essential for correcting these distortions by providing a voxel-wise map of the magnetic field inhomogeneities, allowing for precise image alignment and more accurate localization of brain structures and activity. My 7T Siemens fMRI fieldmap data generated two magnitude images. After going into the JSON files for these, I found that they have different TEs. Different TEs will give slightly different signals, therefore by using both I maximised my sensitivity. My script had a few optimisation steps before running fsl_prepare_fieldmaps to make the most of having multiple magnitude images: First I used fslmaths to calculate the mean of magnitude1 and magnitude2. Then, I performed brain extraction using bet on the generated image. Then, I used fslmaths to erode by 3.8. I then extracted the TE values from each magnitude image by looking at the respective JSON files, I then calculated the difference between these two times and converted the result to milliseconds ("deltaTE"). DeltaTE was then used for further processing in fsl_prepare_fieldmaps.

The next pre-processing stage was slice timing correction. Slice timing correction accounts for the fact that different slices of the brain are acquired at slightly different times during each volume acquisition. Since brain activity changes over time, this can introduce timing discrepancies in the recorded signal. Slice timing correction adjusts the fMRI data by interpolating the signal to align all slices as if they were acquired simultaneously, improving the accuracy of subsequent analyses, such as detecting brain activity patterns and temporal dynamics. I extracted the slice timing array and the TR from the JSON file. I calculated the adjustment factor for converting slice timing values to fractions of the TR (required for FSL slicetimer). I then converted the slice timing into an array and processed each value in the array.

2.4.3.4 Independent Component Analysis (ICA)

Resting-state fMRI has a few additional complexities because the fMRI data are measures of small, spontaneous fluctuations in the MR signal and not fluctuations that are time-locked to an external stimulus, such as a task. This makes the identification of relevant signal among noisy measurements challenging. Resting-state fMRI often uses Independent Component Analysis (ICA) at the single-subject level first to clean

the data. ICA is a model-free approach, meaning that there is no explicit timeseries model of assumed activity specified from a time-varying feature, such as a task, to which the resting state data is fit. Instead, ICA linearly decompose the fMRI data into underlying "components" which, together, maximally explain the data. Each component consists of a timeseries, power spectrum, and associated spatial map (see Figure 14 and 15).

I used MELODIC at the single subject and fMRI run level to decompose my fMRI data into time courses and corresponding spatial maps using ICA. The following pre-statistics processing was applied; motion correction using MCFLIRT Jenkinson *et al*., 2002) ; slice-timing correction using Fourier-space time-series phase-shifting; grand-mean intensity normalisation of the entire 4D dataset by a single multiplicative factor; high pass temporal filtering (Gaussian-weighted least-squares straight line fitting, with sigma=50.0s). Then, registration to high resolution structural and/or standard space images was carried out using FLIRT (Jenkinson and Smith, 2001). Registration from high resolution structural to standard space was then further refined using FNIRT nonlinear registration (Andersson, Jenkinson and Smith, 2007). Single-subject ICA, implemented in MELODIC, was then used to extract independent components.

2.4.3.5 Training a classifier

Categorising "noise" components from "signal" components can then be done using automatic classification toolboxes, though this approach relies on training the algorithm on at pre-trained dataset. Though many pre-trained datasets exist, the training data must be well-matched to one's fMRI data in terms of acquisition, study parameters, participant cohort and other factors. There are limited trained datasets for FIX on high-resolution 7T data. I thus decided to train my own FIX model by manually labelling 44 datasets, from 10 different participants, across my four timepoints (pre-tACS, early-tACS, late-tACS, and post-tACS) to capture the likely variance seen in my dataset. I then used the Leave One Out (LOO) approach to assess the performance of my model. Having achieved a 0.99% correspondence with a threshold of 20, the FIX classification using this model was applied to the rest of the data. Finally, data were smoothed and warped into standard space for higher level processing. **Further details regarding higher level analyses can be found in Chapter 5 (Neuroimaging).**

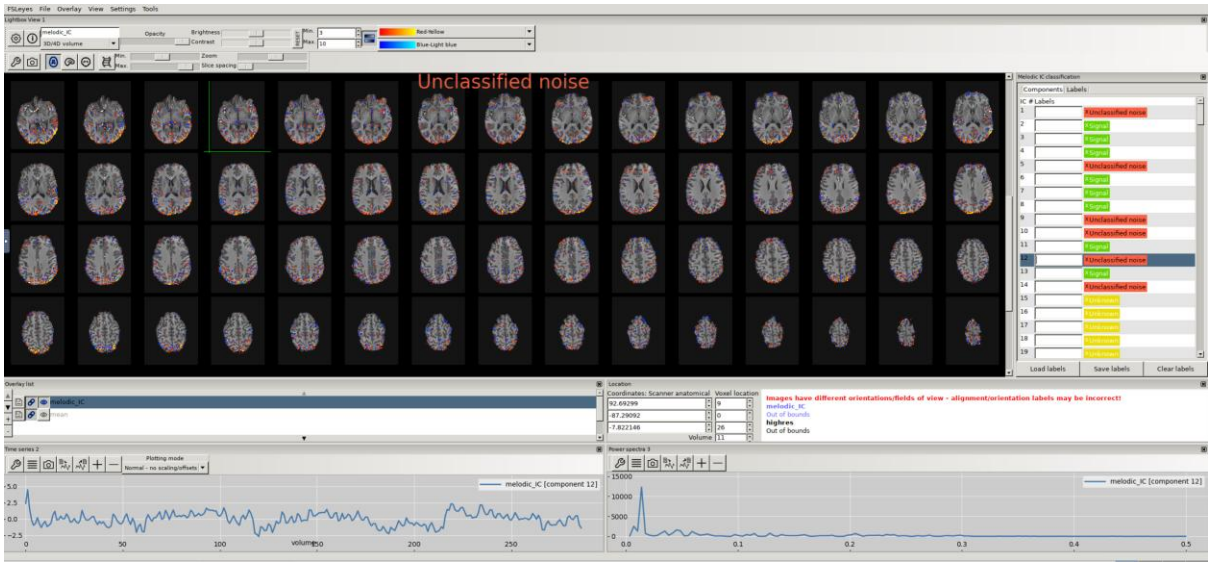

Figure 14: An example of a MELODIC-extracted component. Spatial map (top), timeseries (bottom left), and power spectrum (bottom right). From the information in the spatial map, timeseries, and power spectrum this was manually classified as "noise".

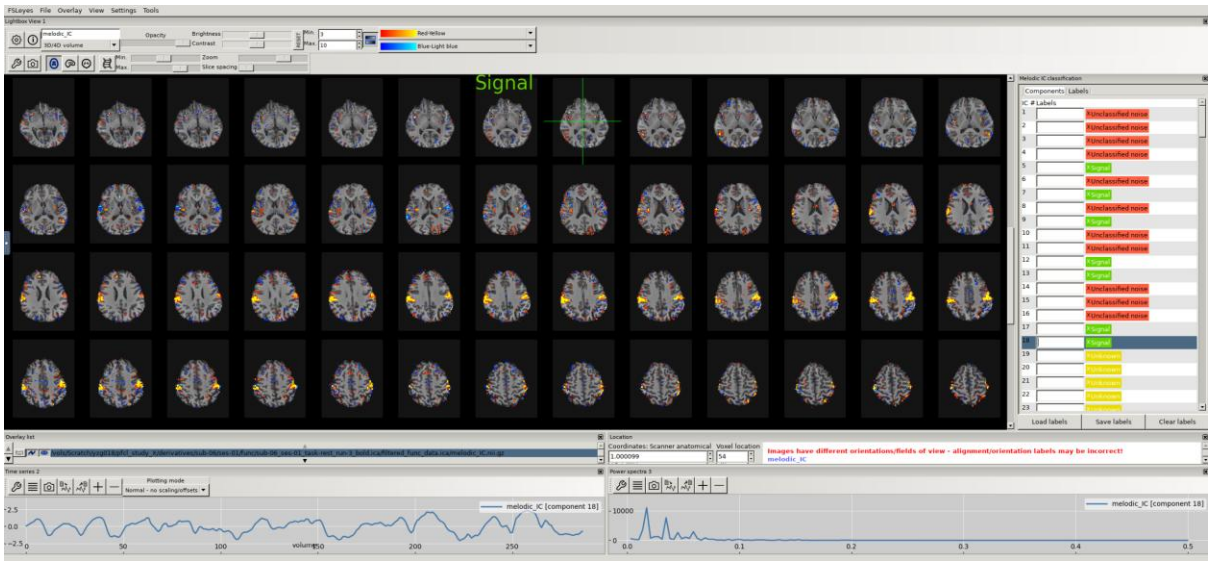

Figure 15: An example of a MELODIC-extracted component. Spatial map (top), timeseries (bottom left), and power spectrum (bottom right). From the information in the spatial map, timeseries, and power spectrum this was manually classified as "signal".

CHAPTER III - Investigating the frequency specificity of θγ oscillations in healthy human motor behaviour

In this first experimental Chapter, I aim to replicate the finding that θγ oscillations improve skill acquisition in a novel motor learning task. I then investigate the frequency-specificity of this effect. Akkad et al. (2021) found that mid-γ (75Hz) in a TGP oscillation plays a key role in motor behaviour. However, whether this effect is specific to mid-γ or whether other γ frequencies (e.g. slow-γ at 45Hz) mediate similar behaviours remain to be causally demonstrated in humans.

3.1 Introduction

Using tACS to artificially entrain 75Hz γ activity, phase amplitude coupled to the positive half of a 6Hz θ wave (θγ peak tACS; *TGP*) has been shown to induce a positive effect on motor behaviour (Akkad *et al.*, 2021). This effect was not seen when entraining 75Hz γ activity, phase amplitude coupled to the negative half of a 6Hz θ wave (θγ trough; *TGT*). Whether this is a purely phase-dependent effect or whether the frequency at which γ activity is delivered within the θ also matters is left to be determined. In this Chapter, I first discuss the existing literature's view on the role of slow- and mid-γ oscillations in motor behaviour and how coupling these to θ may engage different mechanisms. I then aim to replicate the finding that mid-γ TGP is important for motor behaviour whilst further investigating the role of slow-γ activity in the same manner.

3.1.1 Gamma and motor behaviour

In motor areas, γ is a pro-kinetic rhythm. Upon movement execution, M1 neurons synchronise at a γ frequency, known as γ event-related synchronisation (γ ERS; Crone, 1998). This γ ERS is not seen during passive movements (Muthukumaraswamy, 2010), suggesting γ may directly reflect motor output (Crone, 1998). Whilst movement-related desynchronisation (ERD) in neuronal oscillations such as beta ERD are typically detected over bilateral sensorimotor cortices during unilateral movements, γ ERS is detected unilaterally over the contralateral sensorimotor cortex in a somatotopic manner (Crone, 1998).

However, the γ band is very broad and classically defined as activity between 30-100Hz. Increasing evidence points towards the existence of several γ sub-bands that each have distinct functional and neurophysiological mechanisms: slow-γ (human: ~30-60Hz, rodent: ~30-50Hz), mid-γ (human: ~60-90Hz; rodent: ~50-100 Hz), and fast-γ (human >90Hz, rodent >100Hz). In the present study, I focus on exploring the functional role driving slow- and mid-γ sub-bands on human motor behaviour.

3.1.1.1 Slow- and mid-γ: Two distinct movement-related patterns of γ activity

Studies using non-invasive magnetoencephalography (MEG) (Zich *et al.*, 2021) and invasive electrocorticographic spectral analysis (ECoG) (Crone, 1998) measures of neuronal oscillatory activity have shown that slow- and mid-γ ERS have distinct temporal characteristics in response to motor movement (Crone, 1998; Szurhaj *et al.*, 2005). Slow-γ ERS has been reported to arise after movement onset, is sustained throughout (reaching its peak at time of movement offset), and decreases after movement offset (Crone, 1998; Szurhaj *et al.*, 2005; Zich *et al.*, 2021). Mid-γ ERS on the other hand has been reported during (or even slightly before, though this has been contested [(Szurhaj *et al.*, 2005)]) movement onset, reaching its peak between movement onset and offset, and terminates around movement completion (Crone, 1998; Zich *et al.*, 2021). Unlike slow-γ, mid-γ ERS is transient, lasting only 400-1000ms and often precedes the onset of slow-γ ERS (around 200-500ms after movement onset) (Crone, 1998; Zich *et al.*, 2021).

3.1.1.2 Neurophysiological differences between γ sub-bands

The different temporal characteristics of slow- and mid-γ ERS in response to motor movement point towards different, but likely overlapping, neurophysiological mechanisms (Crone, 1998; Szurhaj *et al.*, 2005). Both slow- and mid-γ oscillations are generated via complex interactions between excitatory pyramidal cells and various subtypes of inhibitory interneurons including parvalbumin-positive fast-spiking interneurons (PV-FSi) and somatostatin-expressing interneurons (SST). These pyramidal-interneuron interactions, as well as interneuron-interneuron autoinhibition, are necessary in generating distinct γ states.

However, current models do not consider the diversity of interneuron subtypes in generating different γ frequencies (Keeley, Fenton and Rinzel, 2017). PV-FSis are

generally considered as the key player in γ frequency oscillation generation. Targeting the peri-somatic domain of pyramidal neurons, PV-FSis are adapted for fast synchronisation of network activity, and are capable of precisely controlling spike timing (Pike *et al.*, 2000; Cardin *et al.*, 2009; Antonoudiou *et al.*, 2020). However, the *selective* role of PV-FSis in generating γ oscillations has been challenged by studies in visual cortex (e.g. Chen *et al.*, 2017). For example, a study demonstrated that dendrite-targeting SST interneurons are the main contributors for the generation of slow-γ oscillations, whilst PV-FSis are more important for higher frequency synchronisation (Chen *et al.*, 2017). Therefore, the distinct movement-related profiles of slow- and mid-γ may be, in part, explained by the engagement of different interneuron populations generating different γ frequencies.

3.1.2 The effect of driving θγ oscillations on motor behaviour

To date, literature has highlighted different effects of driving slow (Giustiniani *et al.*, 2019) and mid-γ oscillations alone (Joundi *et al.*, 2012; Nowak *et al.*, 2017; Bologna *et al.*, 2019) on motor behaviour, with slow-γ typically impairing and mid-γ improving behaviour. Taken together with the aforementioned differences in temporal characteristics and neurophysiological mechanisms, the question of whether driving these different γ sub-bands at the peak of a TGP complex has different effects on behaviour arises. *In vitro* work has shown that in region CA1 of the hippocampus, there are three γ bands occurring at different phases of a θ wave: a slow-γ at the descending θ phase; a mid-γ near the θ peak; and a fast γ near the θ trough (Tort *et al.*, 2010; Buzsáki and Wang, 2012). This serves to explain the findings of Akkad *et al*. (2021) in which artificially entraining mid-γ oscillations at the peak of an underlying θ wave affects behaviour since this coupling is endogenous to the brain. However, whether there is an additional γ frequency-specificity mediating this effect remains to be demonstrated. The only causal evidence to date on the effects of different γ sub-bands within TGP on behaviour comes from working memory literature in which Alekseichuk *et al.* (2016) found evidence of enhanced working memory and increased global cortical connectivity when driving high-γ TGP but not low-γ (40Hz) TGP. Therefore, the frequency of γ within TGP appears to be important in mediating behaviour.

3.1.3 Entrainment versus plasticity

The precise neurophysiological mechanisms by which tACS modulates endogenous oscillations remains under contention (see section 1.7.1 *Mechanisms of tACS*). There are currently two major schools-of-thought regarding the mechanisms of tACS: entrainment and spike timing dependent plasticity. Akkad *et al*. (2021) delivered θγ tACS for 20 minutes continuously and report positive behavioural effects both during and up to 60 minutes after stimulation. It is thus likely that tACS had resulted in neuroplastic changes that served the positive modulations in behaviour. However, there are studies reporting no such offline effects of tACS (Pozdniakov *et al.*, 2021; Fabbrini *et al.*, 2022) and computational modelling has provided strong evidence in favour of entrainment as a mechanism of action (Ali, Sellers and Frohlich, 2013). As such, beyond assessing the role of different γ frequency sub-bands within a θγ complex on motor behaviour, I investigated entrainment as a mechanism of action by delivering movement-locked, short bursts (3 seconds) of θγ tACS during motor learning.

3.1.4 Aim of this Chapter

Overall, mid-γ TGP tACS (75Hz/6Hz) has been shown to modulate motor behaviour (Akkad *et al*., 2021). However, whether this effect is unique to high γ is unknown. The γ frequency band is very broad, and there are many patterns of movement-related γ activity in human M1 (slow, mid, fast γ) with different temporal and neurophysiological properties. As such, it is plausible that coupling these to θ will have distinct effects on motor behaviour. In this Chapter I build on the work of Akkad *et al*. (2021) by first seeking to replicate the finding that mid-γ

(75Hz) TGP improves motor behaviour compared to sham stimulation. I then investigate the role of slow- (45Hz) and mid-(75Hz) γ oscillations in TGP on motor behaviour.

3.2 Methods

3.2.1 Participants

A total of 80 right-handed, healthy participants (58 female, 22 male, aged 18-35) gave their written informed consent to participate in this study. Due to equipment failure, nine participants were excluded from analysis. This resulted in a total of 71 participants with 23 participants in 45Hz TGP tACS (18 female, 5 male), 25 in 75Hz TGP tACS (17 female, 8 male), and 23 in sham (16 female, 7 male). Power calculations based on previous literature (Akkad *et al*., 2021) gave n=24 per group (α=0.05, (1-β)=0.8, ηp2=-.12). This project was granted ethics committee approval (Oxford CUREC1: R79659/RE004). Safety exclusion criteria for NIBS included (but was not limited to) a history, or current diagnosis, of a neurological or psychiatric disorder, a family history of epilepsy, a history, or current diagnosis, of migraines or frequent headaches, treatment with psychotropic medication (e.g., antiepileptics, antidepressants, antipsychotics, psychostimulants), the presence of metallic implants in or near the head (such as pacemakers and deep brain stimulators) and pregnancy.

3.2.2 Apparatus and stimuli

3.2.2.1 Transcranial Alternating Current Stimulation (tACS)

2mA peak-to-peak θγ PAC modulated waveforms (6Hz/45Hz and 6Hz/75Hz) were custom-coded in Spike2 and delivered via a Nurostym stimulator using Analogue Mode (see Figure 16). θγ PAC tACS delivery was time-locked to the onset of movement through use of a photodiode which detected cursor movement. tACS was delivered for three seconds per trial (400 trials = 20-minutes of active stimulation delivery, in accordance with previous literature (Akkad *et al*., 2021). Sham-tACS consisted of a custom-coded empty single-cycle θ waveform. The custom coded waveform files were saved as “A”, “B”, or “C” by an independent researcher such that when I ran the waveforms, I was blinded to what condition participants were in.

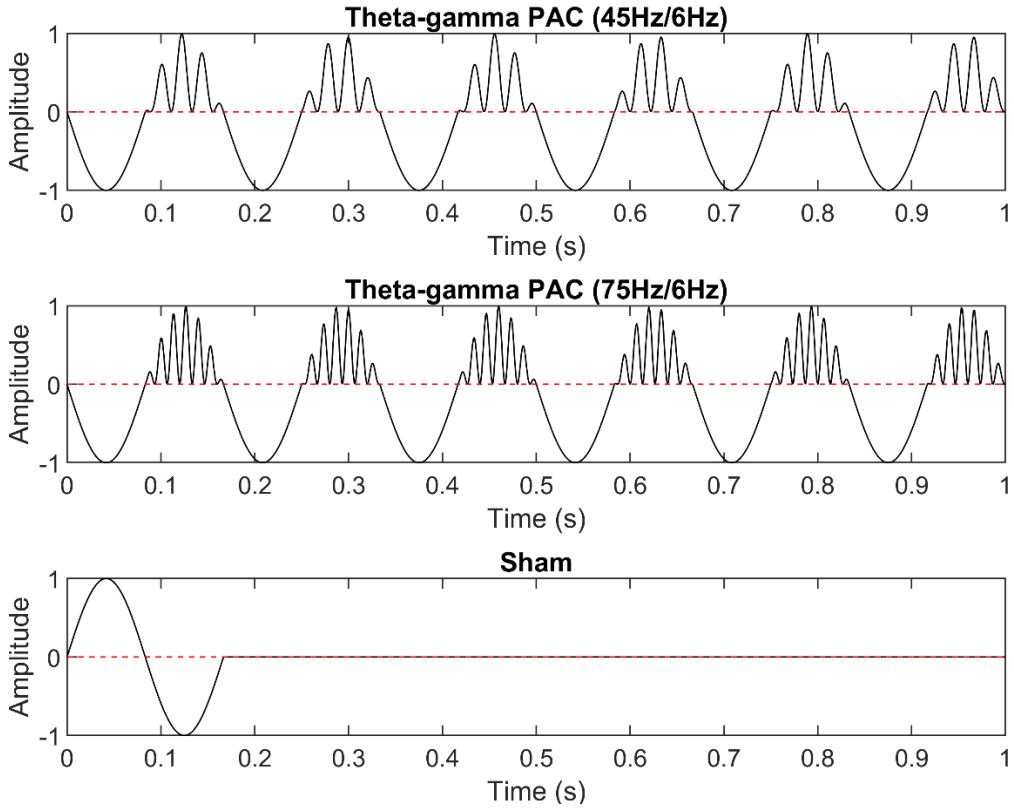

Figure 16: tACS waveforms:45Hzγ-6Hzθ (top), 75Hzγ-6Hzθ (middle), and sham (bottom).

3.2.2.2 Electrode Montage

In accordance with the 10-20 EEG system, 5x5cm rubber conductive tES electrodes were centred over left primary motor cortex (C3) and parietal vertex (Pz). Ten20 electrode paste was used as a conducting medium between the scalp and the electrodes. Impedance was kept below 10kΩ throughout the session. The scalp under C3 and Pz was prepared using abrasive paste (NuPrep) and a cotton tip and wiped clean using an alcohol wipe. The tES electrodes were secured in place using rubber straps and a mesh cotton cap.

3.2.2.3 Behavioural task

A 65g 45x6mm Biometrics Ltd pinchmeter (see Figure 17) was used to convert mechanical load into an electrical output signal that controlled the behavioural task. I developed a custom-coded novel motor task in C++. A stationary three-peak sinusoidal wave was displayed on a 14" screen. A stationary white line was displayed below the three-peak sinusoid wave along the x-axis upon which a red circle was presented at the start. In the absence of force applied to the pinchmeter, the circle travelled at a constant speed of 9.3cm/s along the x-axis. The application of force to the pinchmeter resulted in a linear movement of the circle along the y-axis. Together, with the constant movement along the x-axis and the ability to modulate the movement of the circle along the y-axis, participants were asked to track the sinusoid wave as accurately as possible using the pinchmeter between their right index finger and thumb.

Six yellow targets were displayed along the sinusoid wave (see Figure 6). Participants were instructed to “hit” as many targets as possible (a successful hit resulted in the yellow circle disappearing) and were informed that the best way to achieve this was by tracing the blue sinusoid as accurately as possible. A 15-pixel error margin around

the yellow targets was adopted such that achieving a "hit" was challenging and required learning (avoid ceiling effects), but not so challenging that it was impossible to achieve (avoid floor effects). This reward system has been found to be suitable for this type of behavioural paradigm (Steel *et al.*, 2016, 2019) and closely mirrors the behaviour:reward relationship in the Sala-Bayo *et al.* (unpublished data) mouse study (successful trial = reward / non-successful trial = no reward). Participants took part in four "blocks" of 100 trials with an inter-trial interval of two seconds and a self-paced inter-block interval to avoid fatigue.

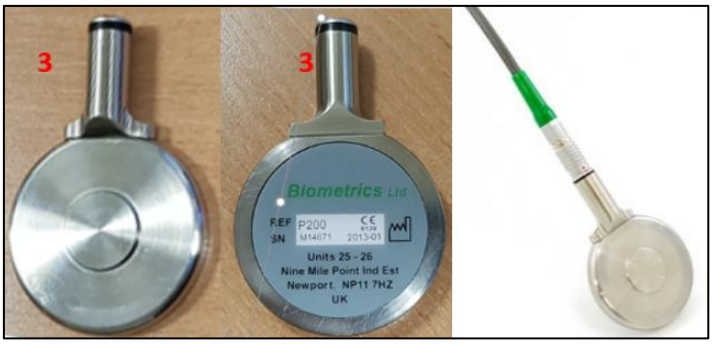

Figure 17: Biometrics Ltd pinchmeter used in the behavioural study.

3.2.3 Procedure

This study is a preregistered (https://osf.io/63tn2), double-blind, sham controlled, between-subjects design. Participants were sent the participant information sheet and invited to an online brain stimulation safety screening interview. Participants were sent a participant information sheet prior to screening and underwent an initial non-invasive brain stimulation safety screening based on (Rossi *et al.*, 2011). On the day of the experiment, participants were screened again and gave informed consent. Participants' heads were measured to calculate the placement of the C3 and Pz electrodes. In line with the 10-20 EEG system, C3 was determined as 20% of the A1:A2 distance from Cz towards the left ear. Pz was determined as 20% of the nasion-to-inion distance from Cz towards the back of the head. The Nurostym Analogue Input Mode was set up and impedance automatically assessed. If impedance was >10kΩ, the area under the electrodes was further cleaned until impendence was <10kΩ.

I then calibrated the pinchmeter to individual participants' strength. Maximum Voluntary Contraction (MVC) was defined by asking participants to perform a precision grip using the pinchmeter using only the pad of the right thumb and index finger to exert an isometric force. MVC for each participant was determined using data from three maximum precision grip trials. The pinchmeter was calibrated to 20% individual MVC as force levels between 10-20% of MVC can be maintained and evoke no fatigue (Voelcker-Rehage and Alberts, 2005).

Participants then completed the four blocks of the task and were debriefed. All participants received financial compensation for participation. A visual depiction of the protocol can be found in Figure 18.

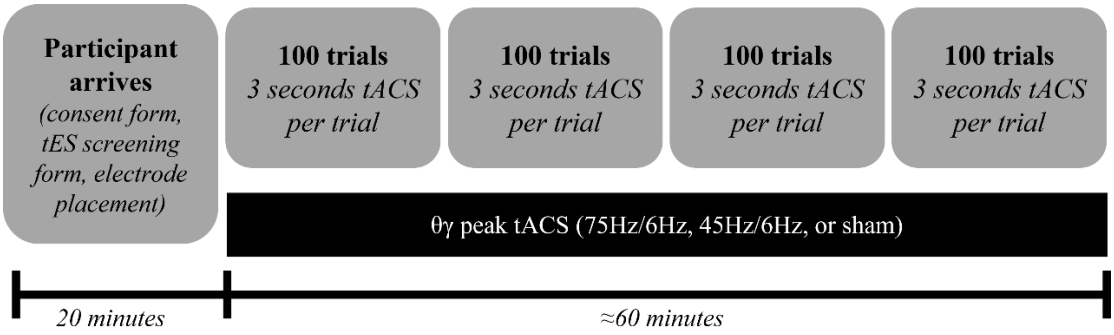

Figure 18: Experimental design (Chapter 3)

3.2.4 Behavioural data pre-processing (targets hit and error)

When first extracting the data, it was clear that there was a period of familiarisation over the first few trials that was not reflective of the same learning mechanism present at later trials (*familiarisation* versus *learning*, a common phenomenon in learning studies). I thus extracted the first 10 trials of block 1 called "block 0". The rest of the trials in this block (i.e. trials 11-100) were re-saved as "block 1" (see Figure 19). Blocks 2,3,4 did not change (n=100 trials).

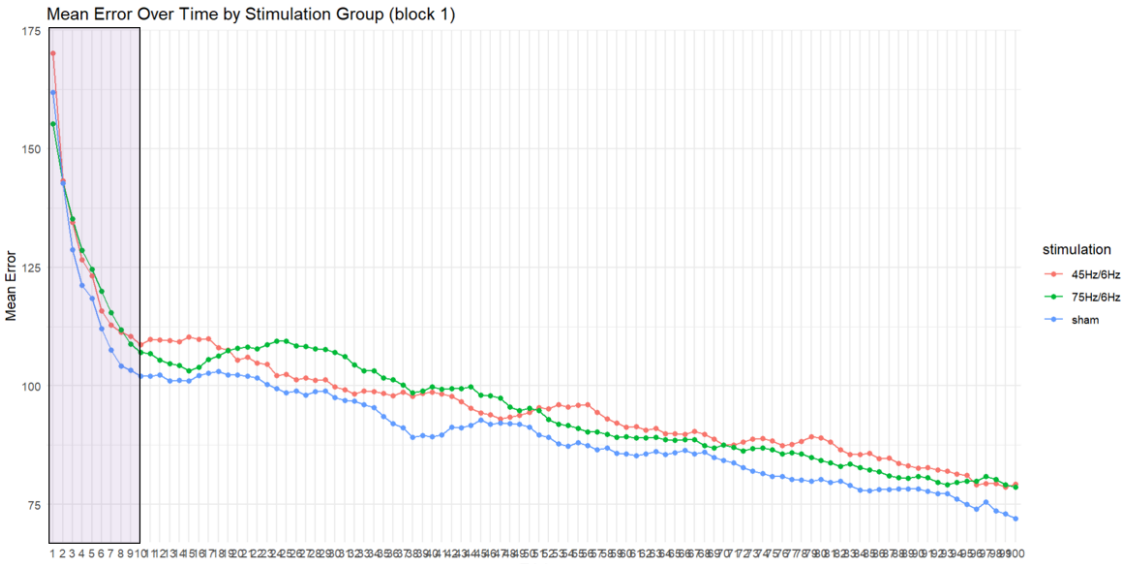

Figure 19: Example error (arbitrary value) for each stimulation condition over the first 100 trials. The purple box shows the steep reduction in error, representing initial familiarisation with the task.

3.2.5 Behavioural data pre-processing (force modulation)

I also investigated the effect of different γ frequencies on participants' ability to modulate force output. At the start of each trial, participants started with no force applied to the pinchmeter (baseline, see Figure 20; red box). Then, participants pinched to hold the circle at the start platform for three seconds (preparatory pinching to begin engaging motor cortical oscillations onto which tACS could entrain to, see Figure 20; orange box). Only once the conditions of the preparatory pinch were met (i.e. three seconds hold) did the circle start to move along the x-axis (force modulation, see Figure 20; green box).

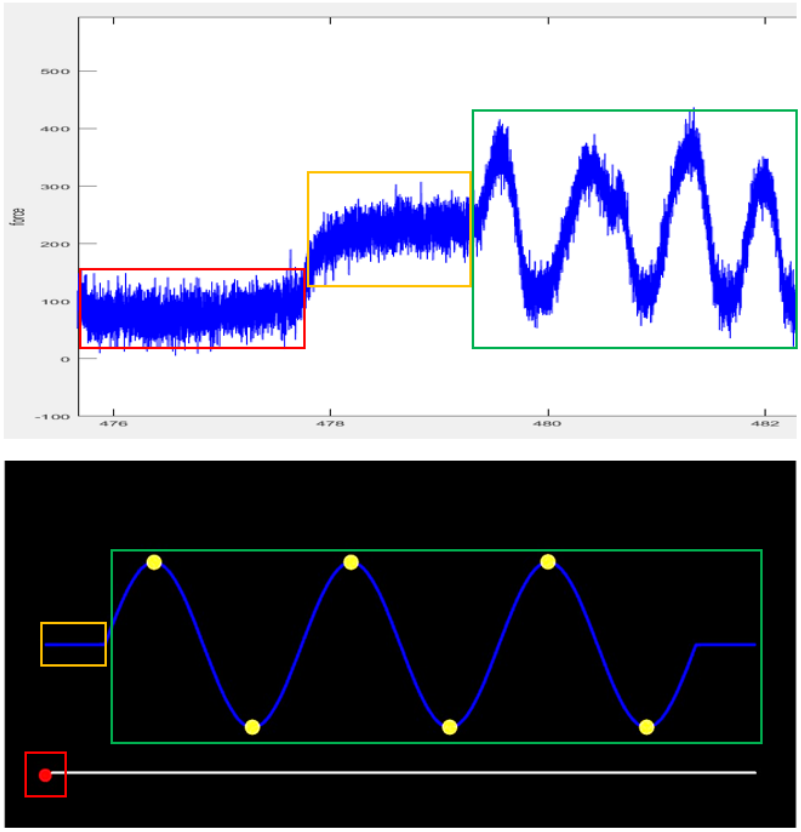

Figure 20: Example of how the task (bottom) matches force data (top) in one trial.

A white circle was coded to appear on the screen (over which a photodiode was applied) at the moment the circle started to move following the preparatory pinching. This way I recorded the exact time at which the circle started to move for each trial (see Figure 21; black line). I then extracted data for 0.5 seconds after this marker for each trial. This ensured that the extracted data always reflected the same first 0.5 seconds of force modulation for each trial/participant/block.

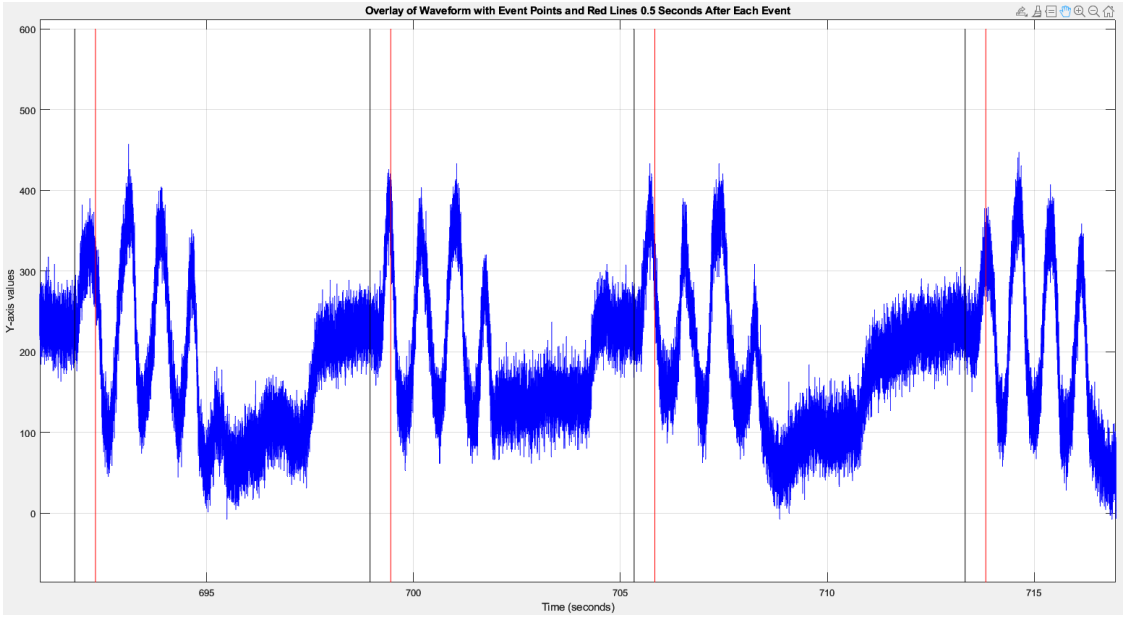

Figure 21: Example of extracting trials and the subsequent 0.5 seconds. Force (blue), start of each trial (black), 0.5s after start of trial (red).

I then further refined the extracted data to account for reaction time (approximately 0.2 seconds). I extracted the data from 0.2 to 100 data points after the max value to maximise fitting. After extracting the tracing data for 0.2 to 100 data points after the max point for each trial, participant, and block, I smoothed each trial using a 100 sliding window average in MATLAB (Mathworks, version 2024a; see Figure 22).

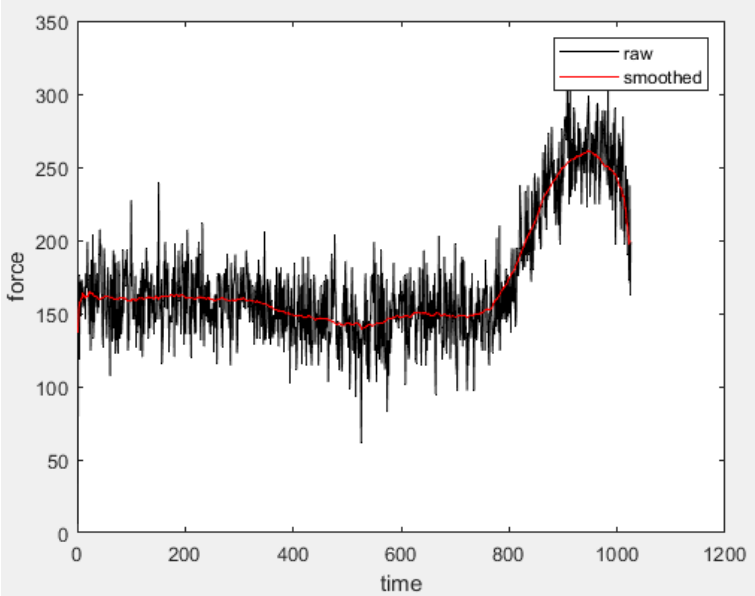

Figure 22: Example of one trial before (black) and after (red) smoothing.

I then applied a Gompertz sigmoidal model to fit each trial (MATLAB, Mathworks, 2024):

$$f(x)=d+(a-d)e^{-e^{-b(x-c)}}$$

In the Gompertz model, *a* and *d* are parameters for the horizontal asymptotes with *c* reflecting the inflection point between the horizontal asymptotes. Of importance to this analysis, *b* is a growth rate parameter and determines how quickly the growth occurs (i.e. steepness) with higher *b* values representing steeper curves. Examples of how trials were fitted with the Gompertz model can be found in Figure 23.

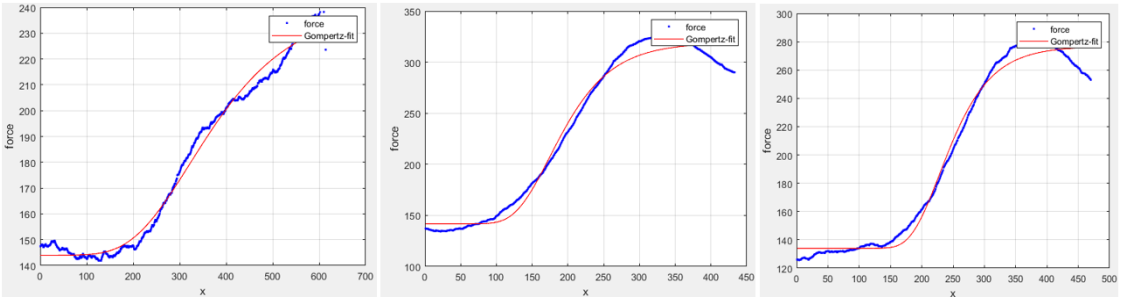

Figure 23: Example of three trials in one participant. Tracing data (blue) and the Gompertz-fitted model (red).

I then plotted the distribution of goodness-of-fits and excluded trials with values less than 0.95 (see Figure 24). I also confirmed that the b-values were normally distributed (see Figure 24).

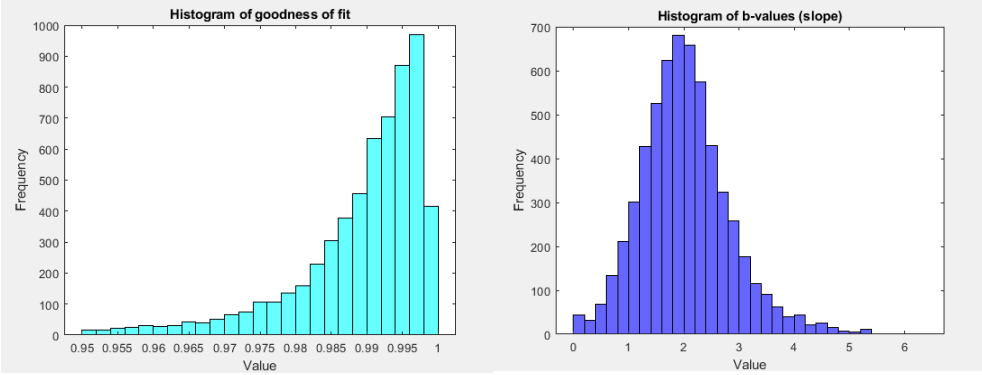

Figure 24: Histogram of the goodness of fits (left) and b-values (right) for Gompertz-fitted models.

3.2.6 Statistical analysis

All analyses included the respective percentage change in performance (***targets hit*** or ***error***) from block 1, using the following equation:

((block n targets hit - block 1 targets hit)/(block 1 targets hit) ×100%)

((block n error - block 1 error)/(block 1 error) ×100%)

All data were z-transformed for each stimulation group and block separately, and Grubbs outlier detection was run on each block for each stimulation condition separately. For error analyses, I calculated the absolute difference in pixels between the subject's position on the screen (i.e. the centre of the red circle) and the sinusoid.

All data were analysed using the linear mixed effects model (lme4) package in R software with **STIMULATION** and **BLOCK** as fixed effects and a **STIMULATION×BLOCK** interaction in the model. I allowed intercepts for different subjects to vary in order to account for covarying residuals within subjects (creating a random intercept model of "subject"). Estimated marginal means for each stimulation condition were computed, and post hoc pairwise comparisons using Tukey-adjusted tests were run on the level of significant main effects. Visual inspection of residual plots did not reveal any obvious deviations from homoscedasticity or normality.

3.3 Results

3.3.1 Number of targets hit

3.3.1.1 No significant difference in the number of targets hit between stimulation groups for block 0

I first ensured that there were no significant differences in the number of targets hit between the stimulation groups at baseline (block 0). Levene's test demonstrated that the assumption of homogeneity of variances was violated, ($F(2,68)=3.282, p=.043$). I therefore ran a Welch's ANOVA with one factor of **STIMULATION** (75Hz, 45Hz, sham) on the number of targets hit in block 0. There was no significant main effect of **STIMULATION** on the number of targets hit in block 1 ($F(2,68)=75.6, p=.140$).

3.3.1.2 No significant difference in the number of targets hit between stimulation groups for block 1

I then ensured that there were no significant differences in the number of targets hit between the stimulation groups in the first true block of learning (block 1). Levene's test demonstrated homogeneity of variance ($F(2,68)=2.04, p=0.138$). I ran a one-way ANOVA to examine the effects of **STIMULATION** on number of targets hit in block 1. There was no significant main effect of **STIMULATION** on the number of targets hit in block 1 ($F(2,68)=1.394, p=0.255$). All subsequent analyses use the data calculated as the percentage change in number of targets hit from block 1.

3.3.1.3 The novel motor learning task results in a significant increase in percentage change in number of targets hit from block 1 over time

I then constructed a linear mixed effects model with **STIMULATION** and **BLOCK** as fixed effects, and varying intercepts for **SUBJECT**. There was a significant main effect of **BLOCK** ($F(2,126)=34.079, p<.001$), a significant main effect of **STIMULATION** ($F(2,67.15)=4.601, p=.013$), but no significant **STIMULATION**×**BLOCK** interaction ($F(4,126)=0.194, p=0.941$, see Figure 25).

To further explore the significant main effect of **BLOCK**, I conducted post-hoc pairwise comparisons between the levels of the **BLOCK** variable using Tukey-adjusted tests. There was a significant increase in the percentage change in number of targets hit from block 1 between block 2 and 3 ($t(137)=-6.42, p<.001$) and between block 2 and 4 ($t(136)=-7.48, p<.001$). There was no significant difference in the percentage change in number of targets hit from block 1 between block 3 and 4 ($t(136)=-1.19, p=.458$).

3.3.1.4 Slow-γ TGP tACS results in significantly fewer number of targets hit compared to sham tACS

To explore the significant main effect of **STIMULATION**, I conducted post-hoc pairwise comparisons between the levels of the **STIMULATION** variable using Tukey-adjusted tests. Participants receiving 45Hz TGP tACS hit significantly fewer targets than participants receiving sham tACS ($t(74.1)=2.920, p=.013$). There was no significant difference between sham and 75Hz ($t(74.3)=1.951, p=.132$) or 45Hz and 75Hz ($t(74)=-1.03, p=.561$).

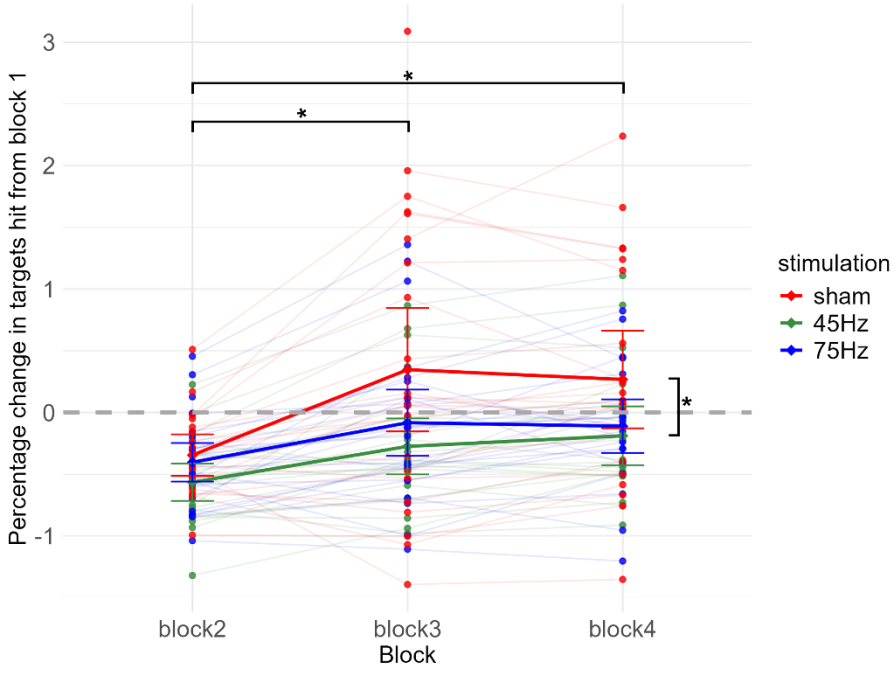

Figure 25: Percentage change in number of targets hit from block 1 (z-transformed). Lines and asterisks represent significant post-hoc contrasts (p<.050).

Thus far, analyses only encompassed the percentage change in the raw number of targets hit. Upon closer examination of the tracing data, it became clear that even if participants were able to successfully reduce the amount of tracing error around the waveform, this was not always fully captured by an increase in the number of targets hit (see Figure 26). This is likely, in part, due to the conservative error margin (15 pixels) adopted around the targets. Therefore, I decided to look at the individual

participants' tracing data and calculate the error in tracing. Error was calculated by subtracting the subject position on screen (trace) from the sinusoid (target).

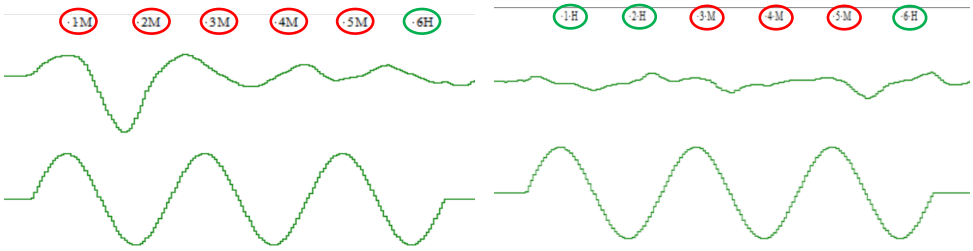

Figure 26: Example of how reductions in tracing error are not always consistently reflected in "number of targets hit". Bottom row: the sinusoid task wave. Top row: trace error data for that trial. The letters/numbers at the top state the target number and whether it was hit (H) or missed (M). Left panel: an individual participant's trace error data on trial 1. Right panel: the same participant's trace error data on trial 400.

3.3.2 Tracing error

3.3.2.1 No significant difference in error between groups in the first 10 trials

I first wanted to ensure that there were no significant differences in error between the stimulation groups at baseline (block 0). The assumption of homogeneity of variances was met, as indicated by Levene's test, ($F(2,68)=0.676, p=.512$). An independent measures ANOVA was run on the three levels of **STIMULATION** on error in block 0. There was no significant main effect of **STIMULATION** on error ($F(2,68)=0.007, p=0.993$), suggesting no significant difference in baseline error between the three stimulation groups.

3.3.2.2 No significant difference in error between groups in block 1

I then wanted to ensure that there were no significant differences in error between the stimulation groups in the first true block of learning (block 1). Levene's test demonstrated homogeneity of variance ($F(2,68)=0.450, p=0.640$). I ran a one-way ANOVA to examine the effects of **STIMULATION** on error in block 1. There was no significant main effect of **STIMULATION** on error ($F(2,68)=0.124, p=0.884$), suggesting no significant differences in the first block of learning between the three stimulation groups.

3.3.2.3 The motor learning task results in significant reductions in error over time

I constructed a linear mixed effects model with **STIMULATION** and **BLOCK** as fixed effects, and varying intercepts for **SUBJECT** (random effect). There was a significant main effect of **BLOCK** ($F(2,137.81)=100.472, p<.001$, see Figure 27). To further explore the significant main effect of **BLOCK**, I conducted post-hoc pairwise comparisons between the levels of the **BLOCK** variable using Tukey-adjusted tests. There was a significant reduction in the percentage change in tracing error from block 1 between block 2 and 3 ($t(144)=9.09, p<.001$), between block 2 and 4 ($t(145)=13.574, p<.001$), and between block 3 and 4 ($t(145)=4.582, p<.001$), suggesting that subjects improved their errors over the whole task.

3.3.2.4 No significant effect of tACS on tracing error over time

With the same linear mixed effects model, there was no significant main effect of **STIMULATION** ($F(2,70.47)=0.323, p=.725$, see Figure 27) and no significant **STIMULATION**×**BLOCK** interaction ($F(4,137.79)=2.015, p=0.096$).

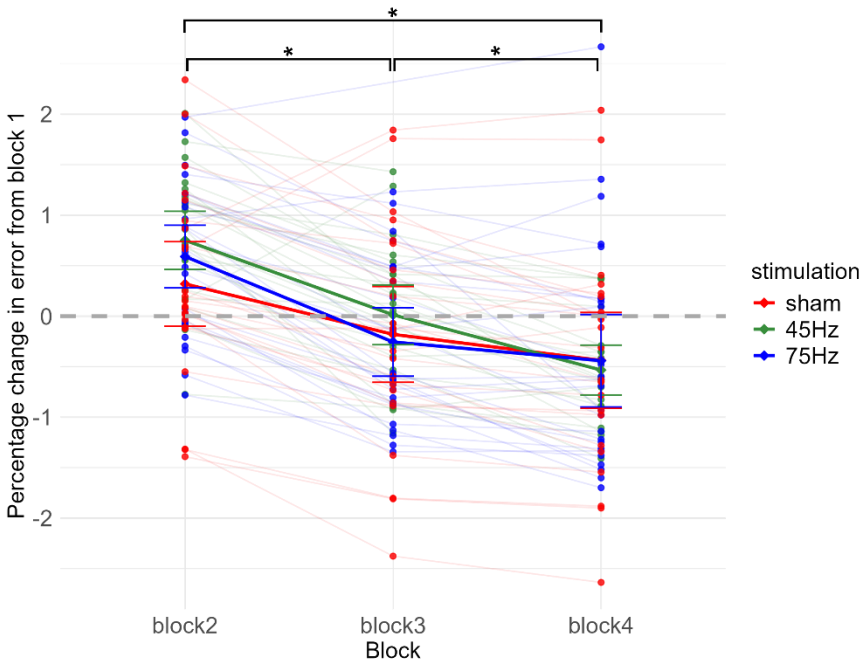

Figure 27: Mean percentage change in error from block 1 (z-transformed). Lines and asterisks represent significant post-hoc contrasts (p<.050).

3.3.3 Force modulation slopes

3.3.3.1 No significant difference in force slopes between groups in the first 10 trials

I first ensured that there were no significant differences in force slopes between the stimulation groups at baseline (block 0). Levene's test demonstrated homogeneity of variance (F(2,66)=0.660,p=.520). I ran a one-way ANOVA to examine the effects of **STIMULATION** on force slope in block 0. There was no significant main effect of **STIMULATION** on error (F(2,66)=0.905,p=.410) suggesting no significant differences in force slopes at baseline between stimulation groups.

3.3.3.2 Significant difference in force slopes between groups in block 1

I then investigated whether there were significant differences in force slope between the stimulation groups in the first true block of learning (block 1). Levene's test demonstrated homogeneity of variance (F(2,68)=0.737,p=0.482). I ran a one-way ANOVA to examine the effects of **STIMULATION** on error in block 1. There was a significant main effect of **STIMULATION** on force slope (F(2,68)=5.915,p=.004), suggesting significant differences in force slopes within the first block of learning between stimulation groups.

3.3.3.3 Slow-γ TGP tACS results in significantly shallower slopes than sham tACS

I constructed a linear mixed effects model with **STIMULATION** and **BLOCK** as fixed effects, and varying intercepts for **SUBJECT** (random effect). There was a significant main effect of **STIMULATION** F(2,71) = 5.228, p = 0.008) and **BLOCK** (F(3,213)=13.523, p<.001; see Figure 28). There was no significant **STIMULATION**×**BLOCK** interaction (F(6,213)=2.08,p=.057). To further explore the significant main effect of **STIMULATION**, I conducted post-hoc pairwise comparisons between the levels of the **STIMULATION** variable using Tukey-adjusted tests. There was a significant difference in the mean slope between sham and 45Hz (t(74.1)=3.13,p=.007) with sham stimulation showing significantly steeper slopes (estimated marginal mean = 2.16, SE = 0.164) than 45Hz (estimated marginal mean = 1.88, SE = 0.160). There was no significant difference between sham and 75Hz (t(74.1)=1.20,p=.457) or 45Hz and 75Hz (t(74.1)=-1.995),p=.120). To further

explore the significant main effect of **BLOCK**, I conducted post-hoc pairwise comparisons between the levels of the **BLOCK** variable using Tukey-adjusted tests. There was a significant reduction in the mean slope across all blocks ($p<.001$) with the exception of between block 1 and 2, and block 3 and 4.

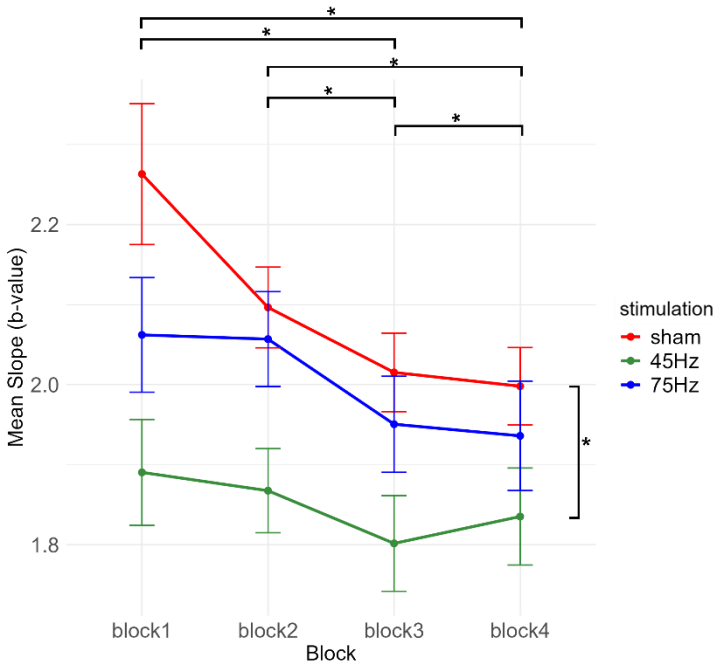

Figure 28: Mean slope by block and stimulation group

3.4 Discussion

In human M1, there are two patterns of movement-related γ activity (slow- and mid-γ) with different temporal, spectral, spatial, and physiological properties. Akkad *et al*. (2021) found that driving mid-γ (75Hz) TGP oscillations causally modulated motor behaviour. In this Chapter, I aimed to demonstrate the γ frequency-specificity of this effect by delivering either slow-(45Hz) or mid-(75Hz) γ activity in a TGP framework and looking at behavioural changes.

3.4.1 Novel motor learning task results in significant motor learning

First, I developed a novel force modulation task for the purposes of this Chapter. I wanted a basic force modulation task (see Methods for a more in-depth discussion around the rationale for the development of this task). I found that this novel task resulted in both significant increases in the number of targets hit over time as well as a significant reduction in tracing error over time. Though these metrics are inherently linked, this highlights the fact that with this task it is possible to investigate both more global and more refined metrics of motor learning.

3.4.2 The effects of slow- and mid-γ TGP on skill acquisition

3.4.2.1 No difference in number of targets hit between sham and 75Hz TGP tACS

I first attempted to replicate the finding of Akkad *et al*. (2021), albeit with a very different task and method of tACS delivery, by looking at the effect of mid-γ TGP tACS on the number of targets hit over time. Though participants receiving 75Hz TGP and sham were both able to refine their newly acquired force modulation skill to meet the spatiotemporal requirements of the task, there was no significant difference between these two groups. This was unexpected given the findings of Akkad *et al*. (2021) as well as previous behavioural (Joundi *et al.*, 2012; Moisa *et al.*, 2016; Nowak *et al.*, 2017) and neurophysiological effects of mid-γ on motor behaviour (Petri *et al.*, 2003; Sohal *et al.*, 2009; Ainsworth *et al.*, 2011). A possible explanation for this result is methodological differences between Akkad *et al*. (2021) and the present study.

Akkad *et al*. (2021) delivered 20 minutes of continuous TGP/TGT tACS during motor behaviour and argue that their positive effects are mediated by neuroplastic changes due to persistent changes in motor behaviour that outlasted the stimulation by 60 minutes. However, the mechanism of action of tACS remains unclear with studies pointing more towards a role for entrainment as opposed to neuroplasticity (Joundi *et al.*, 2012; Moisa *et al.*, 2016). As such, in this study I explored the effect of movement-locked, short bursts (3 seconds) of TGP tACS on motor behaviour to investigate entrainment as a mechanism of action as opposed to neuroplasticity. Since I was not able to replicate the findings of Akkad *et al*. (2021) it is possible that 75Hz TGP mediates its effects through neuroplastic changes and not within an entrainment framework.

3.4.2.2 Participants receiving 45Hz TGP tACS hit fewer targets than participants receiving sham tACS

Whilst I did not find any significant differences between sham and 75Hz TGP, I did find significant differences in the number of targets hit between sham and 45Hz TGP with participants receiving 45Hz TGP hitting significantly fewer targets than participants receiving sham tACS. Surprisingly, this effect was not mirrored in the error analysis. It was assumed that tracing error would provide a more precise metric of skill refinement. It is possible that the 15 pixel error margin around the targets was too liberal, such that participants could obtain a "hit" without significantly reducing their errors. However, based on qualitative feedback from participants, the task was a good level of difficulty.

Though previous literature highlights a role of driving task-relevant γ oscillations on motor learning behaviour (Joundi *et al.*, 2012; Moisa *et al.*, 2016; Nowak *et al.*, 2017), these studies entrained oscillations to mid-γ frequencies only. Studies have shown that M1 slow-γ tACS can in fact disrupt the processes involved in the acquisition and retention of motor sequences. For example, Giustiniani *et al.* (2019) found that slow-γ (40Hz) tACS over M1 during an implicit motor learning task slowed down response times in blocks requiring retrieval of a previously learned sequence following interference from a random block. This effect was repeated in a later study in cerebellar 50Hz tACS during a serial reaction time task where 50Hz γ-tACS applied to the cerebellum impaired performance in sequence learning blocks (and not in pseudorandom sequence blocks), suggesting that slow-γ cerebellar oscillations are crucial for the implicit acquisition and learning of motor sequences (Giustiniani *et al.*, 2021). Together, these results suggest that slow-γ tACS delivered over M1 during motor learning can enhance susceptibility to interference generated by random sequences. A similar disruptive effect of 40Hz tACS has been found in non-motor (auditory) tasks combined with tACS (Rufener *et al.*, 2016). Here, the neuromodulatory effect of tACS was detected (i.e. increased γ amplitudes on EEG) but accompanied by a reduction in task performance.

Explaining the mechanism behind the impaired motor learning for 45Hz γ is challenging but may be due to the disruption in E/I balance. E/I balance determines the efficiency of a given cortical region and can be viewed as an inverted U-shape in which optimal behavioural output is achieved when excitation and inhibition interact efficiently, allowing for stability and plasticity (Krause, Márquez-Ruiz and Kadosh, 2013; Heimrath *et al.*, 2014; Giustiniani *et al.*, 2019). When an optimal level of oscillatory activity is reached, an increase of the specific neuronal oscillation may actually deteriorate performance (Krause, Márquez-Ruiz and Kadosh, 2013; Rufener *et al.*, 2016; Giustiniani *et al.*, 2019). Perhaps in the present study, 45Hz oscillations were being generated by the task and the inconsistent (three second bursts) delivery

of additional 45Hz TGP tACS actually disrupted the endogenously occurring γ activity, which in turn would have disrupted the local E/I balance and subsequent favourable environment in which neuroplastic changes can occur to modulate motor learning behaviour.

3.4.3 Slow-γ TGP tACS significantly reduces force output

Based on Akkad *et al*. (2021)'s results, the authors propose that TGP may act as a "*signature of learning*" due to the detected improvements in skill acquisition. However, these results are perhaps better explained by changes in force output as opposed to changes in skill acquisition mediated by TGP oscillations. Their motor task was a ballistic thumb abduction task, an ideal task for detecting such changes.

γ oscillations are detected around the onset of force production and dissipate, even if there is continued force production (as measured on EMG; Muthukumaraswamy, 2010). This pattern of transient γ activity during constant force suggests that M1 γ oscillations encode kinematic parameters regarding movement rather than subserving muscle contraction itself (Muthukumaraswamy, 2010). In fact, high γ ERS has been shown to be correlated with the time-course of the first time derivative of force (yank) rather than with force itself (Jiang *et al.*, 2020). Causal demonstration of such an effect has been reported, for example Joundi *et al.* (2012) found that driving high γ in M1 using tACS increased force output during a visually-guided go-no-go force generation task. Therefore, the positive behavioural findings of Akkad *et al*. (2021) may not point towards TGP tACS acting as a "*signature of learning*" but rather as modulating the ability of the motor cortex to generate force output. As such, I conducted exploratory analyses on my data to investigated the effect of driving slow- and mid-γ TGP oscillations on initial force production.

Participants receiving sham tACS learnt, over time, to gradually modulate their initial force output to meet the spatiotemporal demands of the task, which translated to significant improvements in behavioural performance over time. However, I found that participants receiving slow-γ TGP tACS had significantly reduced force outputs (shallower curves) from block 1 compared to participants receiving sham tACS. Participants receiving mid-γ TGP tACS also showed reduced force outputs in block 1 compared to participants receiving sham tACS, though this was not statistically significant. The finding of reduced motor output of slow-γ TGP tACS on behaviour appears to be in line with recent optogenetic mouse data (Sala-Bayo *et al*., unpublished data). Briefly, mice were first trained to press a lever three times, consecutively. Once the skill was acquired, an additional timing rule was imposed such that the lever presses had to be performed within a certain time frame in order to obtain a reward. Mice receiving sham stimulation showed evidence of "too fast" presses, disregarding the new timing rules of the novel motor skill. However, ChR2 mice did not show this behaviour (see Figure 29). This result was interpreted as mice learning to "*refine a newly acquired skill*". However, following the results of the present study it is possible that these results are actually a reflection of reduced motor output (i.e. ChR2 mice receiving slow-γ TGP oscillations have reduced motor output which reduces the capability of "too fast" presses). Therefore, θγ oscillations may impact the motor cortex's ability to output force in a behaviourally-meaningful manner.

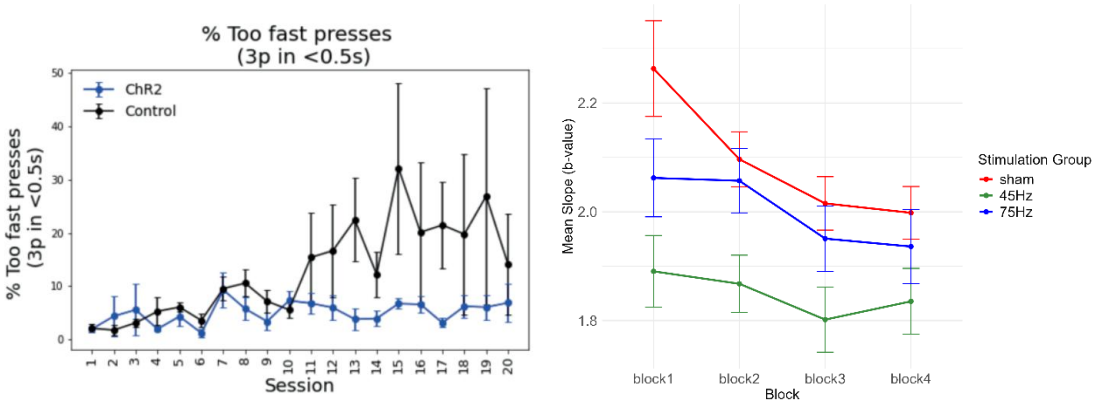

Figure 29: Left: Mouse optogenetic study looking at 45Hz TGP tACS on number of "too fast lever presses". Right: Findings from the present study that 45Hz TGP tACS reduces motor output.

3.4.4 Is slow-γ more closely related to beta?

Though not directly comparable, the finding of reduced motor output with slow-TGP tACS in the present study appears to be in line with results from other slower frequency tACS studies, such as beta (≈12-35Hz). Beta tACS over M1 has been shown to reduces motor output and movement acceleration throughout a motor task by flattening the slope indicative of improving motor performance over training (Pogosyan *et al.*, 2009; Bologna *et al.*, 2019; Leunissen *et al.*, 2022). The value of the division of the oscillatory frequency bands has more recently been questioned and it is possible that considering 45Hz as a sub-band of γ activity and assuming similar neurophysiological underpinnings and mechanisms as higher γ frequencies is an incorrect assumption. Perhaps slow-γ functionally behaves like fast beta, which would serve to explain the findings of the present study.

3.4.5 Evidence for entrainment

The finding of reductions in force output with active tACS from block 1 supports entrainment as a mechanism of action for tACS as opposed to neuroplastic effects. Neuroplastic effects are presumed to take time and would not be expected to be detected in the first block. Likewise, neuroplastic effects are unlikely to have occurred with bursts of three seconds tACS, instead requiring longer periods of stimulation (e.g. 20 minutes continuous delivery, as in Akkad *et al.*, 2021). If I had included a fifth block without tACS, I could have seen whether force output returned to baseline levels (there was no significant difference in the baseline force output across 45Hz TGP, 75Hz TGP, and sham) which would further consolidate the theory that tACS effects on force output are mediated by entrainment as opposed to plasticity. Future research may wish to compared the effect of driving slow- and mid-γ TGP as bursts versus continuously to help establish the mechanisms of tACS on motor physiology.

3.4.6 Conclusion

Overall, the γ frequency band is very broad *(>30Hz)* and there is increasing evidence that the γ sub-bands (slow, mid, fast) may be underpinned by different neurophysiological mechanisms and be involved in different aspects of motor behaviour. Akkad *et al.* (2021) report a significant effect of mid-γ TGP tACS on motor behaviour, and in this Chapter I sought to investigate whether this is a frequency-specific effect, or if other γ sub-bands delivered as part of a TGP complex had similar effects on motor behaviour.

I did not replicate the finding that 75Hz TGP tACS improves skill acquisition (no significant difference between 75Hz TGP tACS and sham on number of targets hit). However, I did find that 45Hz TGP tACS significantly hindered skill acquisition (participants receiving slow-γ TGP tACS hit significantly fewer targets than participants receiving sham tACS) due to significant reductions in force output (participants receiving slow-γ TGP tACS had significantly shallower force curves than participants receiving sham tACS). Together with the findings from a

previous optogenetic mouse study by Sala-Bayo *et al*. (unpublished data), the data from the present study highlight a potentially novel insight into the mechanisms of θγ oscillations on motor behaviour. Whilst it was previously thought that TGP oscillations modulated learning and skill acquisition, here I causally demonstrate for the first time that three second bursts of slow-γ TGP tACS in fact significantly reduces force output in a behaviourally-relevant manner.

Future research should attempt to replicate this effect in a purely force-output task, such as the one used in Akkad *et al*. (2021) and investigate potential entrainment versus neuroplastic effects by driving oscillations for shorts bursts or longer durations. This will allow us to gain a stronger understanding of the potential behavioural effects of θγ oscillations. The next step is understanding what mediates this reduction in force output at a neurophysiological level. In the next Chapter, I will investigate the effect of TGP tACS on changes in receptor-mediated inhibition and excitation using TMS to see if changes in GABAergic inhibition may underpin such reductions in force output.

CHAPTER IV - Investigating the phase specificity of θγ oscillations in healthy human motor behaviour using TMS

In this second experimental Chapter, I investigate the phase-specificity of the findings of Akkad et al. (2021) such that TGP and not TGT mediates positive behavioural changes. I replicate the stimulation protocols of Akkad et al. (2021) and systematically investigate their effects on TMS-metrics of cortical excitability and receptor-mediated excitation and inhibition.

4.1 Introduction

Transcranial Magnetic Stimulation (TMS) is a non-invasive brain stimulation tool that can be used concurrently with tACS to non-invasively assess on- and off-line effects of tACS on cortical excitability (CE; using single pulse TMS) and receptor-mediated inhibition and excitation (using paired pulse TMS). Given that cortical excitability crucially depends on the interaction between excitatory and inhibitory neurons and that weak electric fields polarise both neuron types, it is unclear how tACS modulates excitability at a neurophysiological level (Khatoun, Asamoah and Mc Laughlin, 2017).

4.1.1 The effect of tACS on TMS-derived metrics of cortical excitability and receptor-mediated inhibition/excitation

Previous studies have explored the on- and off-line effects of single frequency β-tACS on TMS metrics of CE with the majority demonstrating increases in M1 excitability (Feurra *et al.*, 2011; Guerra *et al.*, 2016; Nakazono *et al.*, 2016; Pozdniakov *et al.*, 2021) though there are some disagreements between studies (Zaghi *et al.*, 2010; Guerra *et al.*, 2018). In the γ band, however, literature is much scarcer. Nowak *et al*. (2017) found no significant effects of 75Hz γ or 20Hz β-tACS on corticospinal excitability using single pulse TMS. However, they did find a significant, duration-dependent reduction in local resting-state synaptic GABAa inhibition as quantified by short-interval intracortical inhibition (SICI; a TMS protocol for measuring inhibition) (Nowak *et al.*, 2017). Importantly, this change in SICI was closely related to performance in a motor learning task, such that participants who demonstrated a greater increase in GABAa inhibition also showed faster short-term learning (Nowak *et al.*, 2017). This finding points towards γ tACS inducing specific effects on receptor-mediated inhibition as opposed to cortical excitability more generally. However, unfortunately, this effect has not been replicated and thus warrants further investigation.

The effect of cross-frequency coupled oscillations, such as θγ PAC tACS, on TMS-metrics of cortical excitability and receptor-mediated inhibition/excitation has never been explored. In the Chapter 3, I explored the frequency-specificity of γ sub-bands within a θγ PAC complex in mediating the behavioural effects reported by Akkad *et al*. (2021) using a behavioural approach. Here, I explore the phase-specificity of γ oscillations within a θγ PAC complex (i.e. TGP versus TGT) in mediating the behavioural effects reported by Akkad *et al*. (2021) using a neurophysiological approach. Given the findings of Akkad *et al*. (2021) that TGP uniquely improves motor behaviour and the wealth of literature highlighting a relationship between motor learning and GABAergic signalling (Stagg, Bachtiar and Johansen-Berg, 2011; Bachtiar and Stagg, 2014; Nowak *et al.*, 2017; Bachtiar *et al.*, 2018; Nowak, Zich and Stagg, 2018), it is plausible that driving TGP oscillations with tACS modulates local GABAergic signalling, unlike TGT, in a way that is detectable by TMS.

4.1.2 The effects of tACS phase on TMS metrics

Beyond exploring the role of TGP and TGT tACS in modulating cortical excitability and receptor-mediated inhibition and excitation, a secondary advantage of the present study's concurrent tACS-TMS methodology is the possibility of looking at how sampling TMS pulses at different phases of an ongoing entrained oscillation affects MEP amplitude (the primary outcome metric of TMS).

Endogenous ongoing oscillatory activity has been shown to influence MEP amplitude (Desideri *et al.*, 2019), putatively due to the alternating windows of excitation and inhibition imposed by the oscillation. Whether this remains true in the context of an externally driven oscillation (such as with tACS) remains to be reliably demonstrated. On the one hand, Nakazono *et al.* (2016) found that the amplitude of a single pulse TMS MEP was affected by β-tACS in a phase-dependent manner, with the smallest MEPs recorded in the descending phase/trough of the tACS waveform. On the other hand, Guerra *et al.* (2016) report smallest single pulse TMS MEP

amplitudes when sampling at the peak of β-tACS and the largest MEP amplitudes when sampling at the trough. Phase-specific effects have also been reported by Guerra *et al.* (2016) for paired-pulse TMS protocols, ICF and SICI during β-tACS, where sampling at the zero-crossing resulted in the "worse" MEPs (less MEP facilitation with ICF and less inhibition with SICI) and sampling at the trough resulted in the "best" MEPs (more MEP facilitation with ICF and more inhibition with SICI; Guerra *et al.*, 2016). Finally, Vallence *et al.* (2021) reported no differences in MEP amplitude in single pulse and SICI when delivering TMS pulses to the peak and trough phases of α tACS. There thus appears to be conflicting evidence around the effect of tACS phase on TMS MEP amplitudes, and the direction of such an effect. Furthermore, the role of tACS phase on TMS MEP amplitudes has never been explored in a cross-frequency-coupled imposed oscillation with tACS. As more complex, cross-frequency coupled tACS waveforms are being investigated to more closely mimic endogenous oscillatory behaviours, it is important to address this gap to inform the methodology of future combined tACS-TMS studies.

4.1.3 Aim of this Chapter

To date, there has been no systematic investigation looking at how driving TGP and TGT oscillations in human M1 affects TMS-metrics of cortical excitability and receptor-mediated excitation and inhibition. Together, with the behavioural findings from Akkad *et al*. (2021), the results from this Chapter will unveil a potential neurophysiological mechanisms of TGP in positively modulating behaviour. Further exploratory analyses are conducted to look at phase-specific effects of tACS on TMS metrics, providing key methodological insights into future combined tACS-TMS studies.

4.2 Methods

4.2.1 Participants

Twenty-two healthy, right-handed participants took part in the study. Power calculations suggested we required 10 participants per stimulation condition to detect a significant difference between stimulation conditions (α=0.05, (1-β)=0.8, $\eta p2$=-.12). All participants gave their written informed consent to participate in the study, in accordance with granted ethics committee approval (Oxford CUREC2: R81071/RE001). Safety exclusion criteria for NIBS included (but was not limited to) a history, or current diagnosis, of a neurological or psychiatric disorder, a family history of epilepsy, a history, or current diagnosis, of migraines or frequent headaches, treatment with psychotropic medication (e.g., antiepileptics, antidepressants, antipsychotics, psychostimulants), the presence of metallic implants in or near the head (such as pacemakers and deep brain stimulators) and pregnancy.

4.2.2 Procedure

This study is a double-blind, sham-controlled cross-over design. Participants attended three sessions, at least seven days apart. Participants were sent the participant information sheet and invited to an online brain stimulation safety screening interview. Once assessed as stimulation-safe, participants were invited to a testing session and to sign the consent form. Participants' heads were measured to calculate the placement of the C3 and Pz electrodes. I briefly checked that the area marked under C3 was indeed M1 by delivering a few single pulse TMS pulses and checking that these were inducing MEPs.

Following the placement of the tES electrodes over C3 and Pz, I established MT_{1mV} and active MT (aMT) through the tES electrodes (requiring a ~10% increase in maximum stimulator intensity). Participants then completed the pre-, early-tACS, late-tACS, and post-tACS TMS protocol (see Figure 30).

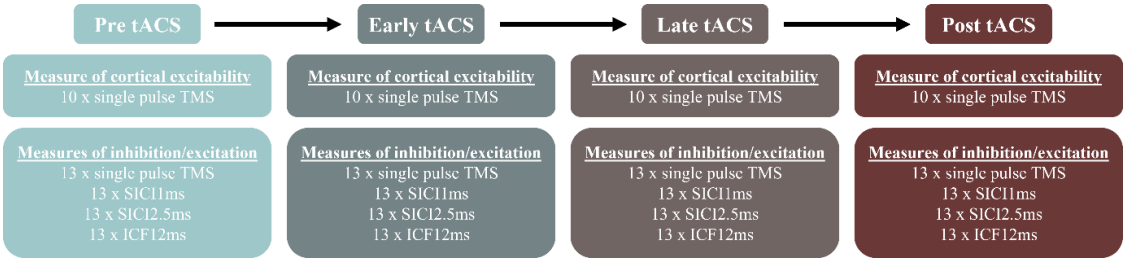

Figure 30: TMS protocols, when they were delivered, and how many MEPs were collected for each protocol. Early-tACS is five minutes into tACS delivery. Late-tACS is 15 minutes into tACS delivery. Post-tACS is immediately post-tACS delivery.

4.2.3 Apparatus and stimuli

4.2.3.1 Transcranial Magnetic Stimulation (TMS)

To interrogate motor cortical excitability, I used a CE-marked Magstim Bistim TMS unit with a standard figure-of-eight 70mm coil delivering monophasic pulses (Magstim Inc). Muscle activity in the right FDI was measured in a belly-tendon montage using surface electromyography (EMG) electrodes, amplified (Digitimer D360 amplifier; Digitimer Ltd), digitised at 5kHz (CED 1401; Cambridge Electronic Design), and stored on a computer for offline analysis (Signal software).

Establishing MT_{1mV}: To find the optimal cortical representation of the right hand FDI within the left M1 as well as the stimulator intensity needed for the study, single pulse TMS (spTMS) was applied over the area marked as C3 with the TMS coil handle pointing posteriorly and laterally to the midsagittal line. I delivered spTMS starting at 40% maximum stimulator output (MSO) and gradually increased in increments of 2% alongside concurrent systematic changes in position of the TMS coil around C3 until I identified the location where MEPs with mean peak-to-peak amplitudes of 1mv in 5/10 subsequent trials in the relaxed FDI muscle were obtained (also known as 1mV motor threshold: MT_{1mV}). This M1 "hotspot" was marked on the scalp using a marker to ensure systematic placement of the coil throughout the session. I adopted an inter-stimulus interval of at least four seconds to avoid any repetitive-TMS entrainment effects.

Establishing aMT: For paired pulse TMS (ppTMS) protocols, a subthreshold conditioning stimulus is required. Here, I calculated the lowest stimulation intensity required to produce MEPs of peak-to-peak amplitudes ≥0.2mV in 5/10 subsequent trials during weak voluntary activation of the contralateral FDI muscle at approximately 30% maximum strength (also known as active motor threshold: aMT). This value was used as the conditioning stimulus in all ppTMS protocols.

Once MT_{1mV} and aMT were established, I used these values to deliver standardised ppTMS protocols. When a subthreshold conditioning stimulus (CS) precedes a suprathreshold test stimulus (TS) by 1-5ms, short-lasting inhibition of MEP amplitude is observed, known as short-interval intracortical inhibition (SICI; Di Lazzaro *et al.*, 1998). Pharmacological studies provide strong evidence that SICI is mediated by GABAa receptor activity (Ilić *et al.*, 2002; Ziemann, 2004). When a subthreshold CS precedes a suprathreshold TS by 10-15ms, short-lasting facilitation of the MEP amplitude is observed, known as Intracortical Facilitation (ICF). Pharmacological studies also provide evidence that ICF is mediated by NMDA-r mechanisms (glutamatergic signalling) since the delivery of NMDA antagonists (such as Dextromethorpan) decreases the magnitude of ICF (Reis *et al.*, 2008).

In the present study, I set the CS at 70% of aMT and the TS to 100% MT_{1mV}. I used three types of ppTMS protocols, defined in Table 1. The data acquisition software,

Signal (version 7; Cambridge Electronic Design), was used to deliver a pseudorandomised combination of four TMS "states" (see Table 1 and Figure 11) to assess cortical excitability and receptor-mediated inhibition and excitation before, during, and after tACS.

State	Type of pulse	ISI (ms)	Neurophysiological correlate
1	Single pulse: MT_{1mV}	--	Cortical excitability
2	Paired pulse: $SICI_{1ms}$	1	Extrasynaptic GABA activity
3	Paired pulse: $SICI_{2.5ms}$	2.5	Synaptic GABAa receptor activity
4	Paired pulse: ICF_{12ms}	12	Glutamatergic activity associated with NMDAR

Table 1: TMS protocols. ISI: Interstimulus interval in milliseconds (ms)

All MEP data underwent quality controls prior to analysis. For spTMS, trials with FDI precontraction (EMG amplitude >0.15mV in the 50ms preceding the test pulse) were excluded. Subsequently, peak-to-peak MEP amplitudes for each trial were calculated. MEPs with peak-to-peak amplitudes >3mV or <0.15mV were excluded. This resulted in 19.7% of spTMS trials being excluded. For ppTMS, trials with an MEP amplitude <0.1mV where the preceding single test pulse had an MEP amplitude <0.15mV were excluded. For all remaining surviving trials, I performed two outlier tests (>2SD from the mean and Grubbs test), and removed any trials which were identified as outliers. This resulted in 21.15% of test pulse trials, 9.97% SICI1ms trials, 9.73% SICI2.5ms trials, and 12.38% ICF12ms trials being excluded.

For each SICI and ICF protocol interval at each timepoint, I calculated the ratio between the mean amplitude of the paired-pulse and the single-pulse MEPs at the adjusted intensity (ppMEP/spMEP), such that smaller values reflected greater levels of GABAergic-mediated inhibition (for $SICI_{1ms}$ and $SICI_{2.5ms}$) and greater values reflected NMDA-receptor mediated facilitation (for ICF_{12ms}). I compared these values between tACS waveform using a two-way repeated measures ANOVA with within-subject factors of **STIMULATION** (TGP, TGT, sham) and **TIMEPOINT** (pre, early, late, post).

4.2.3.2 Transcranial Alternating Current Stimulation (tACS)

I delivered three stimulation protocols per participant (at least seven days apart): TGP, (75Hz γ phase amplitude coupled to the positive half of a 6Hz θ wave), θγ trough (75Hz γ phase amplitude coupled to the negative half of a 6Hz θ wave), and sham (10 seconds empty 6Hz θ at the start and end of the stimulating period; see Figure 31). Each waveform was 2mA peak-to-peak and delivered continuously for 20-minutes. All waveforms were custom-coded in Spike2 (Cambridge Electronic Design, 2024) and delivered to a NeuroConn stimulator (Neurocare, 2024) via Remote Mode. The custom coded waveform files were saved as "A", "B", or "C" by an independent researcher such that when I ran the waveforms, I was blinded to what condition participants were in. The order in which participants received TGP, TGT, and sham stimulation was randomised using a randomisation software and counterbalanced to avoid order-effects. Furthermore, I ensured to control for any time-of-day effects by ensuring that all participants' testing sessions were at the same time.

Two 5x5cm rubber conductive tES electrodes were centred over C3 and Pz, in accordance with the 10-20 EEG system. Ten20 electrode paste was used as a conducting medium between the scalp and the electrodes. Impedance was kept below 10kΩ throughout the session. The scalp under C3 and Pz was prepped using abrasive paste (NuPrep) and a cotton tip and wiped clean using an alcohol wipe to reduce impedance. tES electrodes were secured in place using rubber straps and a mesh cap.

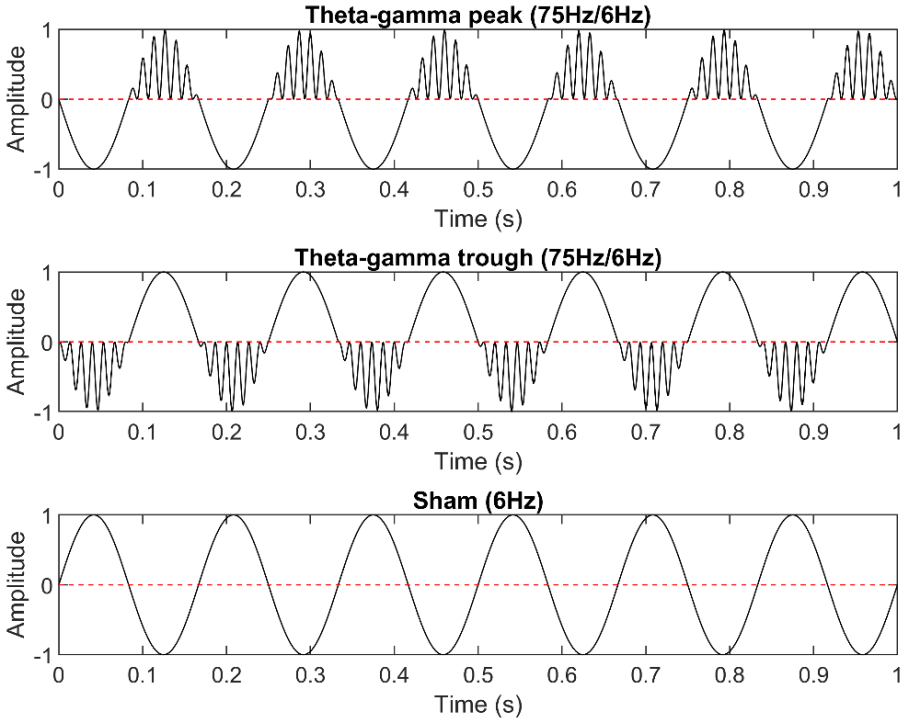

Figure 31: θγ coupled waveforms: θγ peak (top), θγ trough (middle), and sham (bottom).

4.2.4 Phase analysis

During the delivery of tACS, I recorded the phase at which each TMS pulse type (single pulse, SICI1ms, SICI2.5ms, and ICF12ms) was sampled. TMS pulses were stochastically delivered (ISI: 4.2ms) throughout the delivery of tACS to capture the effects of sampling various TMS pulses at the ascending, peak, descending, or trough phase (see Figure 32).

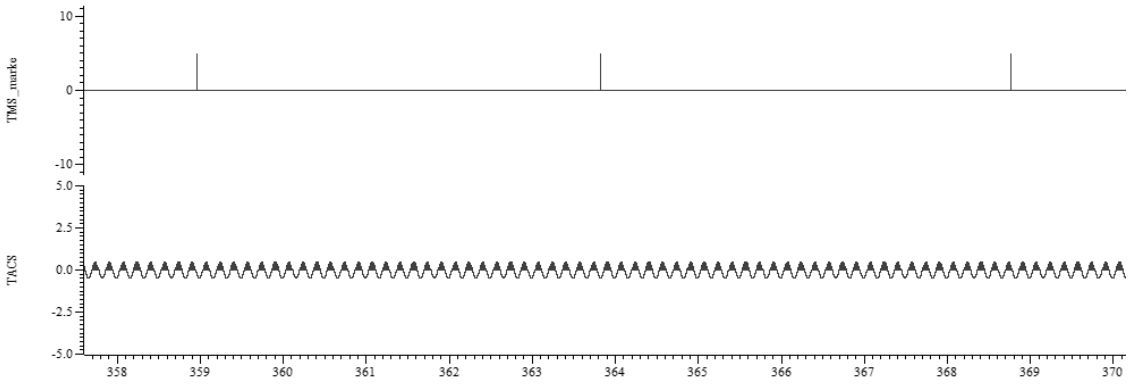

Figure 32: Example of the TMS test stimulus (top) and the delivered tACS waveform (bottom). I used this data to extract the phase at which each TMS pulse was sampled to investigate phase-dependent effects of tACS on MEP amplitude across different TMS protocols.

To extract the phase data, I loaded the file containing the tACS and TMS data on an individual subject-by-subject and session basis (see Figure 33). I calculated the individual time stamps of all of the TMS pulses delivered during tACS and extracted the timestamps of the TMS pulses for which I had recorded MEP data (i.e. excluding any preparatory pulses).

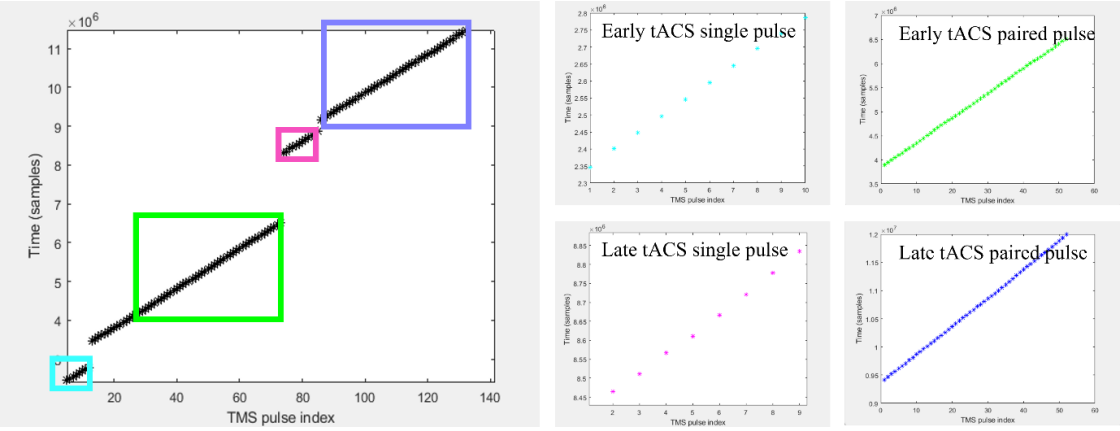

Figure 33: Example of one participant's TMS timestamps over time (left). Blue box: TMS timestamps for early-tACS single pulse (10 pulses), green box: early-tACS paired pulse (52 pulses), pink box: late-tACS single pulse, purple box: late-tACS paired pulse.

In the tACS data, I applied a low-pass Butterworth filter with a cut-off frequency of 20Hz to filter out the γ activity, as this simplified phase calculations (see Figure 34). I then calculated the phase of the filtered tACS waveforms in radians using a Hilbert transform and converted this to degrees (see Figure 34). The resulting phase information was thus in degrees ranging from 180 to -180 degrees. I defined "ascending" as phases between >-136 and ≤-45 degrees, "peak" as >-45 and ≤45 degrees, "descending" as >45 and ≤135 degrees, and "trough" as combined between >135 and ≤180, and ≥-180 and ≤-136 degrees. I then extracted the phase at which each individual TMS timestamp fell along the waveform. Figure 35 shows examples of TMS pulses sampled at different tACS phases (peak [top left], descending [top right], trough [bottom left], and ascending [bottom right]). This data extraction process resulted in a table containing information about stimulation session (TGP, TGT, sham), state (single pulse, SICI1ms, SICI2.5ms, ICF12ms), phase (180 to -180 degrees) and MEP amplitude (mV) of every TMS pulse delivered during tACS.

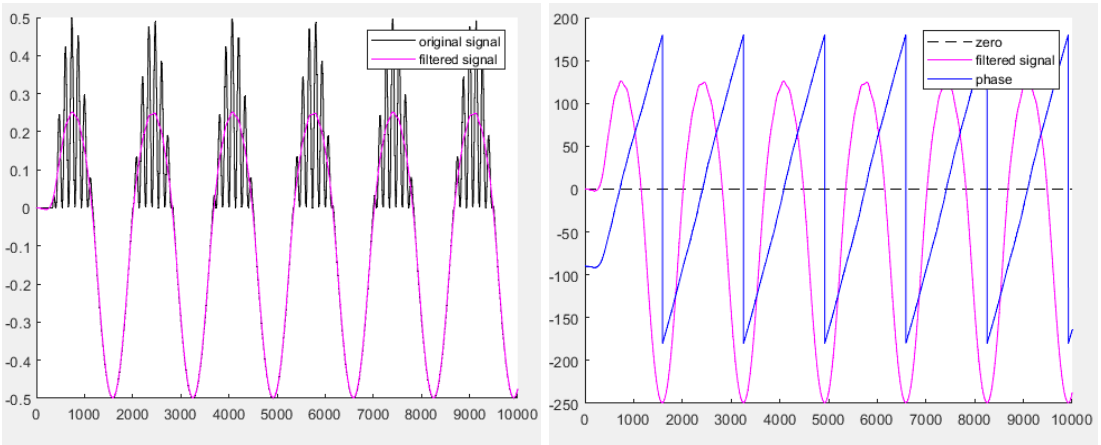

Figure 34: Filtering (left) and calculating phase (right) of the tACS waveform.

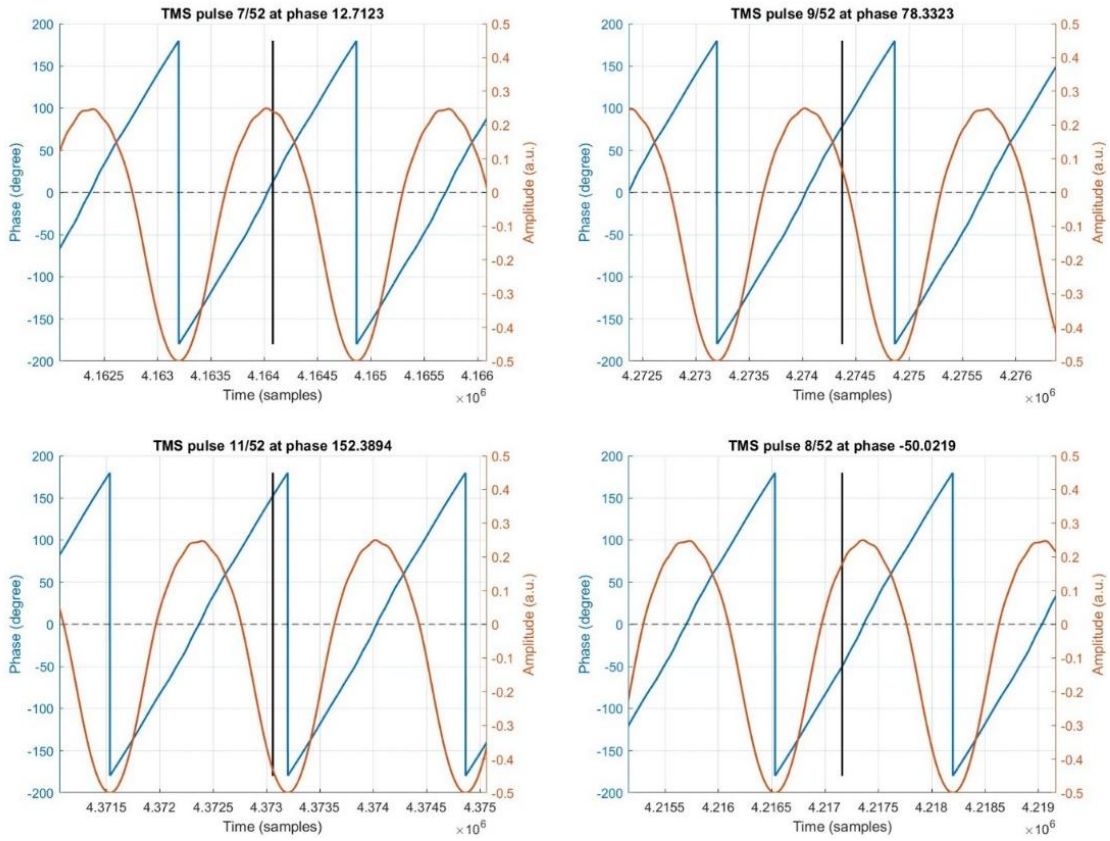

Figure 35: Examples of how phase information was extracted from the individual TMS pulses along the tACS waveform. Red line: Butterworth-filtered tACS waveform. Blue line: Phase as computed by the Hilbert transform. Black line: test pulse of the paired TMS pulse.

4.2.5 Statistical analysis

All TMS analyses look at the respective percentage change in TMS metric from baseline (pre-tACS), using the following equation:

((second measure - baseline measure)/baseline measure)×100%

All data pre-processing was carried out in MATLAB (version R2024a; The MathWorks) and all statistical analyses performed using the linear mixed effects model (lme4) package in R software (Bates *et al.*, 2015). All data were z-transformed across stimulation group and timepoint, and Grubbs outlier detection was run on all individual stimulation by timepoint combinations. As fixed effects, I entered **STIMULATION** and **TIMEPOINT** with a **STIMULATION×TIMEPOINT** interaction into the model.

For the phase analysis, I entered **STIMULATION** and **PHASE** as fixed effects. I allowed intercepts for different subjects to vary in order to account for covarying residuals within subjects (creating a random intercept model of "subject"). Estimated marginal means for each stimulation condition were computed, and post hoc pairwise comparisons using Tukey-adjusted tests were run on the level of significant main effects. Visual inspection of residual plots did not reveal any obvious deviations from homoscedasticity or normality.

4.3 TMS results

4.3.1 No systematic differences in pre-tACS data

I first ensured that there were no systematic differences in my data between sessions at baseline ("pre-tACS"). I extracted the pre-tACS data of interest for each analysis (single pulse, SICI1ms, SICI2.5ms, ICF12ms) and ran a repeated-measures ANOVA with one factor of **STIMULATION** (TGP, TGT, and sham). There was no significant main effect of

STIMULATION on the pre-tACS data for any TMS protocol and all protocols induced the expected inhibition or facilitation (see Table 2 for a summary).

Pre-tACS data	Statistic	Mean MEP amplitude	Expected inhibition/excitation?
Single pulse	(F(2,42)=.250,p=0.780)	1.13mV	--
SICI1ms	(F(2,42)=0.461,p=0.634)	0.52mV	Yes
SICI2.5ms	(F(2,42)=0.882,p=0.422)	0.86mV	Yes
ICF12ms	(F(2,42)=0.792,p=0.460)	1.11mV	Yes

Table 2: Summary statistics of the pre-tACS data across all stimulation conditions.

4.3.2 The effect of θγ oscillations on cortical excitability

Having confirmed that there were no systematic differences between sessions and that my TMS protocols had the expected effects, I examined the effects of driving θγ oscillations on cortical excitability. I first looked at whether there were any changes in cortical excitability over time when participants received sham stimulation to establish a close approximation to what naturally occurs in the brain in the present protocol. I filtered the data to include only the sham data and ran a linear mixed effects model with a fixed effect of **TIMEPOINT** and I allowed intercepts for different subjects to vary in order to account for covarying residuals within subjects (creating a random intercept model of "subject"). There was no significant main effect of **TIMEPOINT** (F(2,41.243),p=.221) on the percentage change in MEP amplitude from pre-tACS when participants received sham stimulation.

When including all groups (TGP, TGT, and sham), there was a significant main effect of **STIMULATION** (F(2,167.55)=4.22,p=.016). There was no significant main effect of **TIMEPOINT** (F(2,167.08)=0.373,p=.689) and no significant **STIMULATION×TIMEPOINT** interaction (F(4,167.29)=1.319,p=.265). To further explore the significant main effect of **STIMULATION**, I conducted post-hoc pairwise comparisons between the levels of the **STIMULATION** variable using Tukey-adjusted tests. There was a significant difference between sham and TGT (estimate=0.389, SE=0.146, t(177)=2.67, p=.023) with participants receiving TGT showing significantly reduced cortical excitability compared to sham. There was no significant difference between sham and TGP (t(176)=2.16,p=.081) nor between TGP and TGT (t(176)=0.536,p=.854).

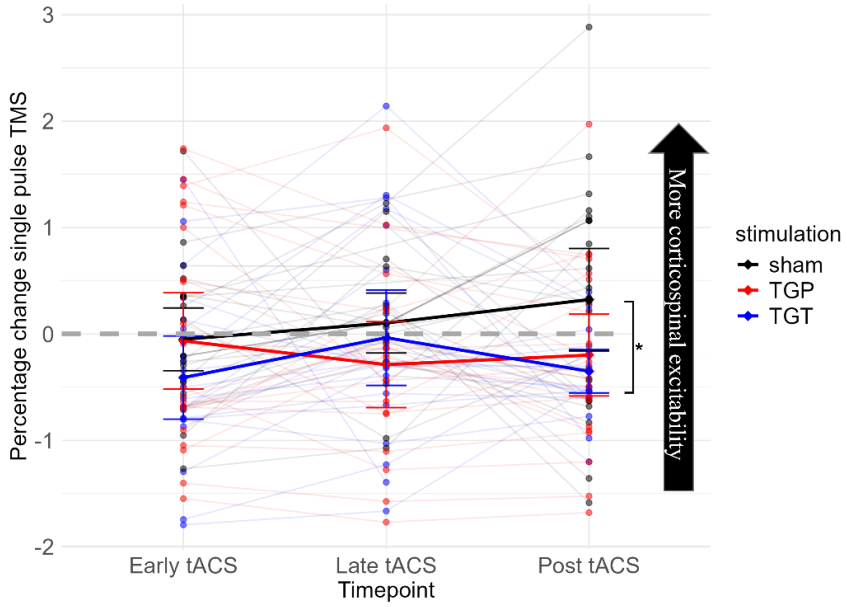

Figure 36: Percentage change in single pulse TMS from pre-tACS over time by stimulation.

4.3.3 The effect of θγ oscillations on receptor-mediated inhibition and excitation

Before running the analyses on the individual ppTMS protocols, I first wanted to confirm that there were no systematic differences in the amplitude of the TS used in the ppTMS protocols

throughout the experiment. Though the TS is also a single pulse, it is important to note that the TS and spTMS are different. The MSO for the ppTMS TS is adjusted throughout the session to account for potential effects of stimulation on cortical excitability and is always kept ≈1mV. The MSO for the spTMS however is kept the same throughout the session to capture changes in cortical excitability. I performed a repeated measures ANOVA with one factor of **STIMULATION** (TGP, TGT, sham) and one factor of **TIMEPOINT** (pre-, early-, late-, post-tACS) on the TS TMS data. There was no significant main effect of **STIMULATION** ($F(2,227.09)=2.146, p=.119$). There was, however, a significant main effect of **TIMEPOINT** ($F(3,227.55)=4.637, p=.003$) with a significant increase in mean TS from pre- to post-tACS ($t(242)=-2.694, p=.038$) and from early- to post-tACS ($t(242)=-3.406, p=.004$). There was no significant **STIMULATION×TIMEPOINT** interaction ($F(6,227)=0.318, p=.926$). Therefore, across all stimulation conditions the TS increased over time. As such, I normalised all of the MEP paired pulse data to their respective sham data by subtracting the mean sham value at each timepoint. All subsequent paired pulse figures thus show the TGP and TGT groups only, normalised to sham.

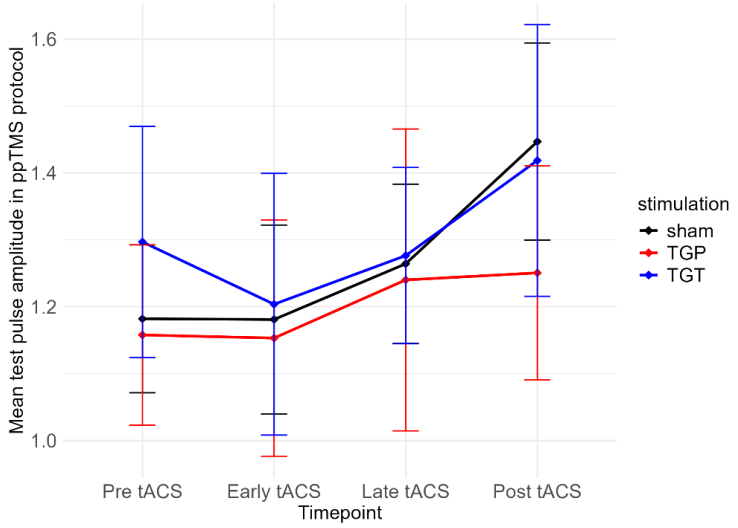

Figure 37: Mean test pulse amplitude used in the ratio calculations of the ppTMS protocols over the four timepoints. Though the amplitude of the test pulse increases over time, this is across all stimulation groups and within the normal limits of TMS literature.

4.3.4 The effect of θγ oscillations on SICI1ms

I then investigated the effects of driving θγ oscillations on local GABAergic and glutamatergic activity, as reflected by MEP amplitudes in my ppTMS protocols (SICI1ms, SICI2.5ms, and ICF12ms). For these analyses, the percentage change SICI1ms from pre-tACS were used.

There was a significant main effect of **STIMULATION** ($F(1,103.28)=5.26, p=.024$) and **TIMEPOINT** ($F(2,103.2)=4.122, p=.019$). There was no significant **STIMULATION×TIMEPOINT** interaction ($F(2,103.4)=1.527, p=.22$). To further explore the significant main effect of **TIMEPOINT**, I conducted post-hoc pairwise comparisons between the levels of the **TIMEPOINT** variable using Tukey-adjusted tests. There was a significant difference between early- and late-tACS ($t(109)=2.424, p=.045$) and between early and post-tACS ($t(109)=-2.442, p=.043$). I then ran exploratory t-tests looking at the difference in percentage change SICI1ms between TGP and TGT at late- and post-tACS. There was a significant difference between TGP and TGT on the percentage change in SICI1ms at late-tACS, with TGP showing greater reductions in inhibition compared to TGT ($t(31.26)=2.068, p=.047$). There was no significant difference between TGP and TGT on the percentage change in SICI1ms at post-tACS ($t(39.80)=1.43, p=.161$).

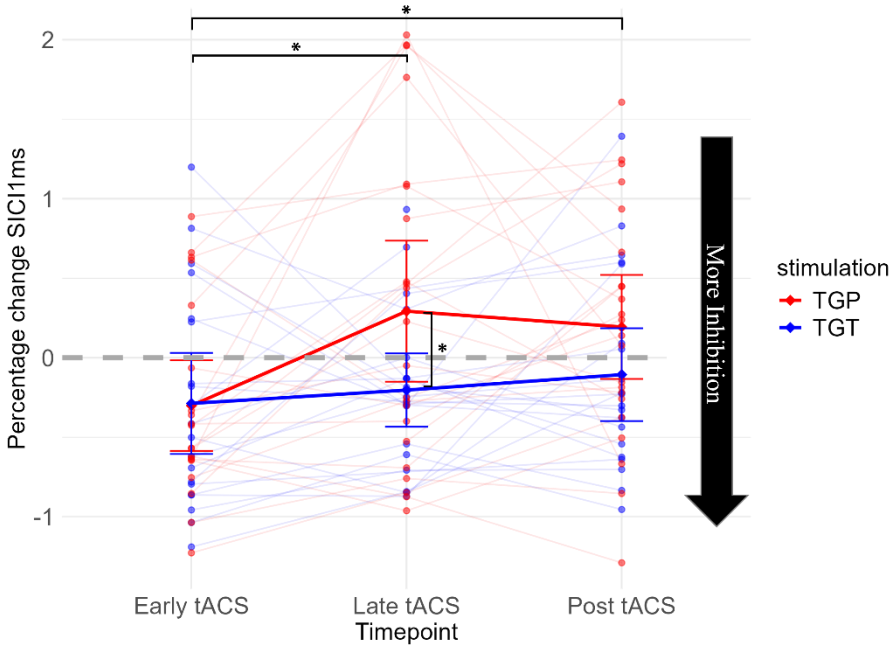

Figure 38: Percentage change in SICI1ms from pre-tACS over time by stimulation (normalised to sham).

4.3.5 The effect of θγ oscillations on SICI2.5ms

For SICI2.5ms, there was no significant main effect of **STIMULATION** (F(1,107.22)=0.772,p=.382). There was a significant main effect of **TIMEPOINT** (F(2,107.3)=6.117,p=.003). There was no significant **STIMULATION×TIMEPOINT** interaction (F(2,107.3)=0.245,p=.783). To further explore the significant main effect of **TIMEPOINT**, I conducted post-hoc pairwise comparisons between the levels of the **TIMEPOINT** variable using Tukey-adjusted tests. There was a significant increase in percentage change of SICI2.5ms from late- to post-tACS (t(113)=-3.414,p=.003).

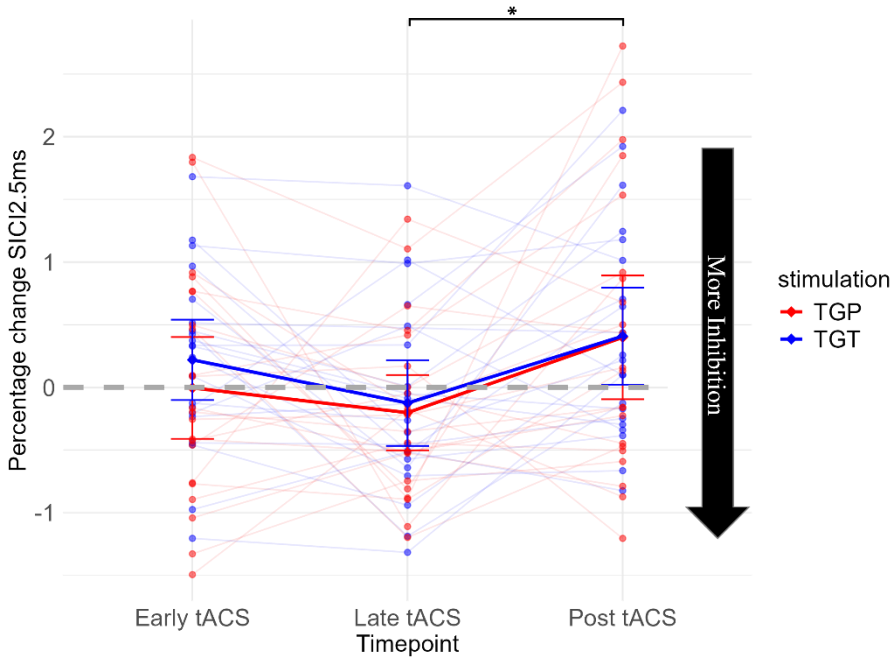

Figure 39: Percentage change in SICI2.5ms from pre-tACS over time by stimulation (normalised to sham).

4.3.6 The effect of θγ oscillations on ICF12ms

Finally, I investigated the effects of stimulation on local glutamatergic activity, as reflected by ICF12ms. There was no significant main effect of **STIMULATION** ($F(1,107.23)=0.932, p=.337$). There was a significant main effect of **TIMEPOINT** ($F(2,107.22)=5.574, p=.005$). There was no significant **STIMULATION×TIMEPOINT** interaction ($F(2,107.22)=2.342, p=.101$). To further explore the significant main effect of **TIMEPOINT**, I conducted post-hoc pairwise comparisons between the levels of the TIMEPOINT variable using Tukey-adjusted tests. There was a significant increase in percentage change ICF12ms from early- to late-tACS ($t(113)=3.109, p=.007$).

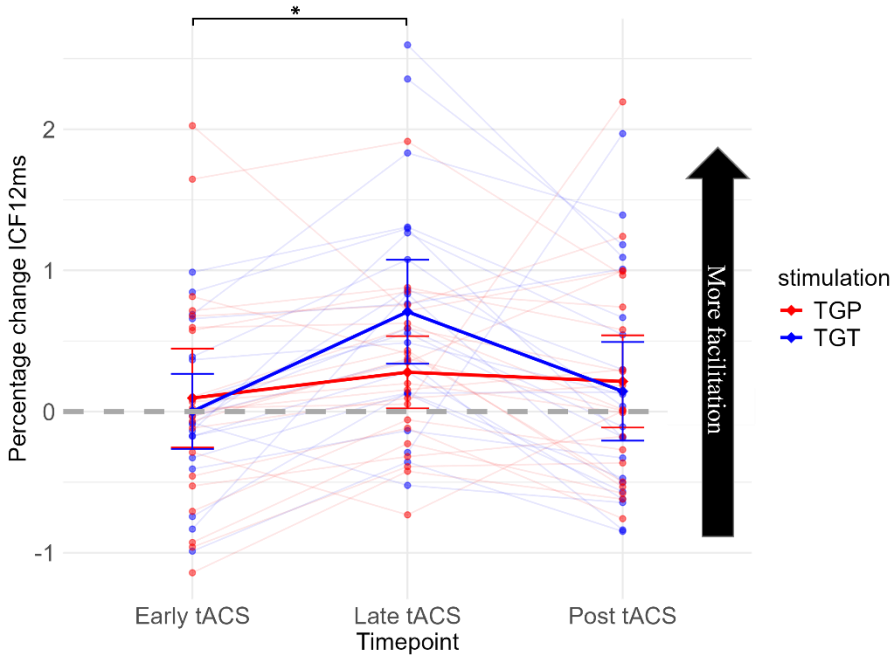

Figure 40: Percentage change in ICF12ms from pre-tACS over time by stimulation (normalised to sham).

4.4 Phase results

4.4.1 Phase distribution of TMS pulses

The same pre-processed MEP data was used for the phase analysis. However, whilst MEPs with peak-to-peak amplitudes >3mV or <0.15mV were excluded in the TMS analysis, in the phase analysis all MEPs of all amplitudes were included. This is because if phase is thought to have an effect on MEP amplitude, then the inclusion of these outliers may provide important information about the effect of tACS phase on MEP amplitude.

First, I first wanted to ensure that the distribution of my sampled phases was stochastically distributed throughout the different tACS waveforms. Polar plots in Figure 41 show the distribution of tACS phases at which the TMS pulses (spTMS and the TS of ppTMS trials) were delivered. I then ran a Chi Square analysis to compare the distributions of TGT and TGP to ensure there were no significant differences in the number of recordings per bin across subjects per TMS pulse type and stimulation condition. There was no significant difference in the distribution of pulses for TGP and TGT for single pulse TMS ($\chi^2(17)=21.037, p=.225$) or SICI1ms ($\chi^2(17)=25.404, p=.086$). However, I did find significant differences in the distribution of pulses for TGP and TGT in SICI2.5ms ($\chi^2(17)=30.081, p=.026$) and ICF12ms ($\chi^2(17)=31.372, p=.018$). Having confirmed that the phases were randomly distributed, I went on to investigate the effect of phase for each type of TMS pulse (spTMS and ppTMS) and at both timepoints (early- and late-tACS).

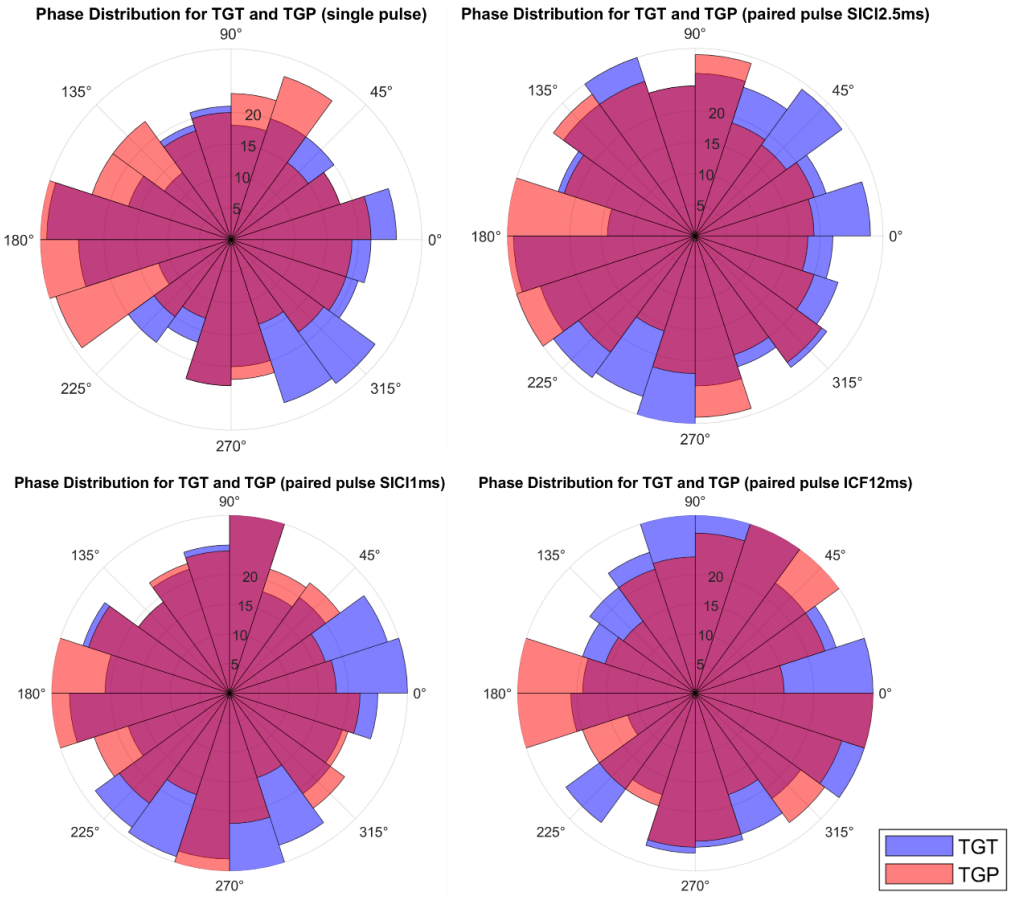

Figure 41: Polar histogram plots showing the distribution of the phase of the TMS pulses along the TGT and TGP waveforms across the four TMS metrics.

4.4.2 The effect of phase on single pulse TMS

I first investigated the effects of phase on spTMS MEP amplitudes. There was a significant main effect of **STIMULATION** (F(1,823.78)=5.984,p=.015. There was no significant main effect of **PHASE** (F(1,828.29)=0.520,p=.669) and no significant **STIMULATION×PHASE** interaction (F(3,830.58)=0.156,p=.093; see Figure 42).

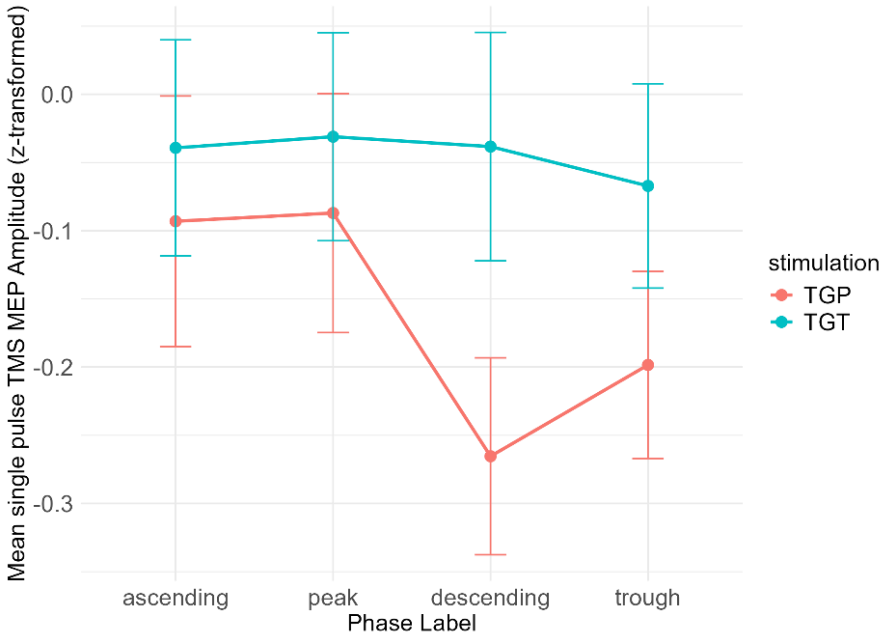

Figure 42: Effect of phase on single pulse TMS MEP amplitude.

4.4.3 The effect of phase on SICI1ms

Next, I investigated the effects of phase on SICI1ms MEP amplitudes. There was a significant main effect of **STIMULATION** (F(1,977.17)=4.025, p=.0451). There was no significant main effect of **PHASE** (F(3,978.18)=2.279,p=.078 and no significant **STIMULATION×PHASE** interaction (F(3,977.55)=0.765,p=.514; see Figure 43).

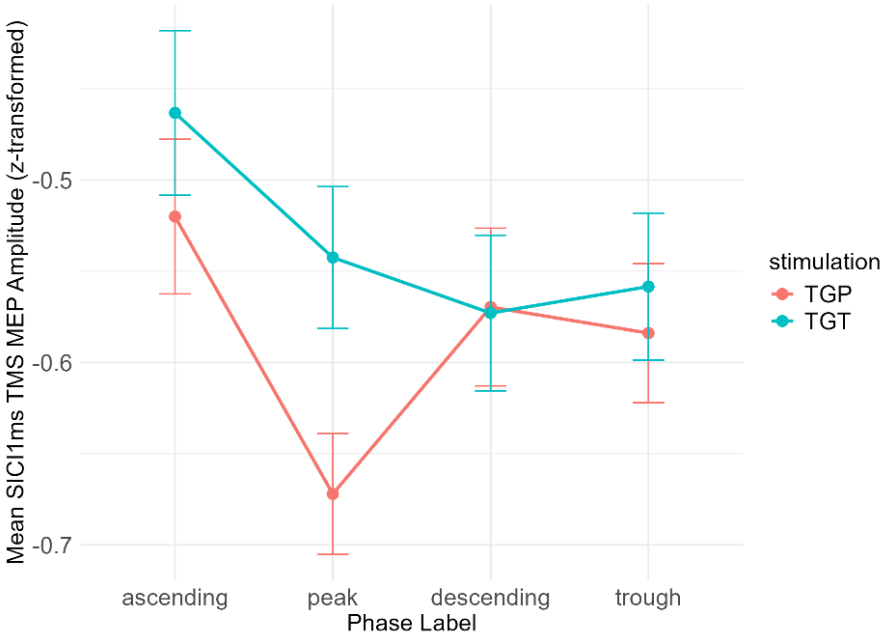

Figure 43: The effect of phase on SICI1ms MEP amplitude.

4.4.4 The effect of phase on SICI2.5ms

Next, I investigated the effects of phase on SICI2.5ms MEP amplitudes. There was no significant main effect of **STIMULATION** (F(1,994.60)=1.623,p=.203), **PHASE** (F(3,997.92)=1.037,p=.376) and no significant **STIMULATION×PHASE** interaction (F(3,996.35)=0.297,p=.827; see Figure 44).

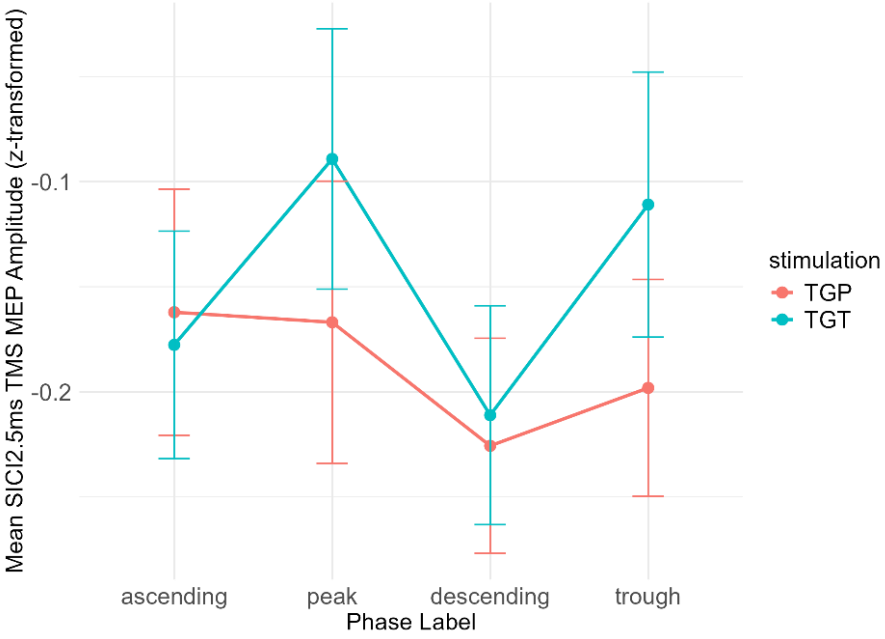

Figure 44: The effect of phase on SICI2.5ms MEP amplitude.

4.4.5 The effect of phase on ICF12ms

Finally, I investigated the effects of phase on ICF12ms MEP amplitudes. There was no significant main effect of **STIMULATION** (F(1,994.71)=2.921,p=.088), **PHASE** (F(3,995.98)=0.852,p=.720) and no significant **STIMULATION×PHASE** interaction (F(3,997.44)=0.447,p=.719; see Figure 45).

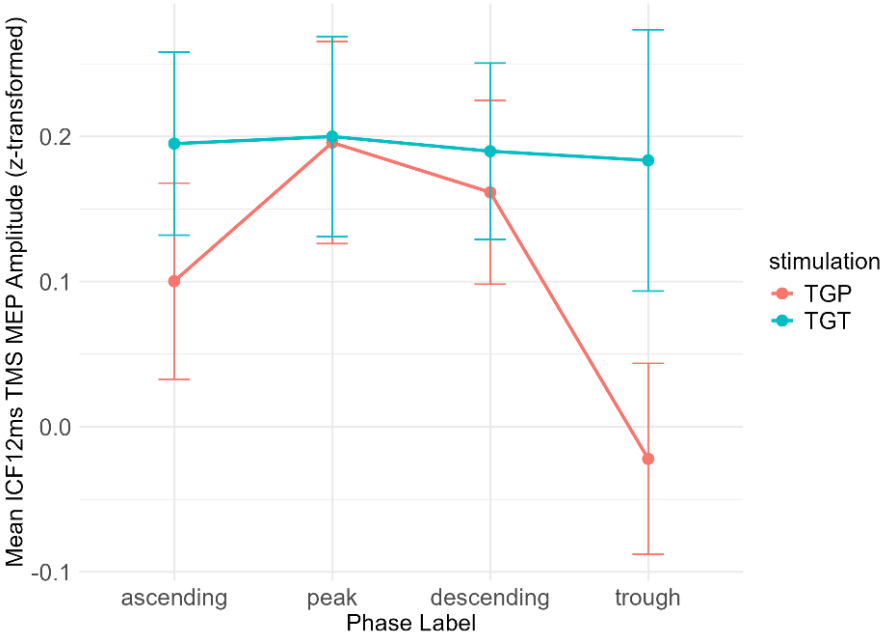

Figure 45: The effect of phase on ICF12ms MEP amplitude.

4.5 Discussion

4.5.1 Summary

The entrainment of TGP (and not TGT) oscillations in healthy human M1 has been shown to improve motor behaviour (Akkad *et al.*, 2021). Hypotheses around the role of changes in excitation/inhibition (E/I) balance, specifically changes in GABAergic signalling, in mediating this effect have been proposed, but never systematically investigated. Here, I investigated the effect of entraining 20 minutes of continuous TGP, TGT, and sham oscillations within the same participant over three sessions affected TMS-metrics of cortical excitability and receptor-mediated inhibition and excitation using single and paired pulse TMS, respectively. I sampled single and paired pulse TMS (SICI1ms, SICI2.5ms, and ICF12ms) at pre-tACS, early-tACS (five minutes into tACS), late-tACS (15 minutes into tACS), and post-tACS. Participants were at rest throughout the entire session. Further exploratory analyses were performed investigating the effect of online tACS phase on the various TMS metrics.

4.5.2 TGT tACS significantly reduced corticospinal excitability compared to sham

I first explored the effects of TGP, TGT, and sham on cortical excitability using single pulse TMS. I sampled single pulse TMS at pre, early-, late-, and post-tACS whilst keeping the test pulse the same throughout the session. I found that the entrainment of TGT oscillations resulted in a significant reduction in corticospinal excitability, compared to sham stimulation. It is possible that TGT oscillations reduced corticospinal excitability due to the mechanisms of θ oscillations in synaptic plasticity and neuronal inhibition. For example, continuous theta burst stimulation literature (cTBS; a repetitive TMS protocol that has been shown to increase θ power in resting-state EEG, Vernet *et al.*, 2013) has reported that driving θ power significantly increases in GABA (as measured with Magnetic Resonance Spectroscopy) and reduces MEP amplitudes (as measured using single pulse TMS; Matsuta *et al.*, 2022). However, if it is the frequency of the θ envelope that drives the effects, then I should have seen this effect for both

TGT and TGP. The fact that I only detected changes in corticospinal excitability with TGT points towards the delivery of phase-specific γ mediating this effect. The troughs of θ oscillations are associated with increased inhibitory processes which can suppress neuronal firing, lead to long-term depression of synaptic activity, and reduce corticospinal output. This is supported by Huerta and Lisman (1996) who found that the delivery of low-frequency stimulation at the negative troughs of an ongoing induced θ oscillation resulted in LTD in hippocampal slices. Therefore, when θ oscillations are at their troughs, they increase local inhibitory tone due to synchronised activity of inhibitory interneurons. When γ activity is nested at the trough of a θ envelope, it is superimposed on a background of inhibition. This inhibitory state limits the ability of γ bursts to entraining firing within local circuits (Sohal, 2016). Therefore, despite the presence of γ oscillations, the ongoing inhibitory tone set by the θ rhythm likely suppresses the net excitability of the cortical network.

4.5.3 TGP tACS significantly reduced extrasynaptic GABAergic tone

I then explored the effects of driving TGP, TGT, and sham oscillations on GABAa receptor-mediated inhibition. GABAa receptors are the major inhibitory receptors in the brain and can be found at both synaptic and extrasynaptic membranes (Wu *et al.*, 2013). Whilst synaptic GABAa receptors mediate phasic inhibition, extrasynaptic GABAa receptors mediate tonic inhibition (Wu *et al.*, 2013). Both phasic and tonic inhibition are necessary in regulating neuronal activity. Paired pulse TMS can be used to probe the activity of these different receptor subtypes. SICI1ms measures extrasynaptic GABAa receptor-mediated inhibition (thus providing insight into levels of tonic inhibition). SICI2.5ms measures synaptic GABAa receptor-mediated inhibition (thus providing insight into the levels of phasic inhibition or the transient inhibitory postsynaptic potentials that follow the synaptic release of GABA). I sampled SICI1ms and SICI2.5ms at pre, early-, late-, and post-tACS whilst changing the TS throughout the session to account for any corticospinal excitability change.

I first investigated whether the TS I used to sample the ppTMS protocols was consistent throughout the sessions and across the stimulation groups (i.e. that the TS was correctly adjusted to ≈1mV throughout the session to account for changes in corticospinal excitability). I found significant increases in the TS over time. Whilst this was unexpected, upon closer examination of the individual values, the greatest discrepancy was 0.4mV which is within the tolerance of noisy TMS data. The TS was challenging to reliably keep around 1mV after tACS. Importantly however, this significant change in test pulse was consistent across groups. Therefore, any significant effects of stimulation in the ppTMS results was likely not simply as a result of changes in TS amplitude. However, to account for these effects, I normalised all TGP and TGT measures to sham by subtracting the mean of the sham group at each timepoint for TGP and TGT. Future analyses may involve covarying the single pulse amplitude in an ANCOVA to account for such effects.

I found that driving TGP oscillations for 15 minutes uniquely reduced extrasynaptic GABAergic tone (as measured with SICI1ms) with no significant effects on synaptic GABAa transmission (as measured with SICI2.5ms). The finding of reduced inhibitory signalling with TGP serves to explain the positive behavioural findings of Akkad *et al*. (2021) since reductions in GABAergic signalling are central to motor plasticity (Stagg, Bachtiar and Johansen-Berg, 2011; Bachtiar and Stagg, 2014; Nowak *et al.*, 2017; Nowak, Zich and Stagg, 2018). I did not include a motor task in the present study, participants received 20 minutes of tACS at rest, and no pre/post measure of motor behaviour was assessed. Providing correlations between this reduction in SICI1ms with behavioural performance would have provided greater insight into the effects of tACS on motor physiology and subsequent behaviour.

The finding of changes in extrasynaptic GABAergic signalling, despite the absence of a task, was unexpected. In Chapter 3, I provided evidence in favour of the theory of entrainment such

that behavioural changes were detected with short bursts of tACS from the start of the experiment. The ability for tACS to successfully entrain endogenous oscillations is dependent on the tACS frequency being at or close to the relevant endogenous frequency (Weinrich *et al.*, 2017; Lazzaro *et al.*, 2022; Vogeti, Boetzel and Herrmann, 2022). As such, it was plausible that since no motor (learning) behaviour was occurring during tACS, the tACS would not have anything to entrain onto and thus not modulate local GABAergic signalling. It is also unlikely that 2mA tACS would entrain *de-novo* oscillations (and thus modulate local neurophysiology in such a way that is detected by TMS). However, the fact that I found changes in SICI1ms after 15 minutes of tACS at rest points towards tACS inducing some form of neuroplastic change that is subserved by modulations in GABAergic signalling that is detectable by TMS.

This neuromodulation hypothesis is corroborated by the findings of the present study. Oscillations represent the dynamic coordination of thousands of micro E/I microcircuits in both phase and time. These oscillatory dynamics crucially depend on the conduction speed of such microcircuits. Extrasynaptic tone, particularly that set by GABAergic conductance, plays a significant role in determining conduction speed and modulating neuronal firing patterns by affecting the regularity of spiking (Pavlov *et al.*, 2014). As such, it can be argued that the coordinated activity of a circuit (i.e. oscillations) is more sensitive to modulations in extrasynaptic tone than phasic inhibition (though this phasic inhibition is inherently vital to the functioning of the circuit and the execution of such modulations in extrasynaptic tone). This is further evidenced by neuropsychiatric conditions, such as schizophrenia, where abnormalities in genes that regulate extrasynaptic GABAergic tone (e.g. 22q11.2 deletion syndrome) significantly reduces γ oscillations (Charych *et al.*, 2009; Mancini *et al.*, 2022). In other words, the significant changes in SICI1ms point towards TGP oscillations modulating extrasynaptic GABAergic tone beyond synaptic inhibition, resulting in general neuromodulatory effects on the E/I circuit as a whole. Overall, the changes in SICI1ms (and not SICI2.5ms) are argued to reflect the neuromodulatory effects of driving oscillations on microcircuit tonic inhibition beyond phasic inhibition. Whilst such microcircuits rely on synaptic signalling to exert their downstream effects, the neuromodulatory effects induced by oscillations (such as changes in resting membrane potential and refractory period) likely rely more on changes in extrasynaptic tone rather than changes in point-to-point phasic synaptic signalling.

It is worth noting, however, that the changes in SICI2.5ms reported by Nowak *et al.* (2017) following γ tACS refute this hypothesis, instead suggesting that driving γ oscillations has a greater effect on synaptic signalling. Though the findings of Nowak *et al*. (2017) provided a starting point towards hypothesising the effects of θγ oscillations on receptor-mediated inhibition, the neurophysiological mechanisms underpinning the effects of single frequency, 75Hz γ tACS cannot be directly compared to a more complex, cross-frequency coupled θγ tACS waveform. These are driving fundamentally different oscillations and likely engaging different mechanisms. Nowak *et al.* (2017) did not sample SICI1ms in their study, thus a direct comparison is not possible.

4.5.4 Active stimulation did not significantly modulate NMDAr-mediated excitation

I then explored the effects of TGP, TGT, and sham on NMDA receptor-mediated glutamatergic facilitation using ICF12ms. I sampled paired pulse TMS at pre, early-, late-, and post-tACS whilst changing the test pulse throughout the session to account for any corticospinal excitability changes. I found that ICF12ms did not significantly differ across stimulation conditions.

4.5.5 No significant effect of tACS phase on TMS metrics

Finally, I explored the effect of tACS phase on all of my TMS metrics (spTMS and ppTMS MEP amplitudes). I did not find any significant effects of tACS phase on any TMS metric. This was unexpected given the evidence that tACS phase affects MEP amplitude in previous

literature (Guerra *et al.*, 2016; Nakazono *et al.*, 2016). A fundamental limitation of tACS studies is the assumption that tACS is entraining oscillations to the frequency and phase at which we think it is being delivered. Here, I extracted the MEP amplitude extracted at the artificial, assumed phase of activity. Without concurrent M/EEG recordings (which is challenging due to significant artefact contamination by tACS), the true relationship between the TMS pulse phase and the endogenous neuronal activity's phase is unknown. Overall, I found no evidence of differences in spTMS or ppTMS MEP amplitudes when sampling at different phases of concurrent tACS. This is, in part, reassuring for future combined tACS-TMS studies such that the precise timings of the TMS pulse delivery along the tACS waveform do not seem to affect MEP amplitude.

4.5.6 Conclusion

Overall, in this concurrent tACS-TMS study, I found that driving TGT oscillations significantly reduced corticospinal excitability whereas driving TGP oscillations significantly reduced extrasynaptic GABAergic tone. A limitation of the present study's design is the fact that no accompanying behavioural metric was used to ascertain the effects of such neurophysiological changes on behaviour. However, the finding that TGP significantly modulated SICI1ms (and not SICI2.5ms) provides insight into the effects of oscillations on general E/I microcircuits such that modulations in extrasynaptic inhibitory tone is more likely to modulate microcircuits beyond phasic synaptic inhibition. The findings from the present study provide a greater insight into the potential neurophysiological mechanisms underpinning the effects of θγ tACS on local M1 E/I circuitry, particularly GABAergic tone. There is increasing evidence that GABAergic tone is important in mediating functional connectivity changes in fMRI. The next experimental Chapter will look at how θγ oscillations at rest and during engagement of the sensorimotor network affects functional connectivity.

CHAPTER V - Investigating the effect of θγ oscillations on sensorimotor network functional connectivity using MRI

In this final experimental chapter, I build upon the finding in Chapter 4 that driving TGP oscillations modulates local extrasynaptic $GABA_a$ receptor-mediated tone. Using a combined tACS-MRI approach, I systematically investigate the effect of driving TGP on network-level resting state sensorimotor functional connectivity, MRS-GABA, and motor learning.

5.1 Introduction

Thus far, I have explored the role of θγ oscillations on motor behaviour (using a novel motor learning task; Chapter 3) and local neurophysiological changes (using TMS; Chapter 4). In Chapter 4, I found evidence that driving M1 θγ peak (75Hz/6Hz) oscillations continuously for 20 minutes significantly modulated local extra-synaptic GABAa signalling at rest. However, how these local M1 cortical changes fit within the wider, functionally connected sensorimotor network remains to be demonstrated.

5.1.1 Resting state fMRI to investigate sensorimotor network functional connectivity

Anatomically-plausible networks of functionally-interconnected brain regions, known as resting state networks (RSNs), have been reliably demonstrated at rest. These networks are robust and spatially consistent across different subjects (Damoiseaux *et al.*, 2006; Smith *et al.*, 2009). An example dataset from Smith *et al.* (2009) showing ten standard RSNs can be found in Figure 46. Capturing such networks can be done using resting state fMRI by recording the low-frequency spontaneous fluctuations of the BOLD signal at rest (<0.1Hz; Bächinger *et al.*, 2017) with the assumption that areas that are functionally-connected show fluctuations in their BOLD signal that follow a similar temporal pattern (i.e. correlated time courses of activation).

The sensorimotor network refers to a set of functionally-connected brain regions that are involved in processing and integrating sensory and motor information to allow motor behaviours. Its activity corresponds closely to the activations seen in bimanual motor tasks (Smith *et al.*, 2009). The sensorimotor network was the first resting state network to be identified in fMRI data and involves a variety of cortical and sub-cortical motor and sensory cortices including, but not limited to, precentral gyrus (M1), postcentral gyrus (S1), supplementary motor area (SMA), supramarginal gyrus (SMG), and the cerebellum (Biswal *et al.*, 1995; Smith *et al.*, 2009).

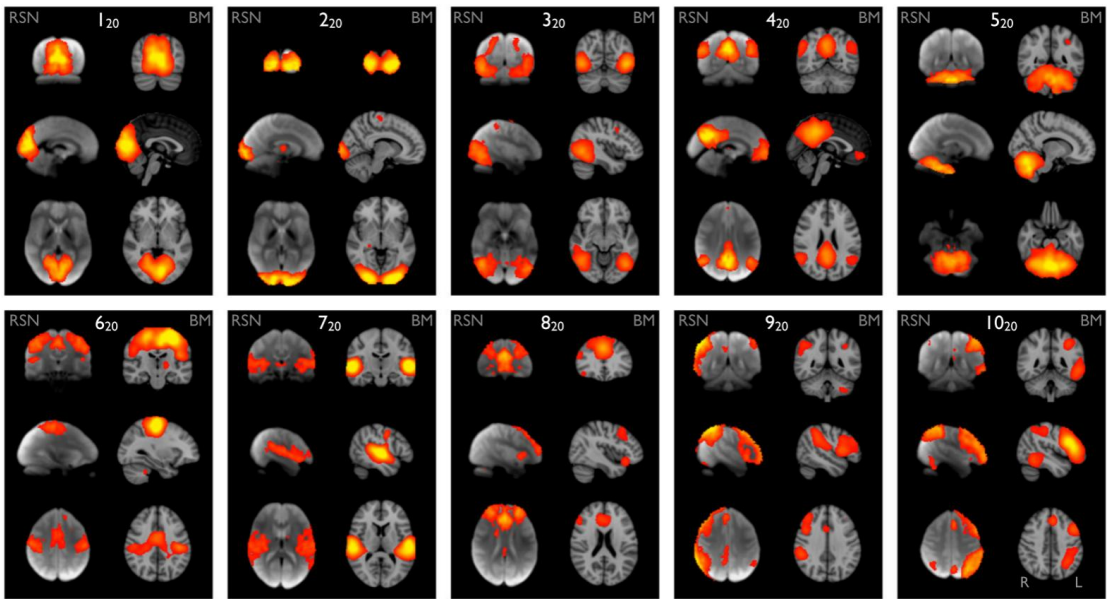

*Figure 46: Ten RSNs from a 20-component analysis from Smith et al. (2009) including the visual medial (1_{20}), visual occipital (2_{20}), visual lateral (3_{20}), default mode network (4_{20}), cerebellar (5_{20}), **sensorimotor (6_{20})**, auditory (7_{20}), salience(8_{20}), executive control (right, 9_{20}), and executive control (left, 10_{20}) network.*

5.1.2 Motor learning and sensorimotor resting-state functional connectivity

The sensorimotor network dynamically adapts to overcome new motor challenges. It is this rapid adaptation of sensorimotor functional connectivity that forms the neurophysiological basis for behavioural adaptation and learning (Bassett *et al.*, 2011). Short-term changes in resting-state functional connectivity in areas known to be involved in the planning and execution of visually-guided movements, including a network of frontal, posterior parietal, and

cerebellar regions (Albert, Robertson and Miall, 2009; Ma *et al.*, 2011; Vahdat *et al.*, 2011; Kraeutner *et al.*, 2021), have been shown to underpin changes in motor learning (Albert, Robertson and Miall, 2009; Vahdat *et al.*, 2011; Kraeutner *et al.*, 2021). This distributed pattern of change is consistent with the idea that a distributed pattern of sensory and motor plasticity accompanies motor learning (Vahdat *et al.*, 2011). In fact, research has shown that subjects who show greater motor learning performance also show greater changes in functional connectivity within these networks (Vahdat *et al.*, 2011; Bonzano *et al.*, 2015) and that resting-state sensorimotor functional connectivity, as measured with EEG, can predict motor learning (Wu *et al.*, 2014; Mottaz *et al.*, 2024). Therefore, network dynamics appear to play a larger role in predicting motor learning than local power changes in motor cortex (Mottaz *et al.*, 2024). This literature thus highlights the fact that neuroplastic changes, driven by motor learning, shapes subsequent spontaneous activity within the resting brain that can be captured using resting-state fMRI.

In a clinical context, the loss and subsequent recuperation of resting state sensorimotor functional connectivity has been shown to underpin post-stroke motor recovery (Van Meer *et al.*, 2010; Kraeutner *et al.*, 2021). Notably, Van Meer *et al.* (2010) demonstrated, using resting-state fMRI, a significant loss of functional connectivity between ipsi- and contra-lesional primary sensorimotor cortices that was accompanied by significant sensorimotor function deficits in the days following an experimental-stroke in rats. Importantly, the temporal pattern of changes in functional connectivity between the bilateral primary sensorimotor cortices significantly correlated with the evolution of sensorimotor function scores (Van Meer *et al.*, 2010). This effect has been replicated in humans by Kraeutner *et al.* (2021) who found increased functional connectivity in the sensorimotor network after stroke, that was correlated with post-stroke motor learning, such that greater connectivity was related to greater motor learning. This suggests that injury to the brain causally induces changes in sensorimotor functional connectivity that correlates with sensorimotor behavioural impairment, and the subsequent re-establishment of interhemispheric functional connectivity within the sensorimotor system underpins recovery.

The association between resting state sensorimotor functional connectivity and motor learning can also be explained, in part, by the neurophysiological mechanisms that govern the strength of resting state networks. Stagg *et al.* (2014) demonstrated a negative relationship between GABA and resting state functional connectivity (such that the higher the levels of GABA, the lower the sensorimotor functional connectivity). Given that reductions in GABAergic signalling are central to motor learning, it is plausible that reductions in GABA result in increases in functional connectivity to serve improvements in learning.

Whilst increases in resting state functional connectivity in the sensorimotor network underpinning motor learning intuitively makes sense, the precise neurophysiology of such changes are likely more complex. For example, it is likely that the sensorimotor network undergoes dynamic changes in functional connectivity at different stages of learning to support the different challenges each learning stage affords. For example, Ma *et al.*, (2011) demonstrated that during a month-long motor skill learning period, there were significant changes in the resting state motor network, particularly in the right postcentral gyrus and bilateral SMG. However, the connectivity strength in these regions fluctuated with initial increases in strength followed by decreases as the learning plateaued. As such, I acquired resting-state fMRI data pre-, during early-tACS (5 minutes into tACS delivery), during late-tACS (15 minutes into tACS delivery), and post-tACS to capture any online dynamic changes in sensorimotor network functional connectivity over time.

Overall, motor learning results in dynamic changes in the resting-state functional connectivity of the sensorimotor network, which highlights the widespread neuroplastic processes occurring across distributed, but functionally-connected, sensorimotor regions.

5.1.3 tACS can modulate functional connectivity

Thus far, I have outlined how changes in resting state sensorimotor functional connectivity in response to brain injury (e.g. stroke) or motor learning changes motor behaviour. However, whether we can artificially change resting state sensorimotor functional connectivity (for example, using tACS) and whether these artificially-driven changes modulate behaviour remains poorly understood.

Using resting-state fMRI to investigate the effects of tACS maps on nicely to an existing hypothesis around the mechanism of tACS: the Communication through Coherence (CTC) hypothesis (Fries, 2005). The CTC posits that only neuronal groups oscillating coherently interact since their communication windows for input/output are open at the same times (Fries, 2005). Therefore, the rhythmic excitability fluctuations imposed by tACS may provide temporal windows for communication across separate but functionally-related brain regions. This hypothesis is likely perfectly captured by resting-state fMRI such that driving θγ oscillations in M1 is hypothesised to entrain these oscillations across the sensorimotor network, meaning areas across the sensorimotor network will oscillate together, a factor that can be detected by resting-state fMRI.

To date, there are some studies looking at the effect of driving various frequency tACS on different RSNs' functional connectivities. For example, Kar *et al.* (2020) found that 10Hz tACS increased functional connectivity between the stimulated area (human motor area) and the dorsal attention network. Using current flow modelling, they highlight a dose-dependent effect such that these changes were related to the strength of tACS-induced electric fields (Kar *et al.*, 2020). Furthermore, Mondino *et al.* (2020) found that 30 minutes of θ tACS delivered over bilateral dorsolateral prefrontal cortex (dlPFC) increased resting state functional connectivity between the left dlPFC and the right inferior parietal lobule. Finally, Cabral-Calderin *et al.* (2016) found that 10Hz and 40Hz tACS induced opposite effects on functional connectivity, with 10Hz tACS increasing and 40Hz tACS decreasing functional connectivity in the left fronto-parietal control network and occipito-parietal regions. These findings suggest that tACS is able to modulate resting state functional connectivity in various RSNs of sufficient magnitude to be detected with resting-state fMRI. However, Weinrich *et al.* (2017) found no evidence that 20Hz tACS resulted in changes in sensorimotor network strength. However, they did find that 20Hz tACS uncoupled M1-M1 functional connectivity and decreased the connectivity between the left M1 and the rest of the sensorimotor network. These effects were not detected with 5Hz control frequency tACS, suggesting frequency-specific modulatory effects of tACS on sensorimotor functional connectivity.

A key methodological consideration for concurrent tACS-fMRI studies is the inclusion of a task. One possible mechanism-of-action for tACS is entrainment (with the notion that the frequency of the endogenous oscillator and the applied frequency of the external driving force must be close to each other to achieve entrainment). In the absence of a task to begin generating oscillations onto which tACS can entrain to, it is surprising to see the positive behavioural effects reported (Cabral-Calderin *et al.*, 2016; Kar *et al.*, 2020; Mondino *et al.*, 2020). To test the hypothesis that the effects of θγ tACS are critically state-dependent, I included two separate, but related studies, one looking at the effects of θγ tACS at rest and one during learning on sensorimotor functional connectivity. This will allow me to disentangle the effects of tACS, motor learning, and their interaction on sensorimotor functional connectivity in supporting behavioural changes.

5.1.4 Aim of this Chapter

Thus far, I have demonstrated the effects of θγ oscillations on cortical excitability and local receptor-mediated excitation and inhibition. However, there remains a lack of understanding about whether the behavioural effects of θγ oscillations (as demonstrated by Akkad *et al*., 2021) are mediated by local changes in neuronal activity or wider, network level functional connectivity. First, I look at how sham tACS with/without motor learning affects sensorimotor functional connectivity (*sham tACS + task* versus *sham tACS + rest*). This will allow me to investigate changes in sensorimotor functional connectivity due to motor learning. I then look at how driving θγ oscillations with/without a task affects sensorimotor functional connectivity (*θγ tACS + task* versus *θγ tACS + rest*). This will allow me to investigate how θγ tACS affects sensorimotor functional connectivity beyond sham stimulation. Finally, I investigate whether the degree of functional connectivity in the sensorimotor network (with/without θγ tACS) serves to explain changes in behavioural performance.

The present study highlights the potential of resting-state fMRI in assessing the spatiotemporal characteristics of functional brain reorganisation due to motor learning, tACS, and their interaction.

5.2 Methods

5.2.1 Overall methods

Participants were invited to take part in one of two related studies (study X or Y). Study X was a three-session, repeated-measures design. Study Y was a single session, independent-measures design. Both studies involved MRI, brain stimulation, and a novel motor learning task. I needed all four sessions to provide necessary scientific controls for the motor learning and the tACS. A summary of the three experimental designs can be found in Figure 47.

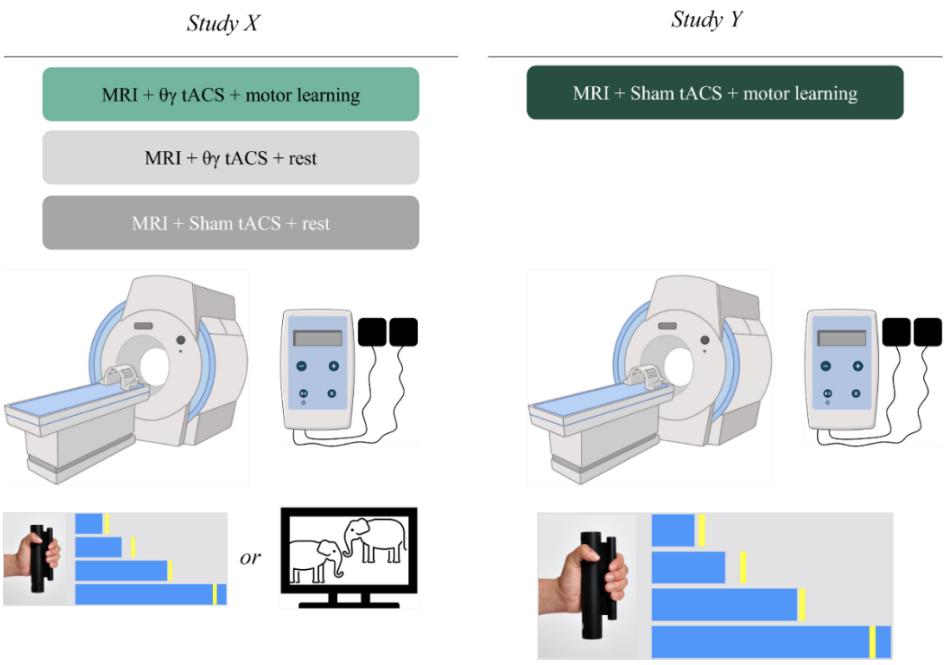

Figure 47: Overview of the experiments in this Chapter. Study X is a repeated-measures, within-subject design in MRI. Study Y is an independent-measures, between-subject design in MRI.

5.2.2 Apparatus and stimuli

5.2.2.1 θγ tACS frequency and duration

A custom-coded, 2mA peak-to-peak θγ PAC tACS waveform (with a 10 second ramp up) was delivered continuously for 20 minutes with a NeuroConn DC Stimulator Plus in Remote Mode using Spike2 (Cambridge Electronic Design, 2024; see Figure 48).

The Neuroconn was located outside of the magnetic field and connected to the electrodes via MR-compatible extension leads.

5.2.2.2 Sham tACS frequency and duration

A custom-coded, 2mA peak-to-peak 6Hz θ wave was delivered with a ramp up of 10 seconds followed immediately by a 10 second ramp down to induce similar early cutaneous sensations to θγ tACS, without entraining any local neuronal oscillations (see Figure 48).

The active and sham custom coded waveforms were saved as "A", "B", or "C" by an independent researcher such that when I ran the waveforms, I was blinded to what condition participants were in.

5.2.2.3 Electrode montage

In line with the 10-20 EEG system, 5×5cm MR-compatible rubber conductive electrodes with 5kΩ safety resistors were centred over left primary motor cortex (C3) and parietal vertex (Pz). Ten20 electrode paste was used as a conducting medium between the scalp and the electrodes. Impedance was kept below 15kΩ throughout the session. The scalp under C3 and Pz was prepped using abrasive paste (NuPrep) and a cotton tip and wiped clean using an alcohol wipe. The tES electrodes were secured in place using rubber straps and a mesh cap.

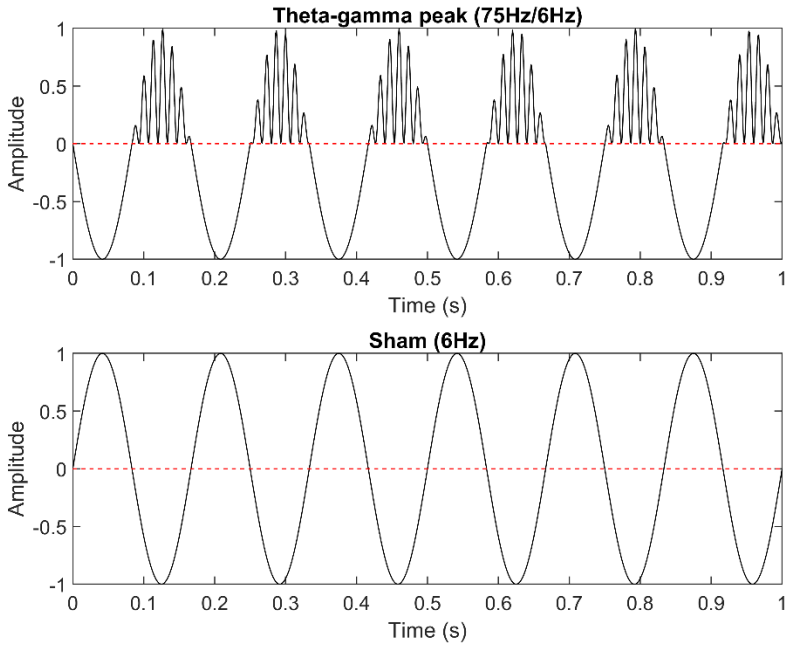

Figure 48: tACS waveforms used in Chapter 5. Top: θγ peak (top). Bottom: sham.

5.2.2.4 Behavioural task

A novel grip force modulation task was developed for Chapter 3. However, this task was not suitable for the present study. Firstly, I did not see a significant effect of 75Hz/6Hz θγ peak tACS on behaviour with this task (see Chapter 3). Secondly, each trial of the previous task lasted three seconds. For an MRI study, this is an insufficient amount of time to detect any BOLD/spectral changes. I considered increasing the duration of each trial but determined that the task was not challenging enough to elicit the anticipated motor learning effects. Finally, the task in Chapter 3 was a pinching task. For an MRI study, this task would likely not produce sufficient signal to noise data for reliable quantification of functional connectivity changes and changes in GABA concentration. I thus decided to adopt a whole hand, grip force modulation

task that would activate a wider spread of motor cortical neurons, increasing the likelihood of higher signal to noise ratio.

A custom-coded novel grip force modulation task was created using MATLAB (MathWorks, version 2022b). The task was translated and adapted from a previously validated task written in Python (Steel *et al.*, 2016). Participants were presented with a "target" (yellow vertical line) that moved smoothly along the X-axis of a 14" screen (see Figure 49). Participants controlled a horizontally moving blue bar of the same width as the yellow target. A hand-held Fibre Optic Grip Force transducer (Current Designs, Inc., Philadelphia, PA) was used to convert mechanical load into an electrical output signal that controlled the blue bar (see Figure 49). The task was coded such that the greater the amount of grip force applied, the further the linear horizontal rightward movement of the blue bar. The aim of the task was to continuously track the yellow target by modulating grip force. The task was calibrated to each participant's 20% maximum voluntary contraction (MVC), such that maximum distance on the screen (right edge) was reached when applying 20% MVC.

The task consisted of six 17-trial blocks. Each trial lasted for 14 seconds, during which the target moved horizontally in a sinusoidal manner. For blocks **1** and **6**, the target motion was random and varied from trial to trial. For blocks **2-5**, the target moved according to a predetermined sequence that was identical across trials (see Figure 50).

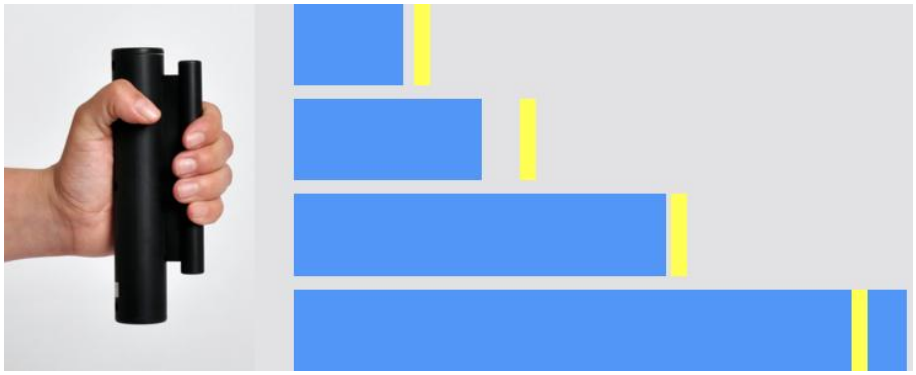

Figure 49: Experimental set up. Left: Grip force transducer. Right: The grip-force modulation task. The yellow bar is a moving target which participants track with the blue bar using force.

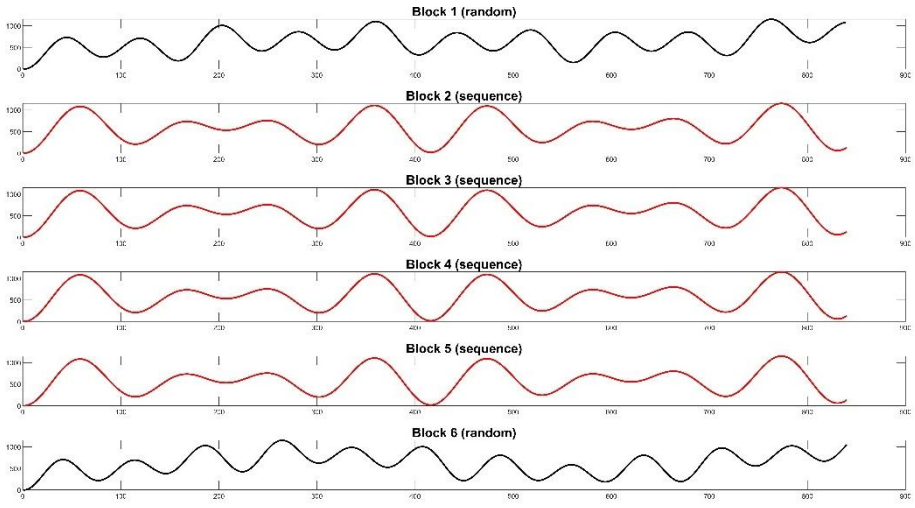

Figure 50: Schematic representation of the target output force required for one trial in each block. Blocks 1 and 6 (black) are random sequences. Blocks 2-5 (red) are a set force sequence to induce motor grip-force sequence learning.

5.2.3 The effect of θγ tACS on sensorimotor functional connectivity (Study X)

Here, I investigated the effect of θγ tACS with and without a task and sham tACS without a task, on sensorimotor functional connectivity and MRS-measured GABAergic signalling in M1.

5.2.3.1 Participants and power calculations

Right-handed participants (n=15, aged 18-35 years, 8 females) took part in the study, under the approval of the local ethics committee (Oxford CUREC2 R88417/RE002). Three participants were excluded due to equipment failure. *A priori* power calculations for 80% power indicated a requirement of n=24 (α=0.05, (1-β)=0.8, η_p^2=-.12), meaning a further nine participants would have needed to be collected for this dataset to have been sufficiently powered. Safety exclusion criteria for NIBS included (but was not limited to) a history, or current diagnosis, of a neurological or psychiatric disorder, a family history of epilepsy, a history, or current diagnosis, of migraines or frequent headaches, treatment with psychotropic medication (e.g., antiepileptics, antidepressants, antipsychotics, psychostimulants), the presence of metallic implants in or near the head (such as pacemakers and deep brain stimulators) and pregnancy.

5.2.3.2 Experimental design

This was a double-blind, sham-controlled, within-subject design. Participants attended three sessions, at least seven days apart. In one session, participants received 20 minutes of continuous TGP tACS and performed the motor learning task. In one session, participants received 20 minutes of continuous TGP tACS in the absence of a task (watching a nature documentary). In one session, participants received the sham tACS protocol in the absence of a task (watching a nature documentary). The session order was randomised using a randomisation software and counterbalanced to avoid order-effects.

5.2.3.3 MRI sequences

All MR data were acquired using an ultra-high field 7T Siemens Magnetom (Siemens, Erlangen) with a 32-channel parallel-transmit head coil at the Centre for Functional MRI of the Brain, University of Oxford. Participants were placed supine and head-first into the scanner. Foam pads were placed between the participants' head and the coil to minimise head movement. A coil-mounted mirror was used to allow participants to view a screen outside of the magnet bore. Functional MRI (fMRI) and MR spectroscopy (MRS) data were acquired **pre**, **during**- (early [5 minutes] and late [15 minutes] into tACS delivery), and **post**-tACS. Linear shims were used to optimize scanning parameters (Lemke *et al*., 2015).

A T1-weighted structural scan was acquired with an MPRAGE sequence for each participant and each session (TR/TE=2600/3.18ms; FOV(AP,FH,RL) = 246×246×176mm^3; voxel size=1mm^3; Flip angle=5°, five minutes). Anatomical landmarks from these images were used to assist in the placement of the left M1 voxel for MRS.

Whole-brain multi-band fMRI data were acquired (TR/TE/FA=1000/20ms/90°; FOV(AP,FH,RL)=220×120×220, voxel size=2mm^3; multi-band factor of 2) in blocks of five minutes. A 2mm fieldmap was acquired to account for geometric distortions in the MR data caused by magnetic susceptibility variations or B0 inhomogeneities.

MRS spectra were acquired over four timepoints: at pre-, early-tACS (5 minutes into tACS delivery), late-tACS (15 minutes into tACS delivery), and post-tACS. Each block of MRS data acquisition took five minutes. MRS data were acquired using a semi-Localization by Adiabatic Selective Refocusing (semi-LASER) sequence (Scheenen *et al*., 2008) with VAPOR water suppression (TR/TE=5000/36ms; water

suppression bandwidth=135Hz; 54 averages; volume of interest (VOI)=20mm^3). Four unsuppressed water spectra were obtained for eddy current correction and water referencing. Participant-and-session unique T1-weighted images were used to place the voxel over the left precentral knob, a landmark for hand motor representation (Yousry, 1997; see Figure 51). Any dura matter overlap was avoided. Following voxel placement, screenshots were taken and used as a reference to replicate the same voxel location across sessions. Transmit voltage amplitude was determined based on the B0 map values in the centre of the MRS voxel, capped at 340V. The flip angle was determined per session to maximise water suppression. The MRS data are not discussed within the scope of this thesis.

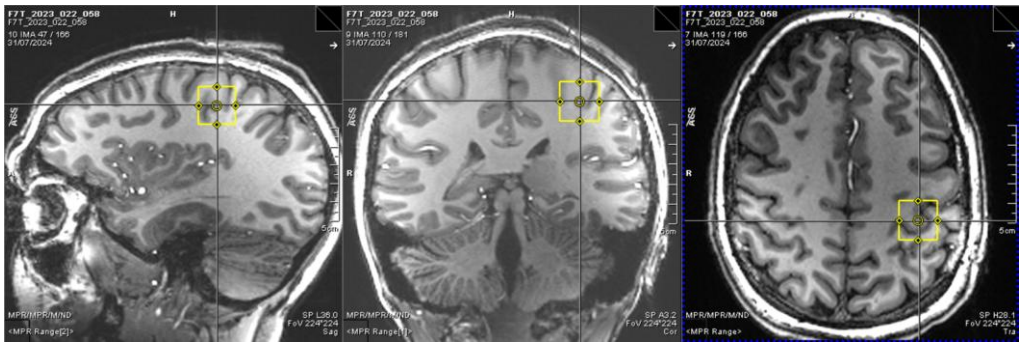

Figure 51: Example MRS voxel placements over left primary motor cortex (M1).

5.2.3.4 Procedure

Participants were sent a participant information sheet prior to screening and underwent an initial non-invasive brain stimulation safety screening interview. On the day of the experiment, participants were screened again and gave informed consent.

Participants' heads were then measured from nasion to inion and bilateral periauricular points (A1 and A2) to localise Cz (10-20 International EEG system, **Figure 2B**). Measurements of 20% distance from Cz to inion and from Cz to A1 were used to centre the tES electrodes over C3 and Pz (see **Figure 2B**). These areas were marked with a marker, and the scalp was prepped with Nuprep and an ethanol wipe to remove any scalp oil and debris. The NeuroConn DC Stimulator Plus was then set to Remote Mode and impedance was checked.

For the task session, participants were shown a demonstration video of the task and were given standardised instructions ("*You will be presented a blue bar on the screen. In the absence of any force applied to the gripper, the blue bar will stay on the far left hand side of the screen. The more force you apply to the gripper, the more the blue bar will move to the right hand side of the screen. You will also see a yellow bar that moves horizontally across the screen. You goal is to track the yellow bar as accurately as possible.")*.

To ensure that all participants experienced the same force modulation requirements, I calibrated the task to individual participant's maximum voluntary contraction (MVC). Participants held the force transducer in their right hand. Participants squeezed the force transducer as hard as they could, maintaining their MVC for three seconds, followed by a three second break, three times, as cued by an in-house MATLAB script (MathWorks, version R2023b). The average force from the maximum peak of each contraction was then used to calculate mean MVC. The task was individually calibrated to 20% of the participant's MVC. This was to ensure participants were not too fatigued and could perform the task continuously for 20 minutes. In the task, 20% MVC was the amount of force required for the blue bar to

travel to the far-right hand side of the screen. Furthermore, the movement of the yellow target in the sequence blocks was also calibrated to this value such that all participants experienced the same task requirements and force modulations. Participants completed the force transducer calibration during the structural scan. After completing the calibration, participants completed run 1 of the task.

After acquiring the structural scan, I performed linear shims in preparation for the pre-tACS resting-state fMRI scan. During the pre-stimulation fMRI scan, participants were shown a white cross on a black background and asked to look at the cross, blink normally, and try not to fall asleep.

I then set up the spectroscopy sequence as outlined in section *5.2.3.3*. During the pre-stimulation MRS scan, participants were shown a white cross on a black background and asked to look at the cross, blink normally, and try not to fall asleep. Towards the end of this scan, I checked the impedance of the electrodes in preparation for the tACS delivery.

I then delivered 20 minutes of continuous stimulation (active or sham). In the task session, participants completed runs 2,3,4,5 (sequence blocks) back-to-back. During these 20 minutes, I acquired fMRI, MRS, fMRI, and MRS scans. In the other two non-task sessions, participants watched a nature documentary during the 20 minutes of stimulation.

After 20 minutes of stimulation, I collected another resting-state fMRI and MRS scan (with a white cross on a black background). At the end of the scan, I acquired a fieldmap for analysis of the fMRI data, during which participants in the task session completed the final random sequence run of the task. An overview of study X can be found in Figure 52.

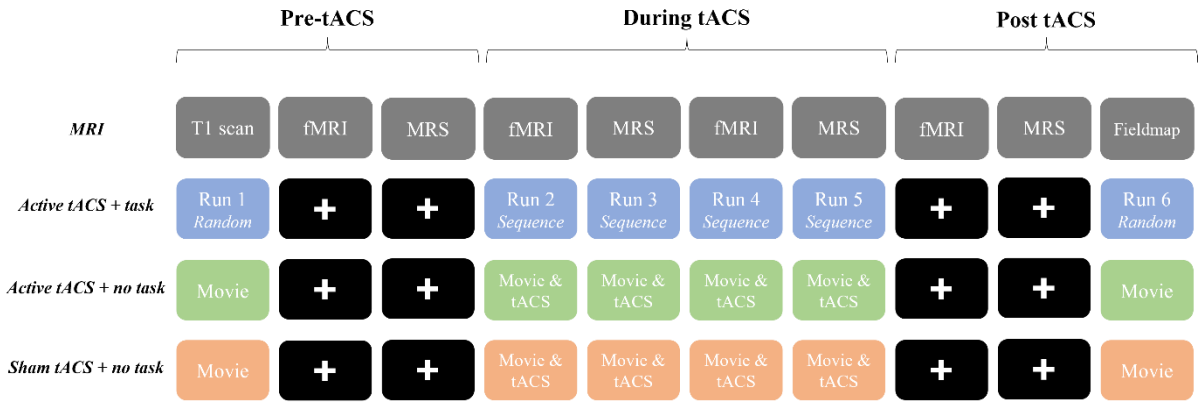

Figure 52: Visual representation of study X design. In this within-subject, repeated measures study, participants attended three sessions, at least seven days apart.

5.2.4 The effect of θγ tACS on sensorimotor functional connectivity (study Y)

Since participants are only able to perform one motor learning session, I required an additional sub-MRI study with a different cohort of participants that act as necessary scientific controls to those in study X.

5.2.4.1 Participants and power calculations

Right-handed participants (n=15, aged 18-35 years, 7 females) took part in the study, under the approval of the local ethics committee (Oxford CUREC R88417/RE002). A priori power calculations for 80% power indicated a requirement of n=24 per group (α=0.05, (1-β)=0.8, η_p^2=-.12), meaning a further 9 participants would have needed to be collected for this dataset to have been sufficiently powered.

5.2.4.2 Experimental design

This was a single-blind study. Participants attended one session during which they received the sham tACS protocol and performed the motor learning task.

5.2.4.3 MRI sequences

The same MRI sequences were used in study Y.

5.2.4.4 Procedure

The same procedure was used as in study X, except for during-tACS participants received sham stimulation. An overview of study Y can be found in Figure 53.

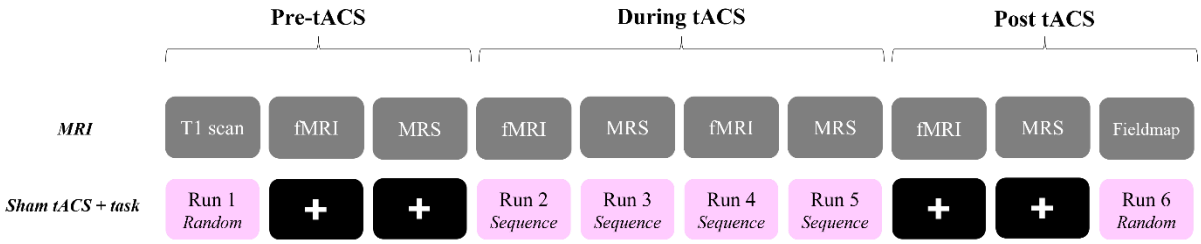

Figure 53: Visual representation of study Y design. In this single session study, participants learnt the motor learning task with sham tACS.

5.3 MRI pre-processing and statistical analysis

All MRI data pre-processing was carried out using FSL (FMRIB's Software Library, version 6.00 (www.fmrib.ox.ac.uk/fsl). I developed of a novel end-to-end pipeline for the pre-processing of 7T SIEMENS structural and resting-state fMRI data.

5.3.1 Structural pre-processing

All subjects' structural T1-weighted MRIs were brain extracted using SynthStrip (Hoopes *et al.*, 2022), segmented and bias field corrected using FAST (Zhang, Brady and Smith, 2001).

5.3.2 Resting-state fMRI pre-processing (study X and Y)

5.3.2.1 Registration (BBR, FLIRT, and FNIRT)

Individual resting-state fMRI scans were registered to their respective T1 structural scan using boundary-based registration (BBR) as implemented in FMRIB Linear Image Registration Tool (FLIRT; (Jenkinson and Smith, 2001; Jenkinson *et al.*, 2002) and then to a standard space template (MNI152, 2mm) using a 7T-optimised non-linear registration (FNIRT; Andersson, Jenkinson and Smith, 2007) configuration file.

5.3.2.2 Motion correction (MCFLIRT)

The data were motion corrected using MCFLIRT (Jenkinson *et al.*, 2002), grand mean intensity normalised, and high pass temporally filtered (equivalent to 100s, 0.01Hz).

5.3.2.3 Single subject ICA (MELODIC)

Single-subject ICA (Probabilistic Independent Component Analysis; Beckmann 2004) as implemented in MELODIC (Multivariate Exploratory Linear Decomposition into Independent Components, version 3.15) was used to remove structured noise. ICA is a model-free approach that linearly decomposes fMRI data into underlying features. Pre-processed data were whitened and projected into a 224-dimensional subspace using probabilistic Principal Component Analysis where the number of dimensions was estimated using the Laplace approximation to the Bayesian evidence of the model order (Minka, 2000; Beckmann and Smith, 2004). The whitened observations were decomposed into sets of vectors which describe signal variation across the temporal domain (time-courses) and across the spatial domain (maps) by optimising for non-Gaussian spatial source distributions using a fixed-point iteration technique (Hyvarinen, 1999). Estimated Component maps were

divided by the standard deviation of the residual noise and thresholded by fitting a mixture model to the histogram of intensity values (Beckmann and Smith, 2004).

5.3.2.4 Training an automated ICA component classifier (FIX)
I trained a FIX classifier by manually labelling 44 datasets, from 10 different participants, across my four timepoints (pre-tACS, early-tACS, late-tACS, and post-tACS).

5.3.2.5 Spatial smoothing (SUSAN)
Spatial smoothing was applied with a 5mm FWHM Gaussian kernel using SUSAN (Smith and Brady, 1997).

5.3.2.6 Standard space (APPLYWARP)
I used applywarp and the previously calculated linear and non-linear transformations and warp files to move the functional data to standard space (MNI152) in a single step.

5.3.2.7 Group ICA (MELODIC) and cross correlation (FSLCC)
I concatenated the pre-processed fMRI data temporally across subject and session into a single 4D data file. I then ran a command line group-level ICA using unconstrained MELODIC. This gave me a set of group level components (group-level networks) which represented the signal that is common across all of my subjects. This generated an eigenspectrum graph which allowed me to interpret approximately how many independent components contributed to explaining the variance in my group-level data (see Figure 54).

I then ran cross-correlations (using fslcc) to compare my data to a 10-component network template (Smith *et al.*, 2009). I prioritised the sensorimotor network component and looked for the dimensionality that resulted in the highest correlation between my data and the template.

An example of how the template sensorimotor network (blue) and study X's MELODIC group level ICA with 13 components for sensorimotor network (red) overlaid on a standard MNI152 2mm brain looks can be found in Figure 55.

The sensorimotor network in my data sits superiorly to the template, likely due to the optimised brain extraction and registration steps taken for my 7T data. For study Y, group-ICA with 9 components generated the largest Pearson's R value for sensorimotor network.

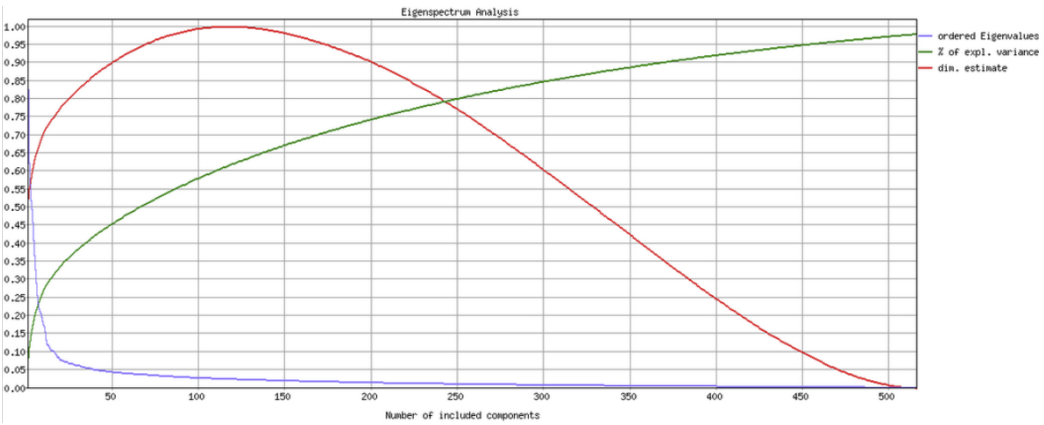

Figure 54: Example PCA estimates from unconstrained group-level ICA for study X using MELODIC. The eigenvalues (i.e. the variance explained) are reflected on the y-axis. The higher the eigenvalue, the greater the variance in the data explained. The cumulative number of components is reflected on the x-axis. A clear drop in the eigenvalue magnitude, known as an elbow, indicates the point where the

variance explained by additional components becomes redundant in the amount of variance explained. This helped me identify how many components I should keep for further analysis (to avoid over-fitting). On the basis of this graph, I ran group-level MELODIC again with 10, 13, and 15 components.

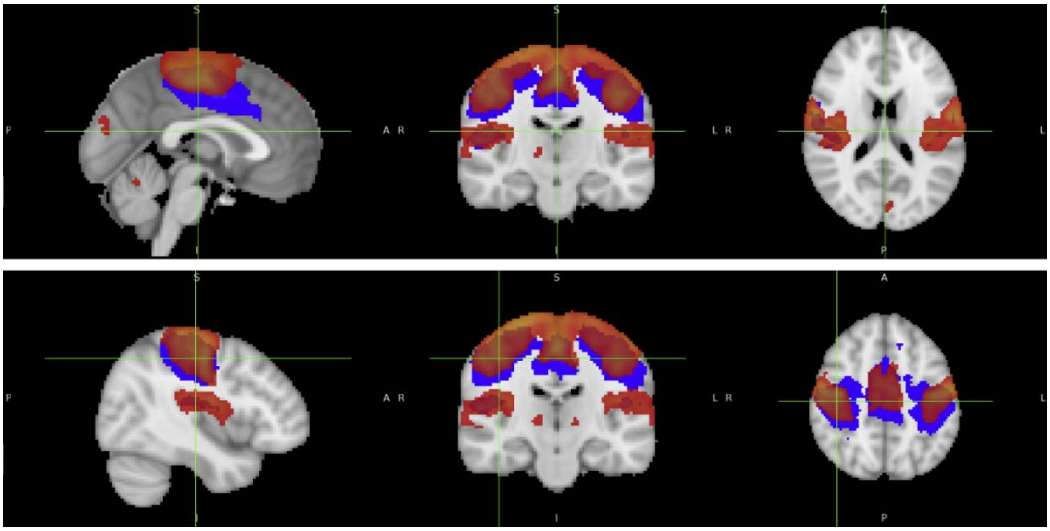

Figure 55: Template sensorimotor network (blue; Smith et al., 2009) and study X's MELODIC group level ICA sensorimotor network (red) with 13 components overlaid on a standard MNI152 2mm brain.

5.3.2.8 Dual regression

After establishing group-level ICA components, I ran standard dual regression on the sensorimotor network to map the group-level sensorimotor network back onto individual subject data to estimate the subject-specific contribution. Dual regression was performed on a subject-by-subject basis and consisted of the following: In stage 1, I inputted the pre-processed fMRI 4D data file for one subject and the group ICA spatial maps (group-level components) and performed a spatial regression to regress the group ICA components onto the subject's 4D fMRI data. This resulted in subject-specific timeseries for each group ICA component. In stage 2, I then fed the subject-specific timeseries from stage 1 into a temporal regression which created subject-specific spatial maps for each group level component. With these two stages, I thus went from having a set of group ICA components to having a set of subject-specific components for each of my subjects.

5.3.2.9 Difference maps

I created individual difference maps for each comparison of interest (i.e. *pre-tACS minus early-tACS, pre-tACS minus late-tACS, pre-tACS minus post-tACS, early-tACS minus late-tACS, early-tACS minus post-tACS, and late-tACS minus post-tACS*). For example, when looking at the change in functional connectivity from pre-tACS to early-tACS, I first extracted the sensorimotor network from the dual regression stage 2 files per subject for the stimulation by timepoint contrast of interest (e.g. active pre-tACS fMRI and active early-tACS fMRI). I then used fslmaths to create a difference map on a subject-by-subject basis (e.g. **sub001_active_pre** minus **sub001_active_early**) and merged them into a group difference map (e.g. **active pre-early**). I then did the same for sham (i.e. **sham pre**-e**arly**). I then concatenated the two merged images in time (**active pre-early and sham pre-early)** and ran randomise to look for effects of stimulation on each stimulation by timepoint contrast.

5.3.2.10 Randomise

I performed nonparametric, permutation-based statistical analyses on the group-level data using RANDOMISE (Winkler *et al.*, 2014). Significant clusters were identified

using cluster-wise thresholding (z-threshold: 3.1, cluster p-threshold: 0.05; Woo *et al*., 2014).

5.3.2.11 Sensorimotor network strength

I quantified the sensorimotor network strength by extracting the arbitrary units of network strength from the subject-and-scan specific network maps masked by the group sensorimotor network mask. I investigated whether the change in sensorimotor network strength correlated with behavioural performance on the grip force modulation task. I calculated the percentage change in network strength as follows.

((second measure - baseline measure)/baseline measure)×100%

I visually assessed the distribution of residuals using diagnostic plots. The residuals appeared evenly distributed around zero in the residuals vs. fitted plot, indicating no clear pattern or systematic bias. The standardized residuals were evenly spread across the range of fitted values, indicating no clear pattern or heteroscedasticity. Normality of residuals was visually assessed using a Q-Q plot. The residuals closely followed the reference line, indicating that the assumption of normality was met.

5.3.2.12 Contrasts

To investigate the effects of tACS (with/without a task), I set up contrasts (see Table 3) comparing active and sham tACS across multiple timepoints.

(active_pre-early)>(sham_pre-early)	(sham_pre-early)>(active_pre-early)
(active_pre-late)>(sham_pre-late)	(sham_pre-late)>(active_pre-late)
(active_pre-post)>(sham_pre-post)	(sham_pre-post)>(active_pre-post)
(active_early-late)>(sham_early-late)	(sham_early-late)>(active_early-late)
(active_early-post)>(sham_early-post)	(sham_early-post)>(active_early-post)
(active_late-post)>(sham_late-post)	(sham_late-post)>(active_late-post)

Table 3: MRI contrasts using the difference maps to look for different activation patterns associated with changes over time and between active/sham tACS.

5.4 Behavioural data pre-processing and statistical analysis

All behavioural data were pre-processed using MATLAB (version R2023b) and statistical analyses were performed using R (RStudio version 2023.12.1+402). Data were visualized using R (RStudio version 2023.12.1+402). Performance in the behavioural task ("error") was quantified as the median distance between the target and the blue bar on a trial-by-trial basis and averaged across trials for each block. I calculated the group mean error ±3SD of each block. I then looked at individual trials within a block, per participant, and excluded trials that fell outside of ±3SD. If a participant had more than 20% of trials excluded in one block, I excluded that block for that participant.

All statistical analyses were performed using the linear mixed effects model (lme4) package in R software (Bates *et al*., 2015). As fixed effects, I entered **STIMULATION** and **TIMEPOINT** with a **STIMULATION×TIMEPOINT** interaction into the model. I allowed intercepts for different subjects to vary in order to account for covarying residuals within subjects (creating a random intercept model of "subject"). Estimated marginal means for each stimulation condition were computed, and post hoc pairwise comparisons using Tukey-adjusted tests were run on the level of significant main effects. Visual inspection of residual plots did not reveal any obvious deviations from homoscedasticity or normality. P-values were obtained by likelihood ratio tests of the full model with the effect in question against the model without the effect in question.

5.5 Results: The effect of θγ oscillations during rest

5.5.1 The effect of θγ oscillations on sensorimotor network strength during rest

I first analysed the two rest sessions during which participants received active or sham stimulation whilst watching a nature documentary. I first confirmed that there were no differences in sensorimotor network strength at baseline (pre-tACS) between active and sham ($t(25.06)=0.66, p=.517$).

There was no significant main effect of **STIMULATION** ($F(1,112)=0.057, p=.812$), **TIMEPOINT** ($F(3,112)=1.48, p=.224$), and no significant **STIMULATION×TIMEPOINT** interaction ($F(3,112)=0.425, p=.736$; see Figure 56).

I also looked at the percentage change in network strength from pre-tACS. There was no significant main effect of **STIMULATION** ($F(1,74.05)=0.87, p=0.355$), **TIMEPOINT** ($F(2,73.68)=2.02, p=0.140$), and no significant **STIMULATION×TIMEPOINT** interaction($F(2, 73.65)=0.04, p=0.960$).

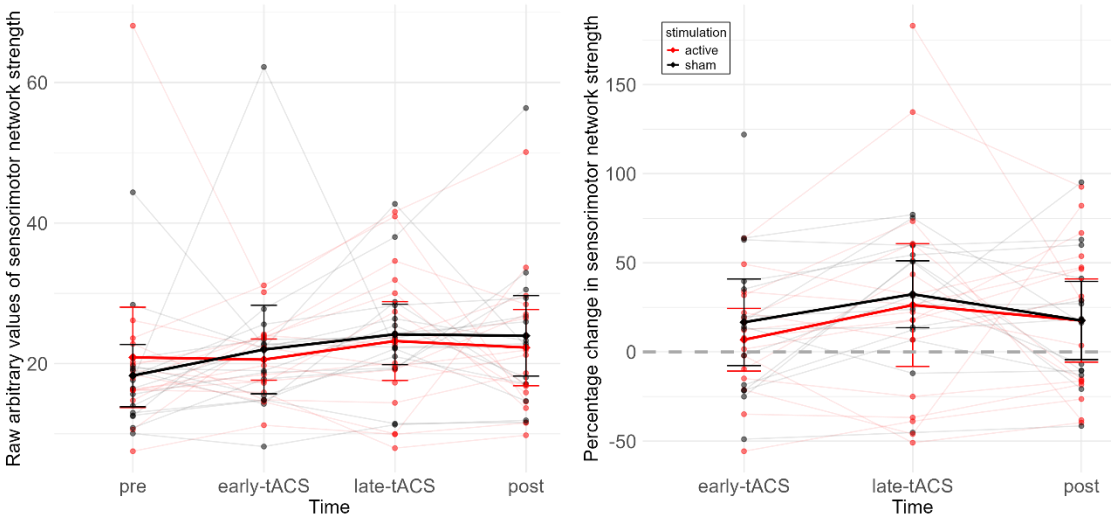

Figure 56: The effect of θγ oscillations on sensorimotor network strength whilst participants were at rest. Left: Raw arbitrary values of network strength. Right: Percentage change in network strength from pre-tACS.

5.5.2 The effect of θγ oscillations on sensorimotor functional connectivity at rest

I then looked at the effect of $\theta\gamma$ oscillations on resting state sensorimotor functional connectivity when participants were at rest. I found no significant difference clusters between active and sham tACS on any stimulation by timepoint functional connectivity measure.

5.6 Results: The effect of θγ oscillations during learning

5.6.1 The effect of θγ oscillations on motor behaviour

I first confirmed that there were no significant differences in error in run 1 between active and sham (t(18.99)=-0.867,p=.397). I then went on to compare learning during task performance with active tACS (study X) and sham tACS (Study Y). I performed a linear mixed effects analysis with one fixed effect of **STIMULATION** (active, sham) and one fixed effect of **TIMEPOINT** (run 1-6). There was no significant main effect of **STIMULATION** (F(1,20.923)=0.047,p=.830). There was a significant main effect of **RUN** (F(5,100.979)=30.237,p<.001; see Figure 57). There was no significant **STIMULATION×TIMEPOINT** interaction (F(5,100.979)=0.872,p=.503). To further explore the significant main effect of **RUN**, I conducted post-hoc pairwise comparisons between the levels of the **TIMEPOINT** variable using Tukey-adjusted tests. There were significant reductions in error between run 1 and runs 2,3,4,5,6 (t(112) = 5.001-10.24, p<.0001) and between run 2 and 5 (t(112)=5.001<.0001). A breakdown of the significant differences can be found in Table 4.

Contrast	Estimate	SE	df	t ratio	p value
run1-run2	**15.263**	**2.87**	**112**	**5.314**	**<.0001***
run1-run3	**22.865**	**2.91**	**112**	**7.849**	**<.0001***
run1-run4	**26.443**	**2.91**	**112**	**9.077**	**<.0001***
run1-run5	**29.831**	**2.91**	**112**	**10.24**	**<.0001***
run1-run6	**22.176**	**2.92**	**112**	**7.589**	**<.0001***
run2-run3	7.602	2.91	112	2.609	0.1035
run2-run4	11.18	2.91	112	3.838	0.0028
run2-run5	**14.568**	**2.91**	**112**	**5.001**	**<.0001***
run2-run6	6.913	2.92	112	2.366	0.1773
run3-run4	3.578	2.95	112	1.211	0.8306
run3-run5	6.966	2.95	112	2.358	0.1804
run3-run6	-0.688	2.96	112	-0.232	0.9999
run4-run5	3.388	2.95	112	1.147	0.8606
run4-run6	-4.267	2.96	112	-1.441	0.7023
run5-run6	-7.655	2.96	112	-2.584	0.1097

Table 4: Breakdown of the significant main effect of RUN.

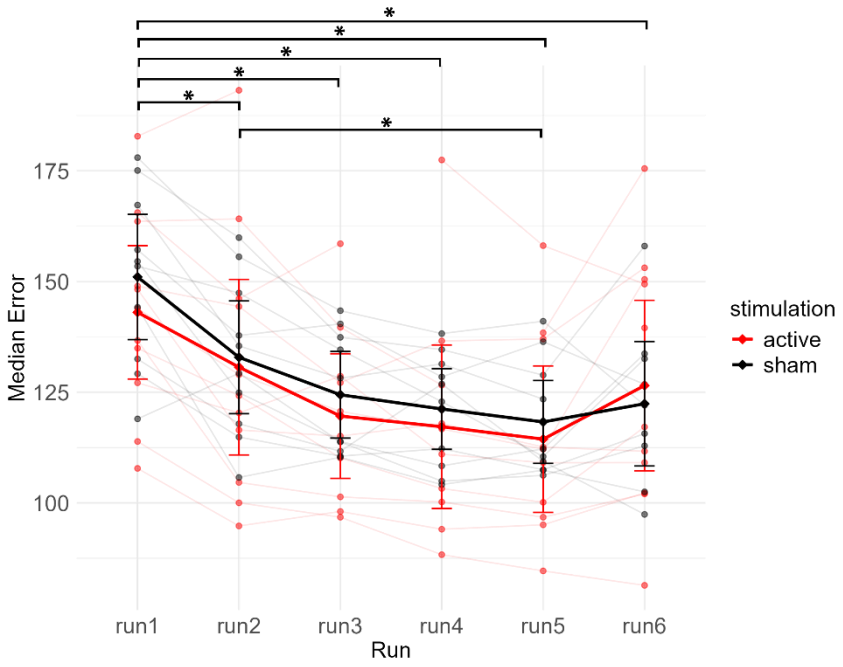

Figure 57: Median error for active and sham over the 6 runs of the motor learning task. Runs 1 and 6 are random movements of the target and runs 2-5 are sequence movements of the target.

5.6.2 The effect of θγ oscillations on sensorimotor network strength during learning

I then went on to compare network connectivity during task performance with active tACS (study X) and sham tACS (Study Y). I first confirmed that there were no differences in sensorimotor network strength at baseline (pre-tACS) between the active and sham conditions (t(17.73)=0.525,p=.606).

I then went on to investigate whether there were any tACS-induced changes in network strength during learning. I performed a linear mixed effects analysis with one fixed effect of **STIMULATION** (active, sham) and one fixed effect of **TIMEPOINT** (pre, early, late, post). There was no significant main effect of **STIMULATION** (F(1,28)=0.005, p=.946). There was a significant main effect of **TIMEPOINT** (F(3,84)=17.163,p<.001). There was no significant **STIMULATION×TIMEPOINT** interaction (F(3,84)=2.426,p=.0713). To further explore the significant main effect of **TIMEPOINT**, I conducted post-hoc pairwise comparisons between the levels of the **TIMEPOINT** variable using Tukey-adjusted tests. There was a significant difference between pre-tACS and early-tACS (t(90.5)=4.29,p<.001), early-tACS and post (t(90.5)=-6.6,p<.001), and late-tACS and post (t(90.5)=-4.38,p<.001).

I also looked at the percentage change in network strength from pre-tACS. There was no significant main effect of **STIMULATION** (F(1,26.856)=2.531,p=0.123). There was a significant main effect of **TIMEPOINT** (F(2,52.697)=24.615, p<.001). There was no significant **STIMULATION×TIMEPOINT** interaction (F(2,52.697)=2.423, p=0.099; see Figure 58). To further explore the significant main effect of **TIMEPOINT**, I conducted post-hoc pairwise comparisons between the levels of the **TIMEPOINT** variable using Tukey-adjusted tests. There was a significant reduction in network strength between early- and post-tACS (t(58.5)=-6.471, p<.0001) and an increase in network strength between late- and post-tACS (t(59.2)=-4.877,p<.0001).

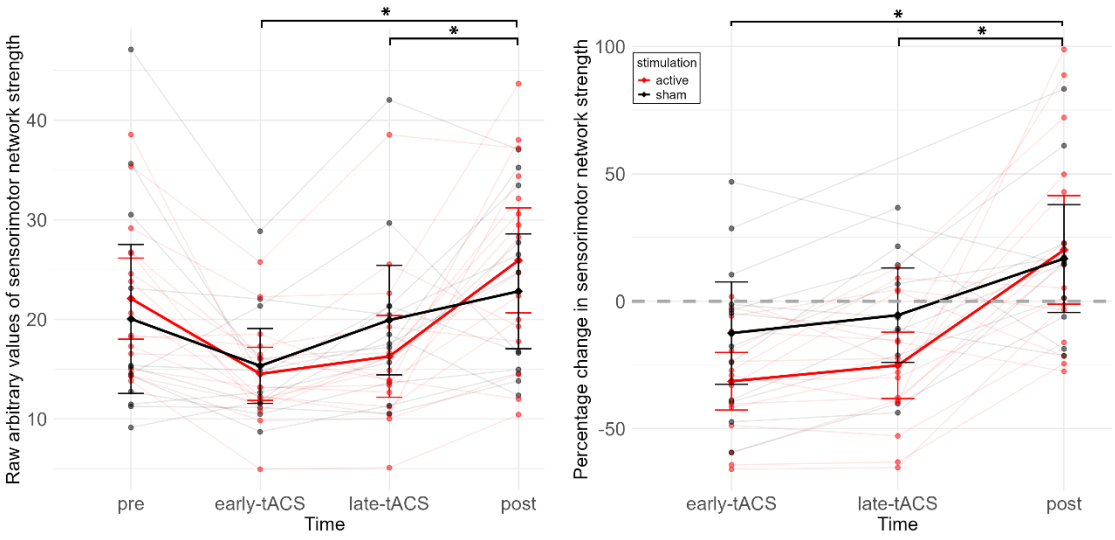

Figure 58: The effect of θγ oscillations on sensorimotor network strength during motor learning. Left: raw arbitrary values of sensorimotor network strength. Right: Percentage change in sensorimotor network strength from pre-tACS.

5.6.3 The effect of θγ oscillations on sensorimotor functional connectivity during learning

I then went on to investigate whether there were any tACS-induced changes in functional connectivity during learning There was a significant difference ($p<.050$) between active and sham tACS on the change in sensorimotor network connectivity from pre-tACS to late-tACS (see Figure 59; green) and from late-tACS to post-tACS (see Figure 59; blue). Maximum intensity voxel as well as centre-of-gravity coordinates in standard space can be found in Table 5 and a visual breakdown of the effect can be found in Figures 60 and 61.

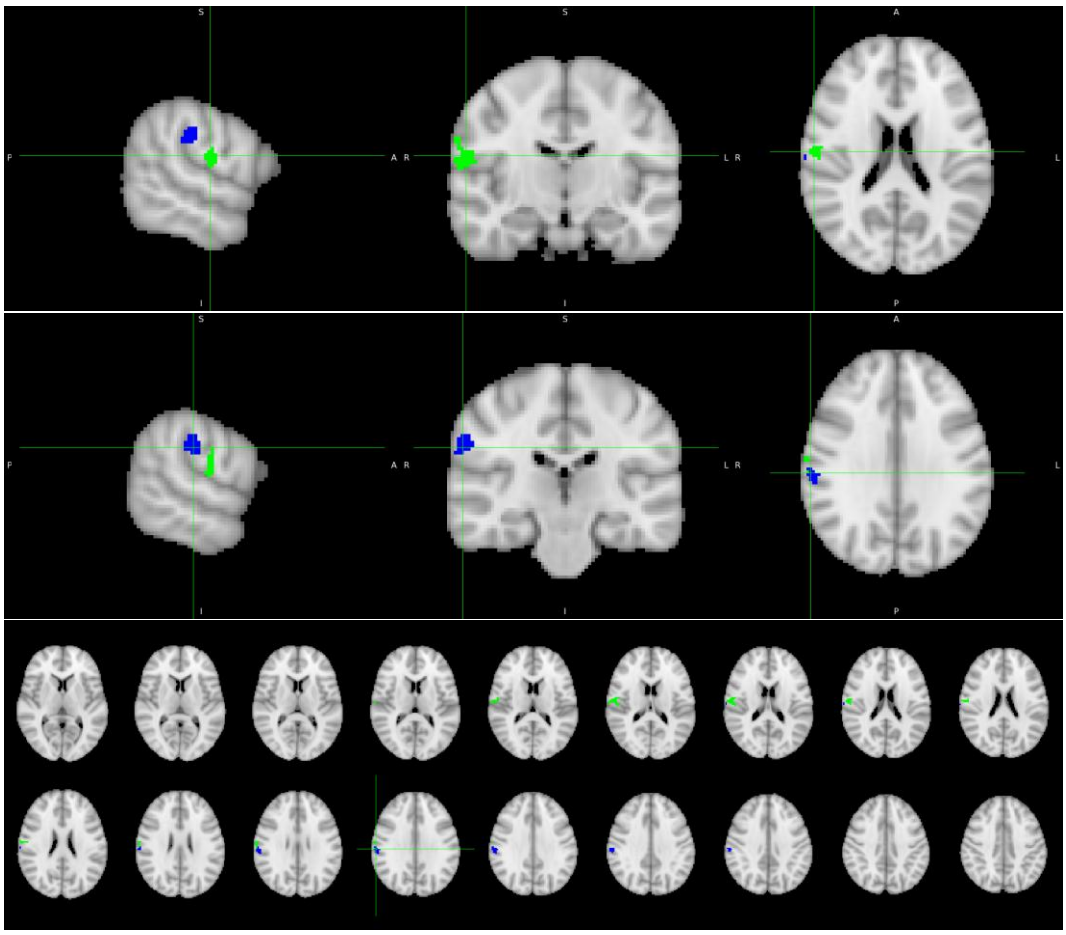

Figure 59: Significant sensorimotor functional connectivity clusters between active and sham for pre-tACS to late-tACS (green; postcentral gyrus) and late-tACS to post-tACS (blue; SMG) during motor learning.

Contrast	Colour	Voxels	MAX	MAX X (mm)	MAX Y (mm)	MAX Z (mm)	COG X (mm)	COG Y (mm)	COG Z (mm)
Pre- to late-tACS	Green	135	0.987	64	-16	12	59.6	-13.3	19.7
Late- to post-tACS	Blue	96	0.964	62	-14	14	61.6	-23.2	29.2

Table 5: The breakdown of the significant sensorimotor functional connectivity clusters by contrast. "Voxels" reports the number of voxels in the detected significant cluster. "MAX" reports the value of the maximum "intensity" within the cluster. "Max X/Y/Z" reports the location of the maximum intensity voxel given in standard space coordinates (mm). "COG X/Y/Z" reports the location of the centre-of-gravity for the cluster (the weighted average of the coordinates by the intensities within the cluster) given in standard space coordinates (mm). Images thresholded to Z=3.1, p=.050.

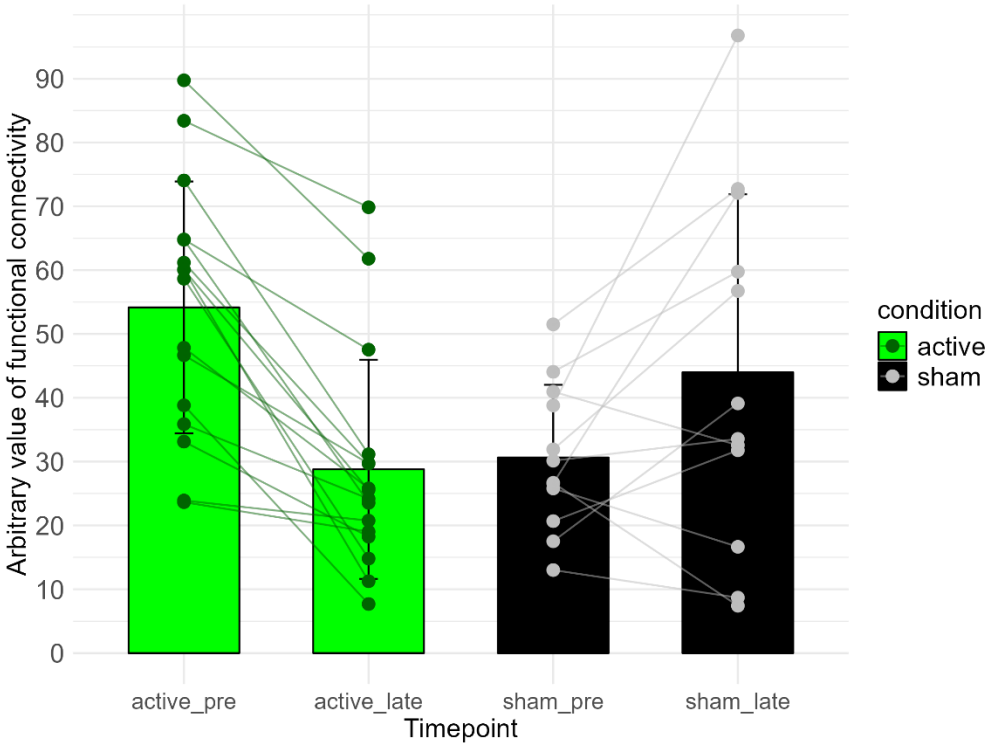

Figure 60: Breakdown of the significant change in functional connectivity between sensorimotor network and the postcentral gyrus from pre-tACS to late-tACS.

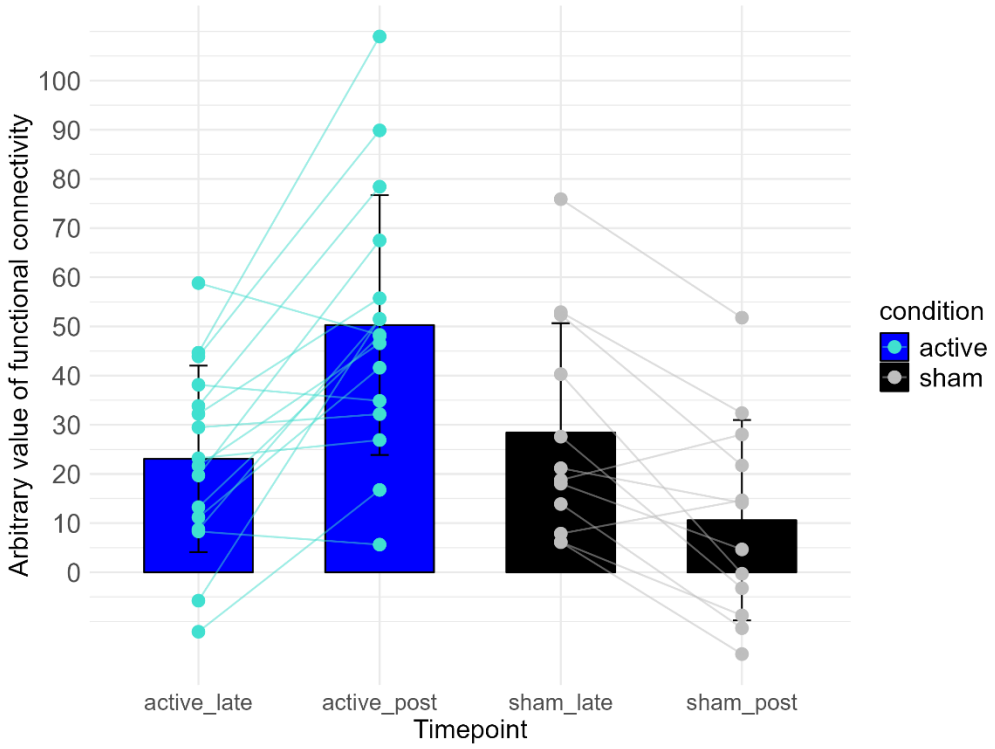

Figure 61: Breakdown of the significant change in functional connectivity between sensorimotor network and the supramarginal gyrus from late-tACS to post-tACS.

5.6.4 Correlation between neuronal changes in contralateral S1 and behaviour

I then wanted to understand whether there was a relationship between the tACS-induced neuronal changes and behaviour. I therefore calculated the slope of errors across learning in the sequence runs (2-5), such that negative slopes indicate greater motor learning. I correlated this behavioural metric with tACS induced functional connectivity changes from pre-tACS to late-tACS in the region shown in green in Figure 59. When calculating the learning-slope, one participant was a significant outlier (G=3.50, U=0.236,p<0.001). This datapoint was removed and no further outliers were detected. A Pearson correlation was then conducted to examine the relationship between slope and connectivity change. There was no significant correlation between the slope of error and sensorimotor-right S1 functional connectivity change from pre- to late-tACS (r=0.34, p= 0.185).

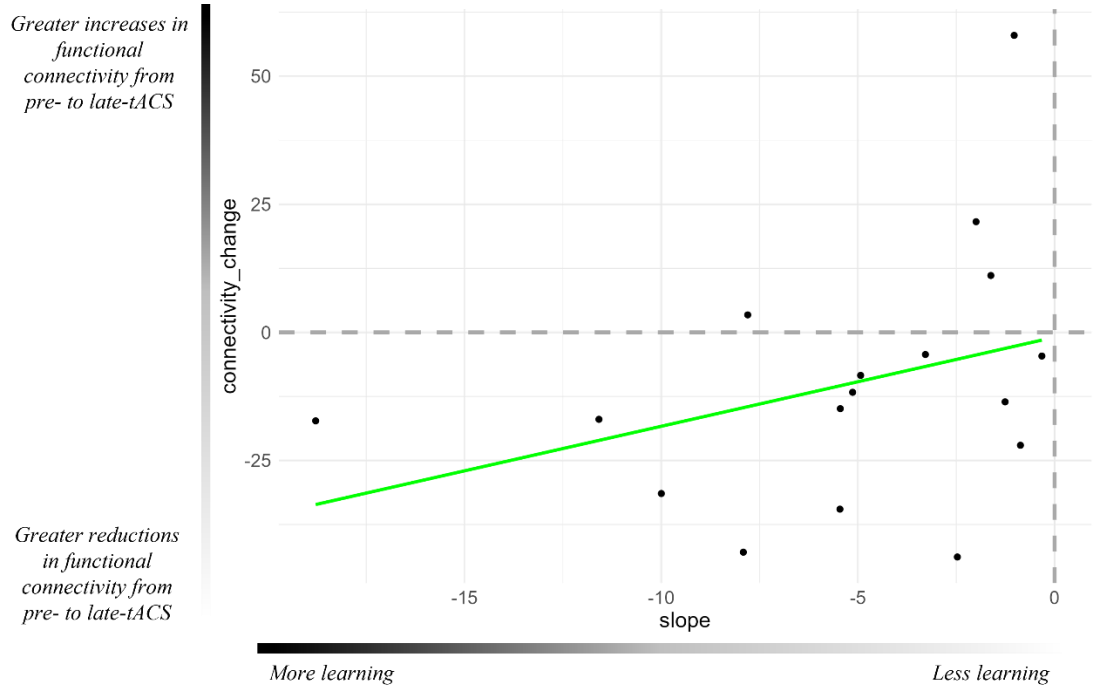

Figure 62: Correlation between the change in sensorimotor-right S1 functional connectivity from pre- to late-tACS and the slope of error reduction in the motor learning task.

5.7 Discussion

To date, there remains a lack of understanding about whether the positive behavioural effects of θγ oscillations on motor behaviour reported by Akkad *et al*. (2021) are mediated by local changes in neuronal activity or by wider, network level changes in functional connectivity. A combined tACS-fMRI methodology allows the causal investigation into the links between neuronal oscillations, network activity, and behaviour. Here, I investigated the effect of TGP tACS on sensorimotor functional connectivity at rest versus during motor learning. This experimental design highlights the potential of resting-state fMRI in assessing the spatiotemporal characteristics of functional brain reorganisation due to motor learning, tACS, and their interaction.

5.7.1 No significant effects of θγ oscillations during rest

I first investigated the effects of driving M1 θγ oscillations when participants were at rest, both at the network level and on a voxel-wise basis.

I found no significant changes in sensorimotor network strength over time, suggesting that in the absence of motor task requirements, the sensorimotor network is stable over time. This confirmed that my experimental protocol did not induce systematic, significant naturally-occurring fluctuations in the sensorimotor network when at rest. I also found no significant differences in sensorimotor network strength between active and sham stimulation. Based on

the results of my TMS study (that 20 minutes tACS at rest can induced changes in extra-synaptic GABAergic inhibition), it was plausible that active tACS may result in changes in sensorimotor network strength in the present study too. However, the lack of stimulation effects on sensorimotor network strength at rest is in line with the entrainment hypothesis of tACS such that without any motor (learning) oscillations occurring, the tACS has nothing to entrain onto. It is thus not able, independently, to induces significant changes in sensorimotor network strength.

Whilst useful, the metric of network strength gives the mean connectivity across the entire network, and therefore may be insensitive to specific regional changes within the wider network. My experimental design was a unimanual, grip force, M1-specific task. As such, looking across the entire network may have missed specific changes within M1. I thus next looked at the effects of driving M1 θγ oscillations on sensorimotor functional connectivity on a voxel-wise basis. I found no significant clusters when looking within the sensorimotor network and between the sensorimotor network and whole brain. Therefore, driving M1 θγ oscillations when participants are at rest had no significant effect on sensorimotor functional connectivity.

Overall, in the absence of motor network engagement, driving θγ M1 oscillations using tACS had no significant effects on sensorimotor network strength or functional connectivity.

5.7.2 The novel motor learning task induces significant motor learning

I then wanted to ascertain whether the novel motor learning task resulted in significant motor learning, quantified as reductions in median error over time, in the absence of stimulation (i.e. sham tACS). Due to the format of the task (*random* > *sequence* > *sequence* > *sequence* > *sequence* > *random*), an inverted-U shape was expected, characterised as reductions in error until the last block of sequence, after which error should increase in the final run. I found that participants were able to learn to modulate their grip force to meets the spatiotemporal demands of the task, reflected as a significant reduction in error between run1 and the rest of the blocks. Furthermore, in the post-hoc breakdown there was a significant difference between run 2 and 5 (the first and last sequence runs). This suggests that participants implicitly learnt to modulate their grip force to perform optimally. However, I did not find a significant difference between the last block of sequence and the last random block, though error did increase. Therefore, it seems that the discrepancy between sequence and general task learning was not fully captured with this design. Future research could look at how performance in the random and sequence runs changes long-term. I would expect that performance in the sequence runs remains high (due to consolidation) whereas performance in the random runs decreases over time (as participants are less in tune with the general spatiotemporal requirements of the task). Furthermore, a limitation of the present study's design, which impacted this behavioural analysis, was participant fatigue. Multiple participants reported fatigue and/or falling asleep inside the scanner. Whilst I tried to ensure this did not happen, a lot of behavioural data had to be removed due to poor quality. Therefore, I am underpowered in terms of behavioural output.

5.7.3 Motor learning significantly increases sensorimotor network strength

I then investigated the effects of motor learning in the absence of stimulation (i.e. sham tACS) on sensorimotor network strength. I found that engaging the sensorimotor network with a motor task significantly increased sensorimotor network strength over time. This effect was expected and in line with previous literature (Albert, Robertson and Miall, 2009; Ma *et al.*, 2011; Vahdat *et al.*, 2011; Kraeutner *et al.*, 2021). This increase in sensorimotor network strength with novel skill acquisition is thought to reflect the necessary integration of novel sensory and motor information to support the new skill, a process which becomes less necessary in the later phases of skill refinement (Ma *et al.*, 2011).

When breaking down the significant effect of timepoint on sensorimotor network strength, I found significant dynamic modulations in sensorimotor network strength characterised by an initial *reduction* in sensorimotor network strength from pre- to early-tACS, followed by an *increase* in sensorimotor network strength from early- to post-tACS and from late- to post-tACS. In other words, the sensorimotor network strength was dynamically modulated to support the different stages of skill acquisition. During the early stages of acquisition (pre- to early-tACS), there was an initial reduction in connectivity followed by an increased during the later stages of learning (early- and late- to post-tACS). This pattern is seen for both active and sham tACS. It is possible that from pre- to early-tACS, the sensorimotor network was actively desynchronising to explore potential motor schemes to meet the imposed challenges of the novel motor skill. As such, the network is less correlated (lower sensorimotor network strength). However, from early- to late- and post-tACS, the sensorimotor network had found the optimal motor scheme and was now synchronising its output to support this execution.

This interpretation is in line with findings from Stagg *et al.* (2014) who reported a negative correlation between the levels of M1 GABA and the strength of the functional connectivity within the sensorimotor network (see Figure 63). During early learning (such as those seen from pre- to early-tACS), there was likely high(er) levels of GABA, and thus less functional connectivity. However, reductions in GABA are known to serve improvements in motor learning behaviour (Stagg, Bachtiar and Johansen-Berg, 2011; Stagg *et al.*, 2011; Bachtiar and Stagg, 2014; Nowak *et al.*, 2017; Grigoras and Stagg, 2021). Therefore, by late motor learning one would expect a reduction in GABAergic signalling, correlated with an increase in functional connectivity. This explains why I found an initial reduction in sensorimotor network strength in early learning compared to gradual increases in later learning. Overall, my data demonstrated that motor learning dynamically modulated (reduced then increased) sensorimotor network strength, but not in a stimulation-dependent manner.

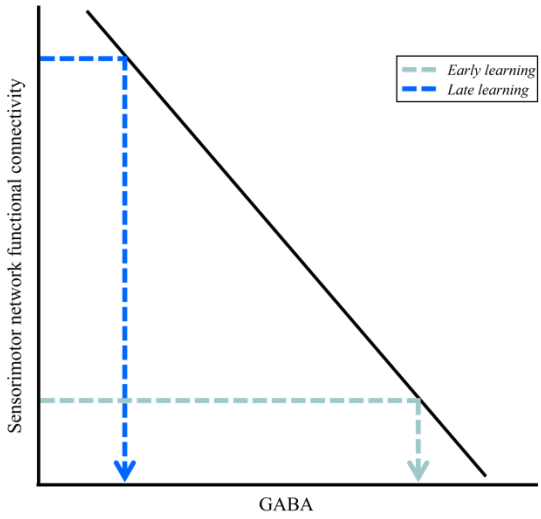

Figure 63: Visual depiction of how the findings from Stagg et al. (2014) may explain the findings of the present study. Stagg et al. (2014) report a negative correlation between sensorimotor network functional connectivity and GABA. In the present study, I find an initial reduction in sensorimotor network strength from pre- to early-tACS. This may be due to initial high(er) levels of GABA in the system. However, as learning goes on, reductions in GABAergic inhibition occur which, in turn, correlate to increases in sensorimotor network functional connectivity (and network strength).

5.7.4 M1-θγ oscillations significantly reduce functional connectivity between sensorimotor network and right S1 from pre- to late-tACS during motor learning

Next, I looked at the effect of driving M1 θγ oscillations on sensorimotor network functional connectivity on a voxel-wise basis. I found two significant clusters that differed significantly

between active and sham tACS. The first was from pre- to late-tACS in right S1 and the second was from late- to post-tACS in the SMG.

If my sham tACS session represents a close approximation to what naturally occurs in the brain during motor learning, there appears to be an increase in functional connectivity between the sensorimotor network and the right S1. This is perhaps unsurprising given the fact that left M1 and right S1 are structurally (Ruddy, Leemans and Carson, 2017) and functionally (Kinnischtzke, Simons and Fanselow, 2014) highly interconnected. Furthermore, corresponding changes in somatosensory regions with motor learning have been reported (Floyer-Lea and Matthews, 2005; Vahdat *et al.*, 2011; Ohashi, Gribble and Ostry, 2019; Pham *et al.*, 2022). In particular, right hemisphere parietal regions dominance during the early stages of motor skill learning have been reported (Halsband and Lange, 2006; Ma *et al.*, 2011). For example, Ma *et al.* (2011) report increased strength of resting state functional connectivity to the right S1 and SMG during early motor learning.

What is intriguing, however, is the seemingly opposite effect being driven by active stimulation. I found a significant reduction in functional connectivity between the sensorimotor network and the right S1 for active compared to sham tACS. In other words, driving θγ oscillations using tACS appears to prevent the naturally-occurring increased functional connectivity between the sensorimotor network and the right S1 during a unimanual grip force task. This apparent "disconnection" of nodes within the sensorimotor network during motor learning with active tACS was unexpected. To date, I have not established the behavioural relevance of such disconnection. However, the study is currently underpowered, especially with regards to the noisy behavioural data. With more participant data, the impact of such left M1-right S1 disconnection with active tACS on motor behaviour will become clearer.

A possible interpretation of such disconnection can be made based on the timing of the significant cluster. This effect is seen from pre- to late-tACS, or from early to late sequence learning. One possible explanation for the reduced functional connectivity between left M1 and right-S1 with active tACS is that over time, as the skill is learnt (with the support of concurrent active tACS), the sensorimotor network becomes less reliant on sensory information processing for the task (i.e. the initial visuomotor grip:force mapping required for the present study's task) and focuses greater attention to the motor execution of the skill.

It is worth noting that there are baseline differences in functional connectivity between active and sham (active pre-tACS and sham pre-tACS) which may be inflating this effect. However, on both an individual and group level, participants show reductions in functional connectivity from pre- to late-tACS when receiving active θγ oscillations, supporting the hypothesis that driving left M1 θγ oscillations disconnects this node from the right S1 node within the sensorimotor network.

5.7.5 M1-θγ oscillations significantly increase functional connectivity between sensorimotor network and right supramarginal gyrus from late- to post-tACS during motor learning

Initially, I thought that the two significant clusters could be one cluster. However, when I changed the threshold (from Z=3.1 to 2.5) these clusters remained spatially-distinct, suggesting that there are independent, functional connectivity changes between the sensorimotor network and two independent brain regions at different time points, perhaps serving different aspects of motor learning. I found significant differences between active and sham on functional connectivity between sensorimotor network and SMG from late- to post-tACS. The SMG is involved in the processing of body schema and proprioception (Sattin *et al.*, 2023). Specifically, unfamiliar (compared to familiar) movements, showed higher activation in the left intraparietal sulcus and in the anterior division of the right SMG (Bischoff *et al.*, 2012). Therefore, the SMG is involved in processing motor unfamiliarity.

If my sham tACS session represents a close approximation to what naturally occurs in the brain when learning, I found that these participants showed a reduction in functional connectivity from the sensorimotor network to the SMG from late- to post-tACS. According to the aforementioned role of the SMG in motor familiarity, the functional connectivity between the sensorimotor network and the SMG may have decreased as prioritising local activity within the SMG (rather than its functional connectivity to the sensorimotor network) occurred to cope with the sudden unfamiliarity of movement in the last run of the task (run 6, random at post-tACS). Therefore, the previously reported increase in functional connectivity from pre- to late-tACS was being driven by sequence learning and familiarity and this was lost when participants were exposed to a random sequence, requiring greater individual activation from the SMG during the random run at post-tACS.

Participants receiving active tACS, however, again show the opposite effect with significant increases in functional connectivity between the sensorimotor network and the right SMG from late- to post-tACS. This is more challenging to explain, however given that active tACS also had opposite effects in the previous significant cluster is it perhaps reassuring that this persists. This suggests that driving M1 θγ oscillations increases the functional connectivity of the sensorimotor network to the right SMG when performing unfamiliar/random movements. The opposite argument can also be taken here, such that active tACS increases the functional connectivity of the SMG to the sensorimotor network to cope with sudden motor unfamiliarity. However, this interpretation is challenging and not currently supported by literature.

5.7.6 Summary of the interpretation of the significant clusters

To summarise, from pre- to late-tACS (i.e. during sequence learning), participants receiving sham stimulation show an increase in functional connectivity between the sensorimotor network and the right S1. This supports previous literature such that increases in sensorimotor network functional connectivity support motor skill acquisition. However, when participants receive active tACS during the same timeframe (i.e. from pre- to late-tACS or during sequence learning), there is a reduction in sensorimotor functional connectivity between the sensorimotor network and the right S1. This apparent "disconnection" of nodes within the sensorimotor network during motor learning with active tACS may serve to reflect the automation of sensorimotor learning, such that less reliance on sensory areas are needed. From late- to post-tACS (i.e. the switch from sequence learning to random pattern and in the absence of stimulation), participants receiving sham show a reduction in functional connectivity between the sensorimotor network and the right SMG. This is interpreted as the SMG disconnecting from the sensorimotor network to focus on the sudden random movements (motor unfamiliarity). In active, however, these participants again show the opposite pattern with increases in functional connectivity between the sensorimotor network and the right SMG. Finally, I looked at changes in functional connectivity between the sensorimotor network and the whole brain but found no additional significant clusters. This suggests that there is no additional activity beyond that occurring within the sensorimotor network that is joining it.

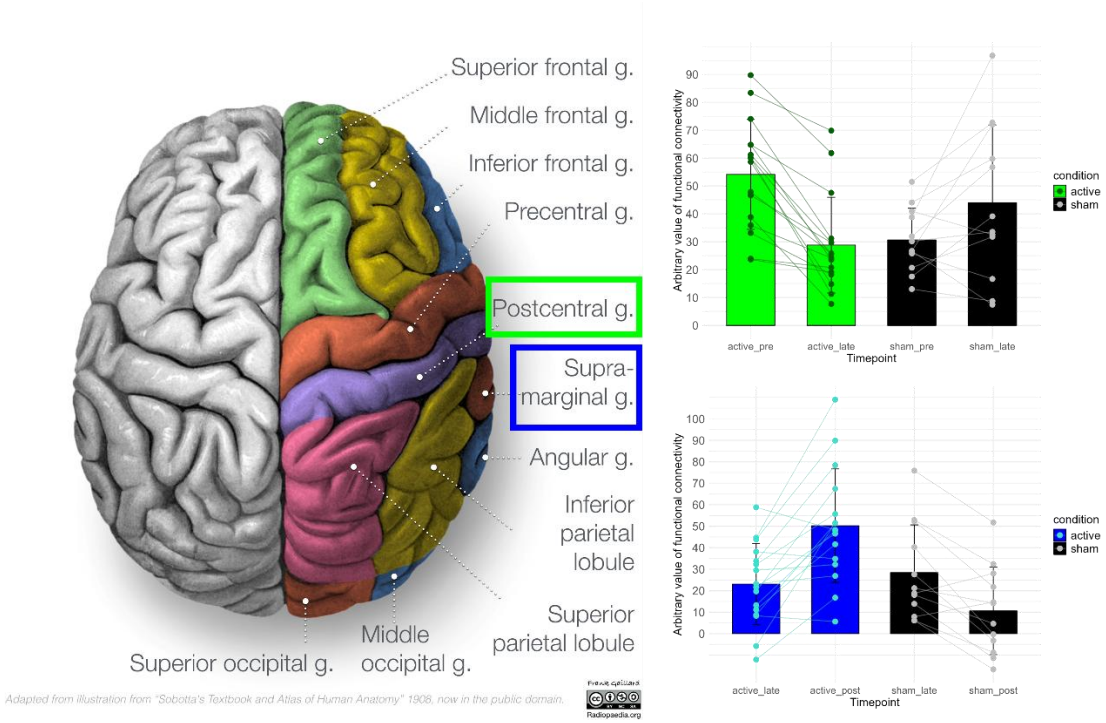

Figure 64: Brain image case courtesy of Frank Gaillard, Radiopaedia.org, rID: 59317 adapted into a visual summary of the findings of the fMRI data. Top (green) is the significant difference between active and sham on sensorimotor to S1 functional connectivity from pre- to late-tACS. Bottom (blue) is the significant difference between active and sham on sensorimotor to SMG functional connectivity from late- to post-tACS.

In summary, the interpretation of these significant clusters is challenging given the paucity of literature around the role of M1 θγ oscillations on sensorimotor network functional connectivity. However, here I provide the first evidence of dynamic modulations in functional connectivity at different time points (from pre- to late-tACS and late- to post-tACS) with spatially independent neuronal correlates (sensorimotor network to right S1 and sensorimotor network to SMG).

5.7.7 Future directions

As part of the data collection for this project, I also acquired blocks of MRS data at the same timepoints as the fMRI. So far, with resting-state fMRI, I have demonstrated dynamic modulations in sensorimotor resting state functional connectivity with active tACS when combined with a motor task. However, whether (and how) these changes in functional connectivity are correlated to neurochemical modulations remains unknown. MRS-measured GABA is thought to measure the total amount of GABA within a voxel and more closely reflect extrasynaptic rather than synaptic GABA activity (Stagg *et al.*, 2011; Stagg, 2014) (Stagg *et al.*, 2011, 2014). Given the changes in sensorimotor functional connectivity and the findings of Stagg *et al*. (2014) I anticipate finding increases in GABA from pre- to late-tACS and reductions in GABA from late- to post-tACS. However, this is dependent on the assumption that these are correlated. I will then also look at how such changes in GABA correlate to motor learning to add to the current wealth of literature supporting the role of GABA in motor learning.

CHAPTER VI - General discussion

In this final chapter, I provide an overview of the research questions, the experiments conducted to address these questions, the findings of the experiments and how together they provide insight into the role of θγ oscillations in human motor neurophysiology. Finally, I address some general limitations of the research questions and methods used throughout the thesis and discuss how future research could address these.

6.1 Summary

In this thesis, I investigated the role of motor θγ phase amplitude coupled oscillations on healthy human motor neurophysiology and learning. I used transcranial alternating current stimulation (tACS) as the non-invasive neuromodulatory technique to entrain θγ oscillations in healthy human motor cortex and, putatively, the wider functionally-connected sensorimotor network. By entraining θγ oscillations, I investigated the effect this had on behaviour (Chapter 2: Behavioural), receptor-mediated inhibition and excitation (Chapter 3: TMS), and sensorimotor functional connectivity (Chapter 4: Neuroimaging). I ran three double-blind, randomised, sham-controlled experiments each asking questions that, together, provide a clearer idea of the role of θγ oscillations on healthy human motor neurophysiology and learning.

In Chapter 1, I first contextualised the significant clinical problem that stroke poses to society and how the acquisition of a new motor skill in the healthy brain is likened to the reacquisition of a lost motor skill in the post-stroke brain. As such, I used healthy human motor learning as a model of post-stroke motor skill recovery. I then defined motor learning for the purposes of the experimental Chapters and outlined the role of the human primary motor cortex and other motor areas in motor learning. I then explored the neurophysiology of different neuronal subtypes, including excitatory pyramidal cells and inhibitory interneurons and how their interactions give rise to oscillations, specifically θ and γ oscillations. I outlined the role of cross frequency coupling between θ and γ, specifically phase amplitude coupling, in hippocampal-dependent learning. I then discussed whether this θγ PAC pattern of oscillatory activity can be extrapolated to non-hippocampal dependent learning, such as *motor* learning. Finally, I outlined tACS as a neuromodulatory technique as well as provide an overview of its hypothesised mechanisms of action.

In Chapter 2, I provided an overview of the methods used throughout this thesis to investigate the role of θγ oscillations on motor neurophysiology and learning. First, I outlined the neuromodulatory technique used to entrain θγ oscillations: tACS. I stated the electrode montage used to induce peak electric fields in M1, as inferred by current flow models and outline the four different tACS waveforms used throughout the thesis: θ-high γ peak (75Hz/6Hz), θ-high γ trough (75Hz/6Hz), θ-low γ peak (45Hz/6Hz), and sham (6Hz). I then went on to outline and explain the development of my two novel grip force modulation tasks I developed in order to answer my research questions in Chapters 3 (Behavioural study) and 5 (Neuroimaging study). Next, I outlined how TMS can be used to probe cortical excitability and receptor-mediated inhibition and excitation due to tACS using single and paired pulse TMS, respectively. Finally, I outlined how (f)MRI can be used to examine functional connectivity within the sensorimotor network and between the sensorimotor network and the whole brain.

I then ran three independent, but linked, experiments to investigate the causal effect of driving θγ oscillations on neurophysiology and behaviour.

6.1.1 Short bursts of 45Hz TGP tACS significantly reduces force output and affects behaviour

In the first experimental Chapter (Chapter 3: Behavioural), I built on the work of Akkad *et al*. (2021) and explored the effect of driving M1 TGP oscillations on motor behaviour. Unlike Akkad *et al*. (2021) who delivered continuous tACS for 20 minutes (presumed to induce neuroplastic changes), here I tested a different mechanism-of-action of tACS (entrainment) by looking at how tACS delivered in short bursts of three seconds, time-locked to movement modulates behaviour. I first aimed to replicate the finding that 75Hz TGP tACS significantly improves motor behaviour, even when delivered in short bursts. I then explored the frequency-specificity of this effect by looking at the difference between driving slow (45Hz) or mid (75Hz) γ oscillations at the peak of the θ envelope on motor performance.

I found no significant effect of 75Hz TGP on motor behaviour as quantified by the number of targets hit. However, I found an effect of 45Hz TGP on the number of targets hit with

participants receiving 45Hz/6Hz TGP hitting significantly fewer targets than participants receiving sham stimulation. This effect did not, however, hold to a more refined metric of motor performance, that of tracing error. This was unexpected, given that the two metrics are inherently linked (a reduction in tracing error = greater chance of hitting the targets). A further exploratory analysis of force output during the first 0.5 seconds of tACS delivery time-locked to movement revealed further information about the role of 45Hz TGP. I found a significant stimulation by time interaction between sham and 45Hz TGP such that in the first two blocks of motor learning, participants receiving 45Hz/6Hz stimulation had significantly shallower force slopes (i.e. reductions in force output) than participants receiving sham stimulation. Together, the findings of fewer targets hit, and shallower slopes can be interpreted as a general reduction in force output induced by 45Hz/6Hz tACS. This is in line with previous animal optogenetic literature and in fact provides new insights and interpretations into this work. Overall, three-second bursts of 45Hz TGP tACS appears to significantly reduce force output in healthy humans compared to sham tACS.

6.1.2 20 minutes of continuous TGP tACS at rest significantly reduces extrasynaptic GABAergic tone

In the second experimental Chapter (Chapter 4: TMS), I investigated the neurophysiological effects of driving motor θγ oscillations on receptor-mediated excitation and inhibition using TMS. Using the same electrode montage (C3-Pz), tACS waveforms (TGP and TGT), intensity (2mA peak-to-peak), and duration (20 minutes) as Akkad *et al*. (2021), I sampled single and paired pulse TMS before, during (early), during (late), and after 20 minutes of TGP, TGT, and sham at rest within-subject across three sessions. This allowed me to start unveiling the potential neurophysiological mechanisms that may underpin the positive behavioural effects of θγ oscillations on motor behaviour reported by Akkad *et al*. (2021).

For single pulse TMS (an index of corticospinal excitability), I found that driving TGT oscillations resulted in a significant reduction in corticospinal excitability, compared to sham stimulation. The trough of θ oscillations are associated with increased levels of inhibition (Huerta and Lisman, 1996) therefore despite the presence of γ oscillations, the ongoing inhibitory tone set by the θ rhythm likely suppressed the net excitability of the cortical network, resulting in significant reductions in corticospinal excitability.

For paired pulse TMS, I looked at metrics of synaptic (SICI2.5ms) and extrasynaptic (SICI1ms) GABAa-receptor mediated inhibition. I found that driving TGP oscillations significantly reduced extrasynaptic GABAergic tone compared to TGT. I found no significant effect of driving θγ oscillations on SICI2.5ms. This suggests that externally-driving oscillations significantly affects the local GABAergic tone as opposed to synaptic signalling. Though this is not in line with previous literature (Nowak *et al*., 2017), given the role of extrasynaptic tone on modulating neuronal firing patterns, it is perhaps unsurprising that artificially driving oscillations affects tonic rather than phasic inhibition.

The finding of changes in extrasynaptic GABAergic tone informed the final experiment. Extrasynaptic GABAergic tone is thought to be correlated to resting state functional connectivity of networks in the brain. Therefore, in the final experiment I looked at the effects of driving θγ oscillations on sensorimotor functional connectivity.

6.1.3 Motor learning significantly increases sensorimotor network strength

In the final experimental Chapter (Chapter 5: Neuroimaging), I investigated the effect of TGP tACS on sensorimotor network functional connectivity using resting-state fMRI. I acquired resting-state fMRI before, during, and after 20 minutes of 75Hz/6Hz TGP tACS and sham combined with/without a grip force modulation task. I also conducted a separate sub-study with participants receiving sham tACS during the same grip force modulation task to act as experimental controls.

I first demonstrated that my novel grip force modulation task significantly changed sensorimotor network strength in participants receive active and sham stimulation. When participants were at rest, the sensorimotor network strength was stable over time. However, dynamic, task-dependent changes in sensorimotor network strength were detected. Intriguingly, I found that network strength initially decreases during early learning, followed by a steady increase. This suggests state-dependent modulations in network dynamics to support the acquisition of a novel motor skill. To date, I did not find a significant effect of driving θγ oscillations on these changes in network strength. However, the study is currently underpowered.

6.1.4 Driving TGP oscillations at rest results in no significant change in functional connectivity within the sensorimotor network

In my TMS experiment, I found that driving 20 minutes of TGP oscillations at rest resulted in significant modulations in extrasynaptic GABAergic tone. Due to the correlation between extrasynaptic GABAergic tone and functional connectivity (Stagg *et al.*, 2014), it was plausible that I might find modulations in functional connectivity within the sensorimotor network when delivering 20 minutes of tACS at rest in the scanner. However, I demonstrated no significant changes in functional connectivity within the sensorimotor network when driving θγ oscillations when participants were at rest.

6.1.5 Driving TGP oscillations during motor behaviour significantly changes functional connectivity within the sensorimotor network

I then investigated the effects of driving θγ oscillations on functional connectivity within the sensorimotor network when participants were engaging the sensorimotor network with a grip force modulation task. The entrainment hypothesis of tACS suggests that tACS requires the endogenous oscillations to be at, or close to, the exogenously-applied oscillations in order to achieve entrainment. This is supported by my previous finding of no change in functional connectivity when participants are at rest, putatively because there are few ongoing θγ oscillations. When actively engaging the sensorimotor network, I found two significant clusters that differed significantly between active and sham tACS. The first was from pre- to late-tACS in right S1 and the second was from late- to post-tACS in the SMG. Whilst a complete breakdown of the interpretation of these clusters for both active and sham tACS can be found in Chapter 5, briefly, I propose that during early sequence learning, active tACS promotes a disconnection between the sensorimotor network and the right S1, reflecting the automation of sensorimotor learning, such that less reliance on sensory areas are needed. From late to post-tACS (i.e. from sequence to random learning), I found that active tACS increases the functional connectivity between the sensorimotor network and the SMG. Here, I argued that this represented an attempt to cope with sudden motor unfamiliarity. However, these interpretations are purely subjective since this, to our knowledge, is the first study looking at the effect of artificially driving θγ oscillations on sensorimotor functional connectivity.

6.2 General limitations and future directions

Study-specific limitations are explored in the respective Chapters' discussion. However, there are overall general limitations regarding the general approach and rationale of this thesis.

6.2.1 Lack of reproducibility in NIBS studies

Though there is evidence that tACS can influence oscillatory neuronal activity in small animal models (Ozen *et al.*, 2010; Ali, Sellers and Frohlich, 2013; Huang *et al.*, 2021), non-human primates (Kar and Krekelberg, 2014), and computational models (Ali, Sellers and Frohlich, 2013) understanding the precise mechanisms of tACS in order to reliably steer its effects on human behaviour has proven to be surprisingly difficult. As a result, there is currently a lack of reproducibility in NIBS studies, limiting the potential of such findings.

6.2.1.1 Neuroanatomical differences

Since the positioning and size of the tES electrodes determines the distribution of the electric field (e-field) in the brain (Datta *et al.*, 2011), I can theoretically "steer" the spatial effects of tES via the selection of an electrode montage with the assumption that regions receiving higher peak e-fields are more likely to be affected by the stimulation, whilst regions with lower e-field intensities are spared (Bikson, Rahman and Datta, 2012). However, the electrical current is delivered noninvasively and must pass through multiple different tissue types (the skull, meninges, grey matter, CSF), each with unique conductance properties, before reaching the target region of interest. Neuroanatomical inter-individual differences in tissue type significantly affects the distribution and strength of the e-field distribution. For example, literature has shown that higher head volume and relative volumes of skin, skull, and CSF were all associated with lower induced e-field strengths in a region of interest (Antonenko *et al.*, 2021; Franco-Rosado *et al.*, 2024). Furthermore, these relationships were more pronounced in older adults, due to differences in grey matter volume which also significantly affects e-field distribution (Franco-Rosado *et al.*, 2024).

Whilst computational models of current flow in the brain (current flow modelling; CFM) have been used to provide insight into the estimated current flow patterns induced by tES (Bikson, Rahman and Datta, 2012), calculating this on an individual basis is time consuming. As such, literature (and the present studies) typically adopt a set electrode montage and current intensity across all of their participants. For instance, throughout this thesis I adopted the C3-Pz montage for all of my participants, following the CFM validation of this montage by Akkad et al. (2021). Due to neuroanatomical differences, for which I did not account for with the montage, this likely resulted in different e-field distributions for each participant, in turn resulting in different effects on neurophysiology, including entrainment and spike-timing dependent plasticity. This was particularly apparent in my TMS study, when the area measured as C3 according to the 10-20 EEG system was, in fact, not the M1 hotspot.

In an ideal world, I would identify functionally-relevant parts of motor cortex on an individual basis using fMRI. I would then use individualised current flow models to calculate the unique electrode montage and current intensity required to induce an e-field of certain intensity in the functionally-defined region of motor cortex. This would ensure targeting of functionally-relevant parts of cortex, individualised on a subject-by-subject level to account for any/all neuroanatomical differences. However, this process is extremely time consuming as well as computationally-expensive and requiring specialist equipment and expertise.

6.2.1.2 Set versus individualised frequency

tACS additionally suffers from the debate of frequency specificity. tACS is assumed to result in frequency-specific entrainment. However, whether we should use a) a set frequency approach across all participants (e.g. 70Hz) or b) an individualised frequency approach (e.g. using M/EEG to establish the peak frequency) remains under contention and the knowledge of how these frequencies interact with local endogenous oscillations remains unclear.

There is evidence that setting the tACS frequency to individual participants' peak endogenous behaviourally-relevant oscillation has positive behavioural benefits in the cognitive (Aktürk *et al.*, 2022; Zhang, Moraidis and Klingberg, 2022) and motor (Spooner and Wilson, 2023; Van Hoornweder *et al.*, 2024) domain. For example, Zhang, Moraidis and Klingberg (2022) found that individualised θ tACS, compared to sham tACS, significantly increased frontoparietal synchrony which was, in turn,

correlated to behavioural improvements in visuospatial working memory and mental rotation. Likewise, individualised γ-tACS over M1 led to enhanced motor performance/learning (i.e. greatest reduction in time to complete motor sequences compared to non-specific γ tACS (Spooner and Wilson, 2023).

There is also evidence that delivering tACS around rather than at the peak frequency may be better. For example, Aktürk *et al.* (2022) found that whilst individualised peak θ tACS maximally modulated resting-state oscillatory power, θ tACS delivered at a frequency slightly below the optimal peak θ frequency was actually better suited to enhance memory capacity performance. This was hypothesised to be because memory capacity scales with the number of γ cycles that can be fitted into the preferred phase of a θ cycle (Aktürk *et al.*, 2022). Thus, artificially slowly down the endogenous peak θ actually allows more γ cycles to be fit, serving improvements in memory.

Standard tACS protocols, even when calibrated to an individual peak frequency, likely does not capture the complexity, or the idiosyncrasy, of the neuronal oscillatory response or endogenous activity (Janssens *et al.*, 2022). In fact, the "peak" value observed in M/EEG spectra often contains a broader range of frequencies, and thus a truly "biologically-calibrated" tACS protocol should contain this full, wider, range of frequencies (Janssens *et al.*, 2022). Such a "broadband" tACS approach has been found to significantly modulate attentional benefits compared to sham, but more research and replication is required in order to disentangle and understand its potential. Overall, depending on the neurophysiological basis of the behavioural performance attempted in being modulated, the delivery of a frequency at or around the peak frequency may be better suited.

Therefore, there appears to be contention around whether the delivery of tACS at/around the peak frequency affects behavioural performance. However, more recently, literature is moving away from the idea that we should be focussing on the frequency of the externally applied current, but that we should rather be looking at how the frequency (regardless of whether it is at/around peak frequency) interacts with what is happening endogenously. Participants' naturally ongoing endogenous neuronal activity has been shown to interact with the effects of tACS (Feurra *et al.*, 2013; Neuling, Rach and Herrmann, 2013; Alagapan *et al.*, 2016; Ruhnau *et al.*, 2016; Kasten and Herrmann, 2020). For example, in the visual domain, the effect of alpha tACS is state-dependent such that when participants have their eyes closed (which naturally increases alpha oscillations) the effect of alpha tACS is reduced (Neuling, Rach and Herrmann, 2013; Ruhnau *et al.*, 2016). Likewise, in the motor domain, increasing beta power via motor imagery has been shown to increase the effectiveness of beta tACS (Feurra *et al.*, 2013). Therefore, tACS clearly interacts with naturally ongoing endogenous oscillations, though the nature of this interaction is unclear (Krause *et al.*, 2021).

Krause *et al.* (2021) more recently explored the hypothesis that tACS in fact competes with ongoing endogenous oscillations for control over spiking activity. Here, they investigated the interaction between ongoing oscillations and tACS by recording single-neuron activity in the non-human primate brain. They found that tACS can entrain neuronal activity, but only when spike entrainment to ongoing activity is weak (Krause *et al.*, 2021). When neurons were strongly locked to ongoing activity, the application of tACS actually resulted in a reduction in entrainment which could only be reversed at higher stimulation amplitudes (Krause *et al.*, 2021). This data thus suggests that tACS competes with ongoing endogenous oscillations for control over spiking activity (Krause *et al.*, 2021). This is further supported by computational

models showing that at low intensities (<0.3mV/mm), tACS desynchronizes neuronal firing relative to the endogenous oscillations, whereas at higher intensities (>0.3mV/mm) neurons are entrained to the exogenous electric field (Zhao, 2023). It is possible that when neurons are strongly locked to an ongoing oscillation, the delivery of additional current actually acts as an injection of noise into the system and disrupts the ongoing oscillatory process.

6.2.2 Future directions

6.2.2.1 Closed loop stimulation

Thus far I have explored how in order to successfully entrain neuronal oscillations noninvasively, the stimulation should either a) target regions and behavioural conditions in which ongoing entrainment is relatively weak (Krause *et al.*, 2021); or b) follow an Arnold Tongue in which the exogenous oscillation frequency should be *at* or *close to* the relevant endogenous frequency of the targeted neuronal network (Weinrich *et al.*, 2017; Lazzaro *et al.*, 2022; Vogeti, Boetzel and Herrmann, 2022). The latter approach is challenging because estimates of frequency and phase provide only transient approximations to the actual oscillations (Cole and Voytek, 2017; Krause *et al.*, 2021) and drift on sub-second timescales (Mansouri *et al.*, 2017; Krause *et al.*, 2021). One way of controlling for this is using closed-loop stimulation approaches. Closed loop tACS protocols involve the real-time adjustment of stimulation parameters based on ongoing brain activity, typically monitored using EEG, to maximise the efficacy of tACS in maintaining alignment with endogenous neuronal oscillations. Such closed loop approaches have been successful (Jones *et al.*, 2023; Martin and Nikolin, 2024) but are technically-challenging, requiring specialist equipment and expertise.

6.2.2.2 Magnetic Resonance Spectroscopy (MRS)

As part of Chapter 5, I also collected 7T-MRS data before, during, and after tACS with/without the motor task. To date, there is no literature looking at the effects of artificially driving θγ oscillations in healthy human motor cortex on MRS-measured GABA. Following the behavioural findings of Akkad *et al*. (2021), the behavioural changes reported in Chapter 3 with 45Hz TPG tACS, the reduction in extrasynaptic GABAergic tone (SICI1ms) reported in Chapter 4 with 75Hz TGP, and the modulations in sensorimotor network functional connectivity reported in Chapter 5 with 75Hz TGP, it is highly likely that TGP tACS modulates GABAergic signalling. Looking at how MRS-measured GABA changes before, during, and after TGP tACS with/without a motor learning task will provide an additional piece to the puzzle of understanding what the effects of θγ motor cortical oscillations are on local and network level neurophysiology. I will also look at how MRS-measured GABA correlates to functional connectivity to build upon the work of Stagg *et al*. (2014).

Whilst MRS quantifies the total concentration of neurochemicals within a voxel, it is not currently capable of distinguishing the relative contributions of different pools of the same chemical from within the voxel (e.g. synaptic versus extrasynaptic GABA; Stagg, 2014). Paired-pulse TMS literature has attempted to elucidate what MRS-measured GABA measures by looking at the correlation between MRS-measured GABA and SICI1ms and SICI2.5. However, this relationship remains unclear. For example, Stagg *et al.* (2011) report a significant correlation between MRS-measured GABA levels and SICI1ms but Dyke *et al.* (2017) more recently reported no correlation between MRS-measured GABA and GABAa or GABAb activity. Therefore, it remains unclear what GABAergic pools are detected with MRS. Future research may wish to look at how driving TGP oscillations affects SICI1ms,

SICI2.5msm and MRS-measured GABAergic metrics, within subject and attempt to correlate them.

6.2.2.3 θ and γ tACS as active controls

When using phase amplitude coupled waveforms, it is difficult to disentangle the effects mediated by the phases of the θ envelope versus the role of the γ activity nested within the θ. There is evidence that whilst θ and γ couple in a phase amplitude manner, they remain mechanistically distinct (Johnson *et al.*, 2017). As such, in order to understand the effects of θγ PAC oscillations, harnessing an understanding of how driving these oscillations independently affects motor cortical neurophysiology is necessary. This would allow us to understand whether independent θ- and γ-tACS and θγ tACS have similar cumulative effects or if they subserve independent aspects of neurophysiology. Future studies may wish to replicate the methodology of Chapter 4 (TMS), using θ-tACS, γ-tACS, and θγ tACS to systematically investigate the effects of each frequency on cortical excitability and receptor-mediated inhibition and excitation.

6.2.2.4 Driving θγ oscillations in the post-stroke brain

Whilst in this thesis I explored the neurophysiological mechanisms of θγ oscillations in the healthy brain, the ultimate aim is to apply this knowledge to the recovery of motor function post-stroke. The post-stroke brain poses additional complexities to the delivery of tACS. Stroke lesions interact with and distort current flow in a target region-of-interest (Johnstone *et al.*, 2021). This is, in part, because the post-stroke necrotic tissue stroke is replaced with highly conductive CSF, affecting the way tES travel across different tissue types. This highlights the importance of the work carried out in this thesis: gaining an understanding of the mechanisms of a method in the healthy brain and how to reliably steer its effects is fundamental before being applied to a more complex clinical brain in an informed and safe manner.

Novel work by Grigutsch *et al.* (2024) found that TGP tACS did not enhance overall skill acquisition in stroke survivors. This is likely because our understanding of the neurophysiological mechanisms of θγ oscillations (and how to reliably drive these using tACS) remains limited. Future research should utilise precise, individualised current flow models in conjunction with the findings of the present studies to investigate the optimal delivery of θγ oscillations (γ frequency specificity, considerations of tonic GABA in the post-stroke brain, engagement of sensorimotor network with a task, concurrent EEG to assess entrainment) in post-stroke survivors.

6.3 Conclusion

In this thesis, I explored the functional role of θγ oscillations on healthy human motor behaviour and neurophysiology. I artificially entrained these oscillations using a non-invasive brain stimulation approach: tACS. The take home messages are as follows:

1. Short bursts of 45Hz TGP tACS significantly reduces force output.
2. 20 minutes continuous 75Hz TGP tACS significantly reduces extrasynaptic GABAergic tone.
3. 20 minutes continuous 75Hz TGP tACS significantly modulates the sensorimotor network's functional connectivity.

Overall, the relatively weak input provided by tACS has the potential to powerfully modulate the temporal structure of neuronal activity, and subsequent downstream neurophysiological mechanisms, noninvasively. Given the recent attention of driving motor cortical θγ oscillations in human motor cortex, the findings of the present studies provide novel, key, foundational insights into understanding the neurophysiological mechanisms of this intervention as well as seeing its potential as a non-invasive neuromodulatory technique.

CHAPTER VII References

Ainsworth, M. *et al.* (2011) 'Dual Gamma Rhythm Generators Control Interlaminar Synchrony in Auditory Cortex', *The Journal of Neuroscience*, 31(47), pp. 17040–17051. Available at: https://doi.org/10.1523/JNEUROSCI.2209-11.2011.

Akkad, H. *et al.* (2021) 'Increasing human motor skill acquisition by driving theta–gamma coupling', *eLife*, 10, p. e67355. Available at: https://doi.org/10.7554/eLife.67355.

Aktürk, T. *et al.* (2022) 'Enhancing memory capacity by experimentally slowing theta frequency oscillations using combined EEG-tACS', *Scientific Reports*, 12(1), p. 14199. Available at: https://doi.org/10.1038/s41598-022-18665-z.

Alagapan, S. *et al.* (2016) 'Modulation of Cortical Oscillations by Low-Frequency Direct Cortical Stimulation Is State-Dependent', *PLOS Biology*. Edited by O. Jensen, 14(3), p. e1002424. Available at: https://doi.org/10.1371/journal.pbio.1002424.

Albert, N.B., Robertson, E.M. and Miall, R.C. (2009) 'The Resting Human Brain and Motor Learning', *Current Biology*, 19(12), pp. 1023–1027. Available at: https://doi.org/10.1016/j.cub.2009.04.028.

Alekseichuk, I. *et al.* (2016) 'Spatial Working Memory in Humans Depends on Theta and High Gamma Synchronization in the Prefrontal Cortex', *Current Biology*, 26(12), pp. 1513–1521. Available at: https://doi.org/10.1016/j.cub.2016.04.035.

Ali, M.M., Sellers, K.K. and Frohlich, F. (2013) 'Transcranial Alternating Current Stimulation Modulates Large-Scale Cortical Network Activity by Network Resonance', *Journal of Neuroscience*, 33(27), pp. 11262–11275. Available at: https://doi.org/10.1523/JNEUROSCI.5867-12.2013.

Aliakbaryhosseinabadi, S. *et al.* (2021) 'Effect of motor learning with different complexities on EEG spectral distribution and performance improvement', *Biomedical Signal Processing and Control*, 66, p. 102447. Available at: https://doi.org/10.1016/j.bspc.2021.102447.

Andersson, J.L.R., Jenkinson, M. and Smith, S. (2007) *Non-linear registration aka Spatial normalisation: FMRIB Technial Report*. TR07JA2.

Antal, A. and Herrmann, C.S. (2016) 'Transcranial Alternating Current and Random Noise Stimulation: Possible Mechanisms', *Neural Plasticity*, 2016, pp. 1–12. Available at: https://doi.org/10.1155/2016/3616807.

Antal, A. and Paulus, W. (2013) 'Transcranial alternating current stimulation (tACS)', *Frontiers in Human Neuroscience*, 7. Available at: https://doi.org/10.3389/fnhum.2013.00317.

Antonenko, D. *et al.* (2021) 'Inter-individual and age-dependent variability in simulated electric fields induced by conventional transcranial electrical stimulation', *NeuroImage*, 224, p. 117413. Available at: https://doi.org/10.1016/j.neuroimage.2020.117413.

Antonoudiou, P. *et al.* (2020) 'Parvalbumin and Somatostatin Interneurons Contribute to the Generation of Hippocampal Gamma Oscillations', *The Journal of Neuroscience*, 40(40), pp. 7668–7687. Available at: https://doi.org/10.1523/JNEUROSCI.0261-20.2020.

Ashe, J. (1997) 'Force and the motor cortex', *Behavioural Brain Research*, 86(1), pp. 1–15. Available at: https://doi.org/10.1016/S0166-4328(96)00145-3.

Axmacher, N. *et al.* (2010) 'Cross-frequency coupling supports multi-item working memory in the human hippocampus', *Proceedings of the National Academy of Sciences*, 107(7), pp. 3228–3233. Available at: https://doi.org/10.1073/pnas.0911531107.

Bächinger, M. *et al.* (2017) 'Concurrent tACS-fMRI Reveals Causal Influence of Power Synchronized Neural Activity on Resting State fMRI Connectivity', *The Journal of Neuroscience*, 37(18), pp. 4766–4777. Available at: https://doi.org/10.1523/JNEUROSCI.1756-16.2017.

Bachtiar, V. *et al.* (2018) 'Modulating Regional Motor Cortical Excitability with Noninvasive Brain Stimulation Results in Neurochemical Changes in Bilateral Motor Cortices', *The Journal of Neuroscience*, 38(33), pp. 7327–7336. Available at: https://doi.org/10.1523/JNEUROSCI.2853-17.2018.

Bachtiar, V. and Stagg, C.J. (2014) 'The role of inhibition in human motor cortical plasticity', *Neuroscience*, 278, pp. 93–104. Available at: https://doi.org/10.1016/j.neuroscience.2014.07.059.

Bassett, D.S. *et al.* (2011) 'Dynamic reconfiguration of human brain networks during learning', *Proceedings of the National Academy of Sciences*, 108(18), pp. 7641–7646. Available at: https://doi.org/10.1073/pnas.1018985108.

Bates, D. *et al.* (2015) 'Fitting Linear Mixed-Effects Models Using lme4', *Journal of Statistical Software*, 67, pp. 1–48. Available at: https://doi.org/10.18637/jss.v067.i01.

Beckmann, C.F. and Smith, S.M. (2004) 'Probabilistic Independent Component Analysis for Functional Magnetic Resonance Imaging', *IEEE Transactions on Medical Imaging*, 23(2), pp. 137–152. Available at: https://doi.org/10.1109/TMI.2003.822821.

Bikson, M., Rahman, A. and Datta, A. (2012) 'Computational Models of Transcranial Direct Current Stimulation', *Clinical EEG and Neuroscience*, 43(3), pp. 176–183. Available at: https://doi.org/10.1177/1550059412445138.

Bischoff, M. *et al.* (2012) 'Motor familiarity: Brain activation when watching kinematic displays of one's own movements', *Neuropsychologia*, 50(8), pp. 2085–2092. Available at: https://doi.org/10.1016/j.neuropsychologia.2012.05.009.

Biswal, B. *et al.* (1995) 'Functional connectivity in the motor cortex of resting human brain using echo-planar mri', *Magnetic Resonance in Medicine*, 34(4), pp. 537–541. Available at: https://doi.org/10.1002/mrm.1910340409.

Bologna, M. *et al.* (2019) 'Transcranial Alternating Current Stimulation Has Frequency-Dependent Effects on Motor Learning in Healthy Humans', *Neuroscience*, 411, pp. 130–139. Available at: https://doi.org/10.1016/j.neuroscience.2019.05.041.

Bonzano, L. *et al.* (2015) 'Functional connectivity in the resting-state motor networks influences the kinematic processes during motor sequence learning', *European Journal of Neuroscience*, 41(2), pp. 243–253. Available at: https://doi.org/10.1111/ejn.12755.

Börgers, C. (2017) 'The PING model of gamma rhythms', in *An Introduction to Modeling Neuronal Dynamics*. Springer International, pp. 249–261. Available at: https://web.njit.edu/~horacio/AdvancedCompNeuro/downloads/BorgersProtobook_Ch30_PING.pdf.

Boto, E. *et al.* (2018) 'Moving magnetoencephalography towards real-world applications with a wearable system', *Nature*, 555(7698), pp. 657–661. Available at: https://doi.org/10.1038/nature26147.

Bott, J.-B. *et al.* (2016) 'Spatial Reference Memory is Associated with Modulation of Theta–Gamma Coupling in the Dentate Gyrus', *Cerebral Cortex*, 26(9), pp. 3744–3753. Available at: https://doi.org/10.1093/cercor/bhv177.

Bragin, A. *et al.* (1995) 'Gamma (40-100 Hz) oscillation in the hippocampus of the behaving rat', *The Journal of Neuroscience: The Official Journal of the Society for Neuroscience*, 15(1 Pt 1), pp. 47–60. Available at: https://doi.org/10.1523/JNEUROSCI.15-01-00047.1995.

Buzsáki, G. (2002) 'Theta oscillations in the hippocampus', *Neuron*, 33(3), pp. 325–340. Available at: https://doi.org/10.1016/s0896-6273(02)00586-x.

Buzsáki, G. *et al.* (2003) 'Hippocampal network patterns of activity in the mouse', *Neuroscience*, 116(1), pp. 201–211. Available at: https://doi.org/10.1016/S0306-4522(02)00669-3.

Buzsáki, G. (2006) *Rhythms of the Brain*. Oxford University Press. Available at: https://doi.org/10.1093/acprof:oso/9780195301069.001.0001.

Buzsáki, G. and Wang, X.-J. (2012) 'Mechanisms of Gamma Oscillations', *Annual Review of Neuroscience*, 35(1), pp. 203–225. Available at: https://doi.org/10.1146/annurev-neuro-062111-150444.

Cabral-Calderin, Y. *et al.* (2016) 'Transcranial alternating current stimulation modulates spontaneous low frequency fluctuations as measured with fMRI', *NeuroImage*, 141, pp. 88–107. Available at: https://doi.org/10.1016/j.neuroimage.2016.07.005.

Cabral-Calderin, Y. and Wilke, M. (2020) 'Probing the Link Between Perception and Oscillations: Lessons from Transcranial Alternating Current Stimulation', *The Neuroscientist*, 26(1), pp. 57–73. Available at: https://doi.org/10.1177/1073858419828646.

Canolty, R.T. *et al.* (2006) 'High Gamma Power Is Phase-Locked to Theta Oscillations in Human Neocortex', *Science*, 313(5793), pp. 1626–1628. Available at: https://doi.org/10.1126/science.1128115.

Canolty, R.T. and Knight, R.T. (2010) 'The functional role of cross-frequency coupling', *Trends in Cognitive Sciences*, 14(11), pp. 506–515. Available at: https://doi.org/10.1016/j.tics.2010.09.001.

Caplan, J.B. *et al.* (2003) 'Human Oscillations Related to Sensorimotor Integration and Spatial Learning', 23(11), pp. 4726–4736.

Cardin, J.A. *et al.* (2009) 'Driving fast-spiking cells induces gamma rhythm and controls sensory responses', *Nature*, 459(7247), pp. 663–667. Available at: https://doi.org/10.1038/nature08002.

Charych, E.I. *et al.* (2009) 'GABAA receptors and their associated proteins: Implications in the etiology and treatment of schizophrenia and related disorders', *Neuropharmacology*, 57(5–6), pp. 481–495. Available at: https://doi.org/10.1016/j.neuropharm.2009.07.027.

Chen, G. *et al.* (2017) 'Distinct Inhibitory Circuits Orchestrate Cortical beta and gamma Band Oscillations', *Neuron*, 96(6), pp. 1403-1418.e6. Available at: https://doi.org/10.1016/j.neuron.2017.11.033.

Cole, S.R. and Voytek, B. (2017) 'Brain Oscillations and the Importance of Waveform Shape', *Trends in Cognitive Sciences*, 21(2), pp. 137–149. Available at: https://doi.org/10.1016/j.tics.2016.12.008.

Colgin, L.L. and Moser, E.I. (2010) 'Gamma Oscillations in the Hippocampus', *Physiology*, 25(5), pp. 319–329. Available at: https://doi.org/10.1152/physiol.00021.2010.

Crone, N. (1998) ‘Functional mapping of human sensorimotor cortex with electrocorticographic spectral analysis. II. Event-related synchronization in the gamma band’, *Brain*, 121(12), pp. 2301–2315. Available at: https://doi.org/10.1093/brain/121.12.2301.

Cuypers, K. and Marsman, A. (2021) ‘Transcranial magnetic stimulation and magnetic resonance spectroscopy: Opportunities for a bimodal approach in human neuroscience’, *NeuroImage*, 224, p. 117394. Available at: https://doi.org/10.1016/j.neuroimage.2020.117394.

Damoiseaux, J.S. *et al.* (2006) ‘Consistent resting-state networks across healthy subjects’, *Proceedings of the National Academy of Sciences*, 103(37), pp. 13848–13853. Available at: https://doi.org/10.1073/pnas.0601417103.

Datta, A. *et al.* (2011) ‘Individualized model predicts brain current flow during transcranial direct-current stimulation treatment in responsive stroke patient’, *Brain Stimulation*, 4(3), pp. 169–174. Available at: https://doi.org/10.1016/j.brs.2010.11.001.

Demiralp, T. *et al.* (2007) ‘Gamma amplitudes are coupled to theta phase in human EEG during visual perception’, *International Journal of Psychophysiology*, 64(1), pp. 24–30. Available at: https://doi.org/10.1016/j.ijpsycho.2006.07.005.

Deng, Z.-D., Lisanby, S.H. and Peterchev, A.V. (2013) ‘Electric field depth–focality tradeoff in transcranial magnetic stimulation: Simulation comparison of 50 coil designs’, *Brain Stimulation*, 6(1), pp. 1–13. Available at: https://doi.org/10.1016/j.brs.2012.02.005.

Desideri, D. *et al.* (2019) ‘Phase of sensorimotor μ-oscillation modulates cortical responses to transcranial magnetic stimulation of the human motor cortex’, *The Journal of Physiology*, 597(23), pp. 5671–5686. Available at: https://doi.org/10.1113/JP278638.

Devanne, H., Lavoie, B.A. and Capaday, C. (1997) ‘Input-output properties and gain changes in the human corticospinal pathway’:, *Experimental Brain Research*, 114(2), pp. 329–338. Available at: https://doi.org/10.1007/PL00005641.

Di Lazzaro, V. *et al.* (2000) ‘Direct demonstration of the effect of lorazepam on the excitability of the human motor cortex’, *Clinical Neurophysiology*, 111(5), pp. 794–799. Available at: https://doi.org/10.1016/S1388-2457(99)00314-4.

Donkor, E.S. (2018) ‘Stroke in the 21st Century: A Snapshot of the Burden, Epidemiology, and Quality of Life’, *Stroke Research and Treatment*, 2018, pp. 1–10. Available at: https://doi.org/10.1155/2018/3238165.

Dyke, K. *et al.* (2017) ‘Comparing GABA-dependent physiological measures of inhibition with proton magnetic resonance spectroscopy measurement of GABA using ultra-high-field MRI’, *NeuroImage*, 152, pp. 360–370. Available at: https://doi.org/10.1016/j.neuroimage.2017.03.011.

Fabbrini, A. *et al.* (2022) ‘Transcranial alternating current stimulation modulates cortical processing of somatosensory information in a frequency- and time-specific manner’, *NeuroImage*, 254, p. 119119. Available at: https://doi.org/10.1016/j.neuroimage.2022.119119.

Feldman, D.E. (2012) ‘The Spike-Timing Dependence of Plasticity’, *Neuron*, 75(4), pp. 556–571. Available at: https://doi.org/10.1016/j.neuron.2012.08.001.

Feurra, M. *et al.* (2011) ‘Frequency-Dependent Tuning of the Human Motor System Induced by Transcranial Oscillatory Potentials’, *The Journal of Neuroscience*, 31(34), pp. 12165–12170. Available at: https://doi.org/10.1523/JNEUROSCI.0978-11.2011.

Feurra, M. *et al.* (2013) 'State-Dependent Effects of Transcranial Oscillatory Currents on the Motor System: What You Think Matters', *The Journal of Neuroscience*, 33(44), pp. 17483–17489. Available at: https://doi.org/10.1523/JNEUROSCI.1414-13.2013.

Fisher, R.J. *et al.* (2002) 'Two phases of intracortical inhibition revealed by transcranial magnetic threshold tracking', *Experimental Brain Research*, 143(2), pp. 240–248. Available at: https://doi.org/10.1007/s00221-001-0988-2.

Floyer-Lea, A. *et al.* (2006) 'Rapid Modulation of GABA Concentration in Human Sensorimotor Cortex During Motor Learning', *Journal of Neurophysiology*, 95(3), pp. 1639–1644. Available at: https://doi.org/10.1152/jn.00346.2005.

Floyer-Lea, A. and Matthews, P.M. (2005) 'Distinguishable Brain Activation Networks for Short- and Long-Term Motor Skill Learning', *Journal of Neurophysiology*, 94(1), pp. 512–518. Available at: https://doi.org/10.1152/jn.00717.2004.

Franco-Rosado, P. *et al.* (2024) 'Addressing the sources of inter-subject variability in E-field parameters in anodal tDCS stimulation over motor cortical network', *Physics in Medicine & Biology*, 69(14), p. 145013. Available at: https://doi.org/10.1088/1361-6560/ad5bb9.

Fries, P. (2005) 'A mechanism for cognitive dynamics: neuronal communication through neuronal coherence', *Trends in Cognitive Sciences*, 9(10), pp. 474–480. Available at: https://doi.org/10.1016/j.tics.2005.08.011.

Fries, P., Nikolić, D. and Singer, W. (2007) 'The gamma cycle', *Trends in Neurosciences*, 30(7), pp. 309–316. Available at: https://doi.org/10.1016/j.tins.2007.05.005.

Galuske, R.A.W., Munk, M.H.J. and Singer, W. (2019) 'Relation between gamma oscillations and neuronal plasticity in the visual cortex', *Proceedings of the National Academy of Sciences*, 116(46), pp. 23317–23325. Available at: https://doi.org/10.1073/pnas.1901277116.

Gandal, M.J. *et al.* (2012) 'GABAb-mediated rescue of altered excitatory–inhibitory balance, gamma synchrony and behavioral deficits following constitutive NMDAr-hypofunction', *Translational Psychiatry*, 2(7), pp. e142–e142. Available at: https://doi.org/10.1038/tp.2012.69.

Ghafoor, U., Yang, D. and Hong, K.-S. (2022) 'Neuromodulatory Effects of HD-tACS/tDCS on the Prefrontal Cortex: A Resting-State fNIRS-EEG Study', *IEEE Journal of Biomedical and Health Informatics*, 26(5), pp. 2192–2203. Available at: https://doi.org/10.1109/JBHI.2021.3127080.

Giustiniani, A. *et al.* (2019) 'Effects of low-gamma tACS on primary motor cortex in implicit motor learning', *Behavioural Brain Research*, 376, p. 112170. Available at: https://doi.org/10.1016/j.bbr.2019.112170.

Giustiniani, A. *et al.* (2021) 'Functional Role of Cerebellar Gamma Frequency in Motor Sequences Learning: a tACS Study', *The Cerebellum*, 20(6), pp. 913–921. Available at: https://doi.org/10.1007/s12311-021-01255-6.

Grigoras, I.-F. and Stagg, C.J. (2021) 'Recent advances in the role of excitation–inhibition balance in motor recovery post-stroke', *Faculty Reviews*, 10. Available at: https://doi.org/10.12703/r/10-58.

Grigutsch, L.S. *et al.* (2024) 'Differential effects of theta-gamma tACS on motor skill acquisition in young individuals and stroke survivors: A double-blind, randomized, sham-controlled study', *Brain Stimulation*, 17(5), pp. 1076–1085. Available at: https://doi.org/10.1016/j.brs.2024.09.001.

Grillner, S. *et al.* (2005) 'Microcircuits in action – from CPGs to neocortex', *Trends in Neurosciences*, 28(10), pp. 525–533. Available at: https://doi.org/10.1016/j.tins.2005.08.003.

Guerra, A. *et al.* (2016) 'Phase Dependency of the Human Primary Motor Cortex and Cholinergic Inhibition Cancelation During Beta tACS', *Cerebral Cortex*, 26(10), pp. 3977–3990. Available at: https://doi.org/10.1093/cercor/bhw245.

Guerra, A. *et al.* (2018) 'Effects of Transcranial Alternating Current Stimulation on Repetitive Finger Movements in Healthy Humans', *Neural Plasticity*, 2018, pp. 1–10. Available at: https://doi.org/10.1155/2018/4593095.

Halsband, U. and Lange, R.K. (2006) 'Motor learning in man: A review of functional and clinical studies', *Journal of Physiology-Paris*, 99(4–6), pp. 414–424. Available at: https://doi.org/10.1016/j.jphysparis.2006.03.007.

Hasenstaub, A. *et al.* (2005) 'Inhibitory Postsynaptic Potentials Carry Synchronized Frequency Information in Active Cortical Networks', *Neuron*, 47(3), pp. 423–435. Available at: https://doi.org/10.1016/j.neuron.2005.06.016.

Hazime, M. *et al.* (2021) 'Prolonged deficit of low gamma oscillations in the peri-infarct cortex of mice after stroke', *Experimental Neurology*, 341, p. 113696. Available at: https://doi.org/10.1016/j.expneurol.2021.113696.

Hebb, D.O. (1949) *The Organization of Behavior: A Neuropsychological Theory*. 1st edition. Mahwah, N.J: Psychology Press.

Heimrath, K. *et al.* (2014) 'Transcranial direct current stimulation (tDCS) traces the predominance of the left auditory cortex for processing of rapidly changing acoustic information', *Neuroscience*, 261, pp. 68–73. Available at: https://doi.org/10.1016/j.neuroscience.2013.12.031.

Helfrich, R.F. *et al.* (2014) 'Entrainment of Brain Oscillations by Transcranial Alternating Current Stimulation', *Current Biology*, 24(3), pp. 333–339. Available at: https://doi.org/10.1016/j.cub.2013.12.041.

Holdefer, R.N., Sadleir, R. and Russell, M.J. (2006) 'Predicted current densities in the brain during transcranial electrical stimulation', *Clinical Neurophysiology*, 117(6), pp. 1388–1397. Available at: https://doi.org/10.1016/j.clinph.2006.02.020.

Hoopes, A. *et al.* (2022) 'SynthStrip: skull-stripping for any brain image', *NeuroImage*, 260, p. 119474. Available at: https://doi.org/10.1016/j.neuroimage.2022.119474.

Huang, W.A. *et al.* (2021) 'Transcranial alternating current stimulation entrains alpha oscillations by preferential phase synchronization of fast-spiking cortical neurons to stimulation waveform', *Nature Communications*, 12(1), p. 3151. Available at: https://doi.org/10.1038/s41467-021-23021-2.

Huang, Y. *et al.* (2017) 'Measurements and models of electric fields in the in vivo human brain during transcranial electric stimulation', *eLife*, 6, p. e18834. Available at: https://doi.org/10.7554/eLife.18834.

Huerta, P.T. and Lisman, J.E. (1996) 'Low-frequency stimulation at the troughs of theta-oscillation induces long-term depression of previously potentiated CA1 synapses', *Journal of Neurophysiology*, 75(2), pp. 877–884. Available at: https://doi.org/10.1152/jn.1996.75.2.877.

Hummos, A. and Nair, S.S. (2017) 'An integrative model of the intrinsic hippocampal theta rhythm', *PLOS ONE*. Edited by W.W. Lytton, 12(8), p. e0182648. Available at: https://doi.org/10.1371/journal.pone.0182648.

Hyvarinen, A. (1999) ‘Fast and robust fixed-point algorithms for independent component analysis’, *IEEE Transactions on Neural Networks*, 10(3), pp. 626–634. Available at: https://doi.org/10.1109/72.761722.

Igarashi, J. *et al.* (2013) ‘A θ–γ Oscillation Code for Neuronal Coordination during Motor Behavior’, *The Journal of Neuroscience*, 33(47), pp. 18515–18530. Available at: https://doi.org/10.1523/JNEUROSCI.2126-13.2013.

Ilić, T.V. *et al.* (2002) ‘Short-interval paired-pulse inhibition and facilitation of human motor cortex: the dimension of stimulus intensity’, *The Journal of Physiology*, 545(1), pp. 153–167. Available at: https://doi.org/10.1113/jphysiol.2002.030122.

Janssens, S.E.W. *et al.* (2022) ‘“Broadband Alpha Transcranial Alternating Current Stimulation”: Exploring a new biologically calibrated brain stimulation protocol’, *NeuroImage*, 253, p. 119109. Available at: https://doi.org/10.1016/j.neuroimage.2022.119109.

Jenkinson, M. *et al.* (2002) ‘Improved Optimization for the Robust and Accurate Linear Registration and Motion Correction of Brain Images’, *NeuroImage*, 17(2), pp. 825–841. Available at: https://doi.org/10.1006/nimg.2002.1132.

Jenkinson, M. and Smith, S. (2001) ‘A global optimisation method for robust affine registration of brain images’, *Medical Image Analysis*, 5(2), pp. 143–156. Available at: https://doi.org/10.1016/S1361-8415(01)00036-6.

Jiang, T. *et al.* (2020) ‘Power Modulations of ECoG Alpha/Beta and Gamma Bands Correlate With Time-Derivative of Force During Hand Grasp’, *Frontiers in Neuroscience*, 14, p. 100. Available at: https://doi.org/10.3389/fnins.2020.00100.

Johnson, N.W. *et al.* (2017) ‘Phase-amplitude coupled persistent theta and gamma oscillations in rat primary motor cortex in vitro’, *Neuropharmacology*, 119, pp. 141–156. Available at: https://doi.org/10.1016/j.neuropharm.2017.04.009.

Johnstone, A. *et al.* (2021) ‘The impact of brain lesions on tDCS-induced electric field magnitude’. bioRxiv, p. 2021.03.19.436124. Available at: https://doi.org/10.1101/2021.03.19.436124.

Jones, A.P. *et al.* (2023) ‘Closed-Loop tACS Delivered during Slow-Wave Sleep Reduces Retroactive Interference on a Paired-Associates Learning Task’, *Brain Sciences*, 13(3), p. 468. Available at: https://doi.org/10.3390/brainsci13030468.

Joundi, R.A. *et al.* (2012) ‘Driving Oscillatory Activity in the Human Cortex Enhances Motor Performance’, *Current Biology*, 22(5), pp. 403–407. Available at: https://doi.org/10.1016/j.cub.2012.01.024.

Kar, K. *et al.* (2020) ‘Transcranial alternating current stimulation attenuates BOLD adaptation and increases functional connectivity’, *Journal of Neurophysiology*, 123(1), pp. 428–438. Available at: https://doi.org/10.1152/jn.00376.2019.

Kar, K. and Krekelberg, B. (2014) ‘Transcranial Alternating Current Stimulation Attenuates Visual Motion Adaptation’, *The Journal of Neuroscience*, 34(21), pp. 7334–7340. Available at: https://doi.org/10.1523/JNEUROSCI.5248-13.2014.

Karakaş, S. (2020) ‘A review of theta oscillation and its functional correlates’, *International Journal of Psychophysiology*, 157, pp. 82–99. Available at: https://doi.org/10.1016/j.ijpsycho.2020.04.008.

Kasten, F.H. and Herrmann, C.S. (2020) ‘The hidden state-dependency of transcranial alternating current stimulation (tACS)’. Neuroscience. Available at: https://doi.org/10.1101/2020.12.23.423984.

Keeley, S., Fenton, A.A. and Rinzel, J. (2017) 'Modeling fast and slow gamma oscillations with interneurons of different subtype', *Journal of Neurophysiology*, 117(3), pp. 950–965. Available at: https://doi.org/10.1152/jn.00490.2016.

Khatoun, A., Asamoah, B. and Mc Laughlin, M. (2017) 'Simultaneously Excitatory and Inhibitory Effects of Transcranial Alternating Current Stimulation Revealed Using Selective Pulse-Train Stimulation in the Rat Motor Cortex', *The Journal of Neuroscience*, 37(39), pp. 9389–9402. Available at: https://doi.org/10.1523/JNEUROSCI.1390-17.2017.

Kida, H. and Mitsushima, D. (2018) 'Mechanisms of motor learning mediated by synaptic plasticity in rat primary motor cortex', *Neuroscience Research*, 128, pp. 14–18. Available at: https://doi.org/10.1016/j.neures.2017.09.008.

Kim, Y. *et al.* (2017) 'Brain-wide Maps Reveal Stereotyped Cell-Type-Based Cortical Architecture and Subcortical Sexual Dimorphism', *Cell*, 171(2), pp. 456-469.e22. Available at: https://doi.org/10.1016/j.cell.2017.09.020.

Kinnischtzke, A.K., Simons, D.J. and Fanselow, E.E. (2014) 'Motor Cortex Broadly Engages Excitatory and Inhibitory Neurons in Somatosensory Barrel Cortex', *Cerebral Cortex*, 24(8), pp. 2237–2248. Available at: https://doi.org/10.1093/cercor/bht085.

Kolasinski, J. *et al.* (2019) 'The dynamics of cortical GABA in human motor learning', *The Journal of Physiology*, 597(1), pp. 271–282. Available at: https://doi.org/10.1113/JP276626.

Kraeutner, S.N. *et al.* (2021) 'Resting State Connectivity Is Modulated by Motor Learning in Individuals After Stroke', *Neurorehabilitation and Neural Repair*, 35(6), pp. 513–524. Available at: https://doi.org/10.1177/15459683211006713.

Krakauer, J.W. (2006) 'Motor learning: Its relevance to stroke recovery and neurorehabilitation':, *Current Opinion in Neurology*, 19(1), pp. 84–90. Available at: https://doi.org/10.1097/01.wco.0000200544.29915.cc.

Krakauer, J.W. *et al.* (2019) 'Motor Learning', *Comprehensive Physiology*, 9(2), pp. 613–663. Available at: https://doi.org/10.1002/cphy.c170043.

Krause, B., Márquez-Ruiz, J. and Kadosh, R.C. (2013) 'The effect of transcranial direct current stimulation: a role for cortical excitation/inhibition balance?', *Frontiers in Human Neuroscience*, 7. Available at: https://doi.org/10.3389/fnhum.2013.00602.

Krause, M.R. *et al.* (2021) 'Brain stimulation competes with ongoing oscillations for control of spike timing in the primate brain'.

Kujirai, T. *et al.* (1993) 'Corticocortical inhibition in human motor cortex.', *The Journal of Physiology*, 471(1), pp. 501–519. Available at: https://doi.org/10.1113/jphysiol.1993.sp019912.

Lazzaro, G. *et al.* (2022) 'Understanding the Effects of Transcranial Electrical Stimulation in Numerical Cognition: A Systematic Review for Clinical Translation', *Journal of Clinical Medicine*, 11(8), p. 2082. Available at: https://doi.org/10.3390/jcm11082082.

Lazzaro, V.D., Ziemann, U. and Lemon, R.N. (2008) 'State of the art: Physiology of transcranial motor cortex stimulation', *Brain Stimulation*, 1(4), pp. 345–362. Available at: https://doi.org/10.1016/j.brs.2008.07.004.

Leung, L.S. and Law, C.S.H. (2020) 'Phasic modulation of hippocampal synaptic plasticity by theta rhythm.', *Behavioral Neuroscience*, 134(6), pp. 595–612. Available at: https://doi.org/10.1037/bne0000354.

Leunissen, I. *et al.* (2022) 'Effects of beta-band and gamma-band rhythmic stimulation on motor inhibition', *iScience*, 25(5), p. 104338. Available at: https://doi.org/10.1016/j.isci.2022.104338.

Li, K.T., Liang, J. and Zhou, C. (2021) 'Gamma Oscillations Facilitate Effective Learning in Excitatory-Inhibitory Balanced Neural Circuits', *Neural Plasticity*. Edited by J. Su, 2021, pp. 1–18. Available at: https://doi.org/10.1155/2021/6668175.

Lisman, J.E. and Jensen, O. (2013) 'The Theta-Gamma Neural Code', *Neuron*, 77(6), pp. 1002–1016. Available at: https://doi.org/10.1016/j.neuron.2013.03.007.

Liu, A. *et al.* (2018) 'Immediate neurophysiological effects of transcranial electrical stimulation', *Nature Communications*, 9(1), p. 5092. Available at: https://doi.org/10.1038/s41467-018-07233-7.

Lopes-dos-Santos, V. *et al.* (2018) 'Parsing Hippocampal Theta Oscillations by Nested Spectral Components during Spatial Exploration and Memory-Guided Behavior', *Neuron*, 100(4), pp. 940-952.e7. Available at: https://doi.org/10.1016/j.neuron.2018.09.031.

Ma, L. *et al.* (2011) 'Changes occur in resting state network of motor system during 4weeks of motor skill learning', *NeuroImage*, 58(1), pp. 226–233. Available at: https://doi.org/10.1016/j.neuroimage.2011.06.014.

Maier, M., Ballester, B.R. and Verschure, P.F.M.J. (2019) 'Principles of Neurorehabilitation After Stroke Based on Motor Learning and Brain Plasticity Mechanisms', *Frontiers in Systems Neuroscience*, 13, p. 74. Available at: https://doi.org/10.3389/fnsys.2019.00074.

Mancini, V. *et al.* (2022) 'Aberrant Developmental Patterns of Gamma-Band Response and Long-Range Communication Disruption in Youths With 22q11.2 Deletion Syndrome', *American Journal of Psychiatry*, 179(3), pp. 204–215. Available at: https://doi.org/10.1176/appi.ajp.2021.21020190.

Mansouri, F. *et al.* (2017) 'A Fast EEG Forecasting Algorithm for Phase-Locked Transcranial Electrical Stimulation of the Human Brain', *Frontiers in Neuroscience*, 11, p. 401. Available at: https://doi.org/10.3389/fnins.2017.00401.

Markram, H. *et al.* (2004) 'Interneurons of the neocortical inhibitory system', *Nature Reviews Neuroscience*, 5(10), pp. 793–807. Available at: https://doi.org/10.1038/nrn1519.

Martin, D.M. and Nikolin, S. (2024) '"Closing the Loop" With Transcranial Electrical Stimulation for Depression', *American Journal of Psychiatry*, 181(9), pp. 793–794. Available at: https://doi.org/10.1176/appi.ajp.20240603.

Matsuta, H. *et al.* (2022) 'Continuous theta-burst stimulation to the sensorimotor cortex affects contralateral gamma-aminobutyric acid level and resting-state networks', *PLOS ONE*. Edited by B.A. Murphy, 17(8), p. e0272268. Available at: https://doi.org/10.1371/journal.pone.0272268.

Minka, T.P. (2000) *Automatic choice of dimensionality for PCA*. 514.

Miranda, P.C., Lomarev, M. and Hallett, M. (2006) 'Modeling the current distribution during transcranial direct current stimulation', *Clinical Neurophysiology*, 117(7), pp. 1623–1629. Available at: https://doi.org/10.1016/j.clinph.2006.04.009.

Miyaguchi, S. *et al.* (2019) 'Gamma tACS over M1 and cerebellar hemisphere improves motor performance in a phase-specific manner', *Neuroscience Letters*, 694, pp. 64–68. Available at: https://doi.org/10.1016/j.neulet.2018.11.015.

Mo, A. *et al.* (2015) 'Epigenomic Signatures of Neuronal Diversity in the Mammalian Brain', *Neuron*, 86(6), pp. 1369–1384. Available at: https://doi.org/10.1016/j.neuron.2015.05.018.

Moisa, M. *et al.* (2016) 'Brain Network Mechanisms Underlying Motor Enhancement by Transcranial Entrainment of Gamma Oscillations', *The Journal of Neuroscience*, 36(47), pp. 12053–12065. Available at: https://doi.org/10.1523/JNEUROSCI.2044-16.2016.

Mondino, M. *et al.* (2020) 'Effects of Transcranial Stimulation With Direct and Alternating Current on Resting-State Functional Connectivity: An Exploratory Study Simultaneously Combining Stimulation and Multiband Functional Magnetic Resonance Imaging', *Frontiers in Human Neuroscience*, 13, p. 474. Available at: https://doi.org/10.3389/fnhum.2019.00474.

Mormann, F. *et al.* (2005) 'Phase/amplitude reset and theta–gamma interaction in the human medial temporal lobe during a continuous word recognition memory task', *Hippocampus*, 15(7), pp. 890–900. Available at: https://doi.org/10.1002/hipo.20117.

Mottaz, A. *et al.* (2024) 'Neural correlates of motor learning: Network communication versus local oscillations', *Network Neuroscience*, 8(3), pp. 714–733. Available at: https://doi.org/10.1162/netn_a_00374.

Muthukumaraswamy, S.D. (2010) 'Functional Properties of Human Primary Motor Cortex Gamma Oscillations', *Journal of Neurophysiology*, 104(5), pp. 2873–2885. Available at: https://doi.org/10.1152/jn.00607.2010.

Nahar, L., Delacroix, B.M. and Nam, H.W. (2021) 'The Role of Parvalbumin Interneurons in Neurotransmitter Balance and Neurological Disease', *Frontiers in Psychiatry*, 12, p. 679960. Available at: https://doi.org/10.3389/fpsyt.2021.679960.

Nakazono, H. *et al.* (2016) 'Phase and Frequency-Dependent Effects of Transcranial Alternating Current Stimulation on Motor Cortical Excitability', *PLOS ONE*. Edited by A. Antal, 11(9), p. e0162521. Available at: https://doi.org/10.1371/journal.pone.0162521.

Nakazono, T., Takahashi, S. and Sakurai, Y. (2019) 'Enhanced Theta and High-Gamma Coupling during Late Stage of Rule Switching Task in Rat Hippocampus', *Neuroscience*, 412, pp. 216–232. Available at: https://doi.org/10.1016/j.neuroscience.2019.05.053.

Neuling, T., Rach, S. and Herrmann, C.S. (2013) 'Orchestrating neuronal networks: sustained after-effects of transcranial alternating current stimulation depend upon brain states', *Frontiers in Human Neuroscience*, 7. Available at: https://doi.org/10.3389/fnhum.2013.00161.

Nowak, M. *et al.* (2017) 'Driving Human Motor Cortical Oscillations Leads to Behaviorally Relevant Changes in Local $GABA_A$ Inhibition: A tACS-TMS Study', *The Journal of Neuroscience*, 37(17), pp. 4481–4492. Available at: https://doi.org/10.1523/JNEUROSCI.0098-17.2017.

Nowak, M., Zich, C. and Stagg, C.J. (2018) 'Motor Cortical Gamma Oscillations: What Have We Learnt and Where Are We Headed?', *Current Behavioral Neuroscience Reports*, 5(2), pp. 136–142. Available at: https://doi.org/10.1007/s40473-018-0151-z.

Ohashi, H., Gribble, P.L. and Ostry, D.J. (2019) 'Somatosensory cortical excitability changes precede those in motor cortex during human motor learning', *Journal of Neurophysiology*, 122(4), pp. 1397–1405. Available at: https://doi.org/10.1152/jn.00383.2019.

Onitsuka, T. and Kanba, S. (2013) 'Application of Brain Oscillations in Neuropsychiatric Diseases'.

Ozen, S. *et al.* (2010) 'Transcranial Electric Stimulation Entrains Cortical Neuronal Populations in Rats', *The Journal of Neuroscience*, 30(34), pp. 11476–11485. Available at: https://doi.org/10.1523/JNEUROSCI.5252-09.2010.

Palmer, E. and Ashby, P. (1992) 'Corticospinal projections to upper limb motoneurones in humans.', *The Journal of Physiology*, 448(1), pp. 397–412. Available at: https://doi.org/10.1113/jphysiol.1992.sp019048.

Pavlov, I. *et al.* (2014) 'Tonic $GABA_A$ conductance bidirectionally controls interneuron firing pattern and synchronization in the CA3 hippocampal network', *Proceedings of the National Academy of Sciences*, 111(1), pp. 504–509. Available at: https://doi.org/10.1073/pnas.1308388110.

Petri, S. *et al.* (2003) 'Distribution of $GABA_A$ Receptor mRNA in the Motor Cortex of ALS Patients', *Journal of Neuropathology & Experimental Neurology*, 62(10), pp. 1041–1051. Available at: https://doi.org/10.1093/jnen/62.10.1041.

Pham, M.V. *et al.* (2022) 'Changes in excitability and GABAergic neuronal activity of the primary somatosensory cortex after motor learning', *Frontiers in Neuroscience*, 16, p. 794173. Available at: https://doi.org/10.3389/fnins.2022.794173.

Pike, F.G. *et al.* (2000) 'Distinct frequency preferences of different types of rat hippocampal neurones in response to oscillatory input currents', *The Journal of Physiology*, 529(1), pp. 205–213. Available at: https://doi.org/10.1111/j.1469-7793.2000.00205.x.

Pogosyan, A. *et al.* (2009) 'Boosting Cortical Activity at Beta-Band Frequencies Slows Movement in Humans', *Current Biology*, 19(19), pp. 1637–1641. Available at: https://doi.org/10.1016/j.cub.2009.07.074.

Pozdniakov, I. *et al.* (2021) 'Online and offline effects of transcranial alternating current stimulation of the primary motor cortex', *Scientific Reports*, 11(1), p. 3854. Available at: https://doi.org/10.1038/s41598-021-83449-w.

Ranganathan, R., Lee, M.-H. and Krishnan, C. (2022) 'Ten guidelines for designing motor learning studies', *Brazilian Journal of Motor Behavior*, 16(2), pp. 112–133. Available at: https://doi.org/10.20338/bjmb.v16i2.283.

Reato, D. *et al.* (2010) 'Low-Intensity Electrical Stimulation Affects Network Dynamics by Modulating Population Rate and Spike Timing', *The Journal of Neuroscience*, 30(45), pp. 15067–15079. Available at: https://doi.org/10.1523/JNEUROSCI.2059-10.2010.

Reis, J. *et al.* (2008) 'Contribution of transcranial magnetic stimulation to the understanding of cortical mechanisms involved in motor control', *The Journal of Physiology*, 586(2), pp. 325–351. Available at: https://doi.org/10.1113/jphysiol.2007.144824.

Robertson, E.M. (2007) 'The Serial Reaction Time Task: Implicit Motor Skill Learning?: Figure 1.', *The Journal of Neuroscience*, 27(38), pp. 10073–10075. Available at: https://doi.org/10.1523/JNEUROSCI.2747-07.2007.

Roshan, L., Paradiso, G.O. and Chen, R. (2003) 'Two phases of short-interval intracortical inhibition', *Experimental Brain Research*, 151(3), pp. 330–337. Available at: https://doi.org/10.1007/s00221-003-1502-9.

Rosso, C. and Lamy, J.-C. (2018) 'Does Resting Motor Threshold Predict Motor Hand Recovery After Stroke?', *Frontiers in Neurology*, 9, p. 1020. Available at: https://doi.org/10.3389/fneur.2018.01020.

Ruddy, K.L., Leemans, A. and Carson, R.G. (2017) 'Transcallosal connectivity of the human cortical motor network', *Brain Structure and Function*, 222(3), pp. 1243–1252. Available at: https://doi.org/10.1007/s00429-016-1274-1.

Rufener, K.S. *et al.* (2016) '40Hz-Transcranial alternating current stimulation (tACS) selectively modulates speech perception', *International Journal of Psychophysiology*, 101, pp. 18–24. Available at: https://doi.org/10.1016/j.ijpsycho.2016.01.002.

Ruhnau, P. *et al.* (2016) 'Eyes wide shut: Transcranial alternating current stimulation drives alpha rhythm in a state dependent manner', *Scientific Reports*, 6(1), p. 27138. Available at: https://doi.org/10.1038/srep27138.

Saint Amour Di Chanaz, L. *et al.* (2023) 'Gamma amplitude is coupled to opposed hippocampal theta-phase states during the encoding and retrieval of episodic memories in humans', *Current Biology*, 33(9), pp. 1836-1843.e6. Available at: https://doi.org/10.1016/j.cub.2023.03.073.

Sattin, D. *et al.* (2023) 'An Overview of the Body Schema and Body Image: Theoretical Models, Methodological Settings and Pitfalls for Rehabilitation of Persons with Neurological Disorders', *Brain Sciences*, 13(10), p. 1410. Available at: https://doi.org/10.3390/brainsci13101410.

Schmidt, S.L. *et al.* (2014) 'Endogenous Cortical Oscillations Constrain Neuromodulation by Weak Electric Fields', *Brain Stimulation*, 7(6), pp. 878–889. Available at: https://doi.org/10.1016/j.brs.2014.07.033.

Schwab, B.C., König, P. and Engel, A.K. (2021) 'Spike-timing-dependent plasticity can account for connectivity aftereffects of dual-site transcranial alternating current stimulation', *NeuroImage*, 237. Available at: https://doi.org/10.1016/j.neuroimage.2021.118179.

Smith, S.M. *et al.* (2009) 'Correspondence of the brain's functional architecture during activation and rest', *Proceedings of the National Academy of Sciences*, 106(31), pp. 13040–13045. Available at: https://doi.org/10.1073/pnas.0905267106.

Smith, S.M. and Brady, J.M. (1997) 'SUSAN—A New Approach to Low Level Image Processing'.

Sohal, V.S. *et al.* (2009) 'Parvalbumin neurons and gamma rhythms enhance cortical circuit performance', *Nature*, 459(7247), pp. 698–702. Available at: https://doi.org/10.1038/nature07991.

Sohal, V.S. (2016) 'How Close Are We to Understanding What (if Anything) γ Oscillations Do in Cortical Circuits?', *The Journal of Neuroscience*, 36(41), pp. 10489–10495. Available at: https://doi.org/10.1523/JNEUROSCI.0990-16.2016.

Song, S., Miller, K.D. and Abbott, L.F. (2000) 'Competitive Hebbian learning through spike-timing-dependent synaptic plasticity', *Nature Neuroscience*, 3(9), pp. 919–926. Available at: https://doi.org/10.1038/78829.

Sotero, R.C. (2015) 'Modeling the Generation of Phase-Amplitude Coupling in Cortical Circuits: From Detailed Networks to Neural Mass Models', *BioMed Research International*, 2015, pp. 1–12. Available at: https://doi.org/10.1155/2015/915606.

Spooner, R.K. and Wilson, T.W. (2023) 'Spectral specificity of gamma-frequency transcranial alternating current stimulation over motor cortex during sequential movements', *Cerebral Cortex*, 33(9), pp. 5347–5360. Available at: https://doi.org/10.1093/cercor/bhac423.

Stagg, C.J. *et al.* (2011) 'Relationship between physiological measures of excitability and levels of glutamate and GABA in the human motor cortex', *The Journal of Physiology*, 589(23), pp. 5845–5855. Available at: https://doi.org/10.1113/jphysiol.2011.216978.

Stagg, C.J. *et al.* (2014) 'Local GABA concentration is related to network-level resting functional connectivity', *eLife*, 3, p. e01465. Available at: https://doi.org/10.7554/eLife.01465.

Stagg, C.J. (2014) ‘Magnetic Resonance Spectroscopy as a tool to study the role of GABA in motor-cortical plasticity’, *NeuroImage*, 86, pp. 19–27. Available at: https://doi.org/10.1016/j.neuroimage.2013.01.009.

Stagg, C.J., Bachtiar, V. and Johansen-Berg, H. (2011) ‘The Role of GABA in Human Motor Learning’, *Current Biology*, 21(6), pp. 480–484. Available at: https://doi.org/10.1016/j.cub.2011.01.069.

Steel, A. *et al.* (2016) ‘The impact of reward and punishment on skill learning depends on task demands’, *Scientific Reports*, 6(1), p. 36056. Available at: https://doi.org/10.1038/srep36056.

Steel, A. *et al.* (2019) ‘Differential impact of reward and punishment on functional connectivity after skill learning’, *NeuroImage*, 189, pp. 95–105. Available at: https://doi.org/10.1016/j.neuroimage.2019.01.009.

Stewart, J.C., Tran, X. and Cramer, S.C. (2014) ‘Age-related variability in performance of a motor action selection task is related to differences in brain function and structure among older adults’, *NeuroImage*, 86, pp. 326–334. Available at: https://doi.org/10.1016/j.neuroimage.2013.10.016.

Szurhaj, W. *et al.* (2005) ‘Intracerebral study of gamma rhythm reactivity in the sensorimotor cortex’, *European Journal of Neuroscience*, 21(5), pp. 1223–1235. Available at: https://doi.org/10.1111/j.1460-9568.2005.03966.x.

Taylor, J.A., Krakauer, J.W. and Ivry, R.B. (2014) ‘Explicit and Implicit Contributions to Learning in a Sensorimotor Adaptation Task’, *The Journal of Neuroscience*, 34(8), pp. 3023–3032. Available at: https://doi.org/10.1523/JNEUROSCI.3619-13.2014.

Thiele, C. *et al.* (2021) ‘Amplitude modulated transcranial alternating current stimulation (AM-TACS) efficacy evaluation via phosphene induction’, *Scientific Reports*, 11(1), p. 22245. Available at: https://doi.org/10.1038/s41598-021-01482-1.

Tort, A.B.L. *et al.* (2010) ‘Measuring Phase-Amplitude Coupling Between Neuronal Oscillations of Different Frequencies’, *Journal of Neurophysiology*, 104(2), pp. 1195–1210. Available at: https://doi.org/10.1152/jn.00106.2010.

Traub, R.D. *et al.* (1996) ‘A mechanism for generation of long-range synchronous fast oscillations in the cortex’, *Nature*, 383(6601), pp. 621–624. Available at: https://doi.org/10.1038/383621a0.

Trepel, C. and Racine, R.J. (2000) ‘GABAergic modulation of neocortical long-term potentiation in the freely moving rat’, *Synapse (New York, N.Y.)*, 35(2), pp. 120–128. Available at: https://doi.org/10.1002/(SICI)1098-2396(200002)35:2<120::AID-SYN4>3.0.CO;2-6.

Ursin, M.H. *et al.* (2019) ‘Gait and balance one year after stroke; relationships with lesion side, subtypes of cognitive impairment and neuroimaging findings—a longitudinal, cohort study’, *Physiotherapy*, 105(2), pp. 254–261. Available at: https://doi.org/10.1016/j.physio.2018.07.007.

Vahdat, S. *et al.* (2011) ‘Functionally Specific Changes in Resting-State Sensorimotor Networks after Motor Learning’, *The Journal of Neuroscience*, 31(47), pp. 16907–16915. Available at: https://doi.org/10.1523/JNEUROSCI.2737-11.2011.

Vallence, A. *et al.* (2021) ‘Examining motor evoked potential amplitude and short-interval intracortical inhibition on the up-going and down-going phases of a transcranial alternating current stimulation (tacs) imposed alpha oscillation’, *European Journal of Neuroscience*, 53(8), pp. 2755–2762. Available at: https://doi.org/10.1111/ejn.15124.

Van Hoornweder, S. *et al.* (2022) 'Addressing transcranial electrical stimulation variability through prospective individualized dosing of electric field strength in 300 participants across two samples: the 2-SPED approach', *Journal of Neural Engineering*, 19(5), p. 056045. Available at: https://doi.org/10.1088/1741-2552/ac9a78.

Van Hoornweder, S. *et al.* (2024) 'The Causal Role of Beta Band Desynchronization: Individualized High-Definition Transcranial Alternating Current Stimulation Improves Bimanual Motor Control'. Neuroscience. Available at: https://doi.org/10.1101/2024.10.30.621096.

Van Meer, M.P.A. *et al.* (2010) 'Recovery of Sensorimotor Function after Experimental Stroke Correlates with Restoration of Resting-State Interhemispheric Functional Connectivity', *The Journal of Neuroscience*, 30(11), pp. 3964–3972. Available at: https://doi.org/10.1523/JNEUROSCI.5709-09.2010.

Van Wassenhove, V. and Nagarajan, S.S. (2007) 'Auditory Cortical Plasticity in Learning to Discriminate Modulation Rate', *The Journal of Neuroscience*, 27(10), pp. 2663–2672. Available at: https://doi.org/10.1523/JNEUROSCI.4844-06.2007.

Vernet, M. *et al.* (2013) 'Insights on the neural basis of motor plasticity induced by theta burst stimulation from TMS – EEG', *European Journal of Neuroscience*, 37(4), pp. 598–606. Available at: https://doi.org/10.1111/ejn.12069.

Vida, I., Bartos, M. and Jonas, P. (2006) 'Shunting Inhibition Improves Robustness of Gamma Oscillations in Hippocampal Interneuron Networks by Homogenizing Firing Rates', *Neuron*, 49(1), pp. 107–117. Available at: https://doi.org/10.1016/j.neuron.2005.11.036.

Vithlani, M., Terunuma, M. and Moss, S.J. (2011) 'The Dynamic Modulation of $GABA_A$ Receptor Trafficking and Its Role in Regulating the Plasticity of Inhibitory Synapses', *Physiological Reviews*, 91(3), pp. 1009–1022. Available at: https://doi.org/10.1152/physrev.00015.2010.

Vivekananda, U. *et al.* (2021) 'Theta power and theta-gamma coupling support long-term spatial memory retrieval', *Hippocampus*, 31(2), pp. 213–220. Available at: https://doi.org/10.1002/hipo.23284.

Vogeti, S., Boetzel, C. and Herrmann, C.S. (2022) 'Entrainment and Spike-Timing Dependent Plasticity – A Review of Proposed Mechanisms of Transcranial Alternating Current Stimulation', *Frontiers in Systems Neuroscience*, 16, p. 827353. Available at: https://doi.org/10.3389/fnsys.2022.827353.

Vossen, A., Gross, J. and Thut, G. (2015) 'Alpha Power Increase After Transcranial Alternating Current Stimulation at Alpha Frequency (α-tACS) Reflects Plastic Changes Rather Than Entrainment', *Brain Stimulation*, 8(3), pp. 499–508. Available at: https://doi.org/10.1016/j.brs.2014.12.004.

Vosskuhl, J., Strüber, D. and Herrmann, C.S. (2018) 'Non-invasive Brain Stimulation: A Paradigm Shift in Understanding Brain Oscillations', *Frontiers in Human Neuroscience*, 12, p. 211. Available at: https://doi.org/10.3389/fnhum.2018.00211.

Wang, X.-J. and Buzsáki, G. (1996) 'Gamma Oscillation by Synaptic Inhibition in a Hippocampal Interneuronal Network Model', *The Journal of Neuroscience*, 16(20), pp. 6402–6413. Available at: https://doi.org/10.1523/JNEUROSCI.16-20-06402.1996.

Wang, Y. *et al.* (2023) 'Excitability changes induced in the human auditory cortex by transcranial alternating current stimulation', *Neuroscience Letters*, 792, p. 136960. Available at: https://doi.org/10.1016/j.neulet.2022.136960.

Weinrich, C.A. *et al.* (2017) 'Modulation of Long-Range Connectivity Patterns via Frequency-Specific Stimulation of Human Cortex', *Current Biology*, 27(19), pp. 3061-3068.e3. Available at: https://doi.org/10.1016/j.cub.2017.08.075.

White, J.A. *et al.* (2000) 'Networks of interneurons with fast and slow γ-aminobutyric acid type A ($GABA_A$) kinetics provide substrate for mixed gamma-theta rhythm', *Proceedings of the National Academy of Sciences*, 97(14), pp. 8128–8133. Available at: https://doi.org/10.1073/pnas.100124097.

Whittington, M.A. and Traub, R.D. (2003) 'Interneuron Diversity series: Inhibitory interneurons and network oscillations in vitro', *Trends in Neurosciences*, 26(12), pp. 676–682. Available at: https://doi.org/10.1016/j.tins.2003.09.016.

Winkler, A.M. *et al.* (2014) 'Permutation inference for the general linear model', *NeuroImage*, 92, pp. 381–397. Available at: https://doi.org/10.1016/j.neuroimage.2014.01.060.

Wischnewski, M. *et al.* (2019) 'NMDA Receptor-Mediated Motor Cortex Plasticity After 20 Hz Transcranial Alternating Current Stimulation', *Cerebral Cortex*, 29(7), pp. 2924–2931. Available at: https://doi.org/10.1093/cercor/bhy160.

Wu, J. *et al.* (2014) 'Resting-state cortical connectivity predicts motor skill acquisition', *NeuroImage*, 91, pp. 84–90. Available at: https://doi.org/10.1016/j.neuroimage.2014.01.026.

Wu, X. *et al.* (2013) 'Homeostatic Competition between Phasic and Tonic Inhibition', *Journal of Biological Chemistry*, 288(35), pp. 25053–25065. Available at: https://doi.org/10.1074/jbc.M113.491464.

Yao, B. *et al.* (2018) 'Motor Unit Properties of the First Dorsal Interosseous in Chronic Stroke Subjects: Concentric Needle and Single Fiber EMG Analysis', *Frontiers in Physiology*, 9, p. 1587. Available at: https://doi.org/10.3389/fphys.2018.01587.

Yousry, T. (1997) 'Localization of the motor hand area to a knob on the precentral gyrus. A new landmark', *Brain*, 120(1), pp. 141–157. Available at: https://doi.org/10.1093/brain/120.1.141.

Yuasa, A. *et al.* (2022) 'Systematic determination of muscle groups and optimal stimulation intensity for simultaneous TMS mapping of multiple muscles in the upper limb', *Physiological Reports*, 10(23), p. e15527. Available at: https://doi.org/10.14814/phy2.15527.

Zaghi, S. *et al.* (2010) 'Inhibition of motor cortex excitability with 15Hz transcranial alternating current stimulation (tACS)', *Neuroscience Letters*, 479(3), pp. 211–214. Available at: https://doi.org/10.1016/j.neulet.2010.05.060.

Zewdie, E. and Kirton, A. (2016) 'TMS Basics', in *Pediatric Brain Stimulation*. Elsevier, pp. 3–22. Available at: https://doi.org/10.1016/B978-0-12-802001-2.00001-1.

Zhang, D.-W., Moraidis, A. and Klingberg, T. (2022) 'Individually tuned theta HD-tACS improves spatial performance', *Brain Stimulation*, 15(6), pp. 1439–1447. Available at: https://doi.org/10.1016/j.brs.2022.10.009.

Zhang, Y., Brady, M. and Smith, S. (2001) 'Segmentation of brain MR images through a hidden Markov random field model and the expectation-maximization algorithm', *IEEE Transactions on Medical Imaging*, 20(1), pp. 45–57. Available at: https://doi.org/10.1109/42.906424.

Zhao, Z. (2023) 'Intensity- and frequency-specific effects of transcranial alternating current stimulation are explained by network dynamics'.

Zich, C. *et al.* (2020) ‘Dissecting Transient Burst Events’, *Trends in Cognitive Sciences*, 24(10), pp. 784–788. Available at: https://doi.org/10.1016/j.tics.2020.07.004.

Zich, C. *et al.* (2021) ‘Human motor cortical gamma activity relates to GABAergic signalling and to behaviour’. Neuroscience. Available at: https://doi.org/10.1101/2021.06.16.448658.

Ziemann, U. *et al.* (1998) ‘Dextromethorphan decreases the excitability of the human motor cortex’, *Neurology*, 51(5), pp. 1320–1324. Available at: https://doi.org/10.1212/WNL.51.5.1320.

Ziemann, U. (2004) ‘TMS and drugs’, *Clinical Neurophysiology*, 115(8), pp. 1717–1729. Available at: https://doi.org/10.1016/j.clinph.2004.03.006.